Presynaptic function of the voltage-gated calcium channel DmCa1D in *Drosophila* larval motoneurons

Dissertation
Zur Erlangung des Grades
Doktor der Naturwissenschaften

Am Fachbereich Biologie
Der Johannes Gutenberg Universität Mainz

Aylin Klein
geb. am 12.04.89 in Brackenheim

Mainz, 2016

Tag der mündlichen Prüfung: 19.12.2016

Table of contents

Summary

Voltage-gated calcium-channels (VGCCs) are indispensable for neuronal information processing. The different functions mediated by VGCCs are dependent on their conductance, activation and inactivation kinetics and their location in different compartments. These include exocytosis of synaptic vesicles from presynaptic terminals, generating of plateau potentials, modifications of action potential-shape, frequency, and propagation along the axon, as well as amplification of postsynaptic potential in dendrites. In *Drosophila* there are three different genes for VGCCs: DmCa1D (Ca_v1), DmCa1A (Ca_v2) and DmCa1G (Ca_v3), each of which is homolog to one vertebrate family.

This work addresses the functions of DmCa1D L-type channels in different compartments of larval motoneurons. In collaboration with other members of the Duch lab we show that axonal and dendritic DmCa1D channels increase motoneuron firing rates. Ca^{2+} influx into motoneuron dendrites may amplify postsynaptic potentials, thus increasing firing rates and burst durations. During high frequency motoneuron firing, Ca^{2+} influx through axonal DmCa1D channels causes fast de-inactivation of sodium channels via transient BK channel activation, thus shortening the refractory period. Therefore, in *Drosophila* larvae axonal and dendritic DmCa1D channels enhance motoneuron firing and thus synaptic vesicle release to the muscle. Based on these findings I then focused on the question whether DmCa1D channels may also enhance synaptic vesicle turn-over.

In *Drosophila*, synaptic vesicle release requires presynaptic Ca^{2+} influx through DmCa1A channels at active zones. In multiple systems, including the *Drosophila* neuromuscular junction, the recycling of synaptic vesicles is also affected by Ca^{2+}. I provide evidence that DmCa1D channels mediate presynaptic Ca^{2+} influx to enhance synaptic vesicle retrieval at larval motoneuron terminals. DmCa1D channels localize to the periactive zone of motoneuron synaptic terminals, but there is no co-localization with the active zone marker Bruchpilot. Localization is in agreement with a potential role in synaptic vesicle endocytosis. This is further supported by increased synaptic depression upon genetic manipulation of presynaptic DmCa1D channels. Moreover, pharmacological blockade of DmCa1D reduces SV endocytosis while exocytosis is likely not affected. In sum, localization of DmCa1D to three different compartments of motoneurons provides three separate mechanisms that cooperatively augment maximum motoneuron firing rates with sustainable information transfer to the muscle.

1 Introduction

Throughout the nervous system calcium ions fulfill two important functions. First, they act as intracellular messengers thereby regulating numerous cellular processes. Second, they are charge carriers when passing the membrane through Ca^{2+} channels (Clapham 1995; Campiglio & Flucher 2015). As second messenger Ca^{2+} takes part, amongst others, in neurotransmitter release and the regulation of enzymatic processes (Tsien 1988; Catterall 2000; Kawasaki et al. 2004). To address these tasks calcium ions need to be precise in concentration and location. At rest, $[Ca^{2+}]_i$ lies at ~100 nM. To initiate synaptic vesicle exocytosis, a concentration from 10-100 µM has to be achieved (Xiong et al. 2002; Guo et al. 2005). Calcium concentrations above physiological doses are toxic for the neuron (Berridge 1998). Besides, neurons are equipped with several mechanisms to reduce $[Ca^{2+}]$, local elevations in calcium concentration are needed to initiate Ca^{2+} regulated processes (Clapham 1995). Calcium can either be released from internal stores, like the endoplasmatic reticulum, or by passage through the membrane via calcium channels from the extracellular space. Activity dependent Ca^{2+} influx is given by voltage-gated calcium channels (VGCCs) which open at depolarizing membrane potentials (Berridge 1991). In *Drosophila* there are three genes for VGCCs (Littleton & Ganetzky 2000). Localization and function of these channels are still not completely clarified. We use motoneurons to directly measure the effect on motor output (Heckmann 2003). In this study we focus on localization and function of the DmCa1D channel in larval motoneurons.

1.1 The dual role of calcium ions in neurons

By passing the membrane through calcium channels, calcium ions are charge carriers and additionally, they act as intracellular messengers (Clapham 1995; Campiglio & Flucher 2015). Because the extracellular Ca^{2+} concentration of 2 mM is 20,000 times higher than the cytosolic Ca^{2+} concentration (100 nM Ca^{2+}), the opening of calcium channels will force Ca^{2+} along its electromotive force into the cell, which in turn causes a membrane depolarization (Berridge 1993; Clapham 1995). As second messenger Ca^{2+} takes part for example in muscle contraction, cell growth, hormone and neurotransmitter release, membrane excitability, homeostasis of neuronal activity, gene expression and the regulation of enzymatic processes (Tsien et al. 1988; Tsien & Tsien 1990; Hardingham et al. 1997; Dolmetsch et al. 1998; Turrigiano 1999; Catterall 2000; Davis & Bezprozvanny 2001; Marder & Prinz 2002; Kawasaki et al. 2004; Peng & Wu 2007). Consequently, the cytosolic Ca^{2+} concentration has to be strictly regulated to allow

normal cell function. This is mainly achieved by Ca^{2+}-buffering proteins (Allbritton et al. 1992), Na^{2+}/$Ca2^{+}$ exchangers (Reuter & Seitz 1968; Baker et al. 1969; Dipolo & Beaugé 2006) and P-type ATPase pumps. Aforementioned pumps consume 1 to 2 ATPs to convey one Ca^{2+} ion into cell organelles like the endoplasmic reticulum (ER) or the extracellular space. The most famous family of pumps is the sarcoplasmic endoplasmic reticulum Ca^{2+} ATPases, better known as SERCA-pump, which transports Ca^{2+} into ER or SR (sarcoplasmic reticulum) (Pederson & Carafoli 1987; Lytton and MacLennan 1988; Gunteski-Hamblin et al. 1988; Lytton et al. 1989; Burk et al. 1989; Clapham 1995). High ER Ca^{2+} concentrations serve as reservoir of Ca^{2+} for intracellular signaling, and furthermore, calcium ions are required in protein synthesis and processing in the lumen ER. Finally, high cytosolic Ca^{2+} concentrations above physiological doses (~100 nM at rest) activate Ca^{2+} sensitive protein-digesting enzymes which can lead to cell death via necrosis (Berridge et al. 1998, 2000; Orrenius et al. 2003; Boehning et al. 2003).

1.2 Calcium channels

A membrane protein which is selectively permeable for calcium ions is named a calcium channel. Opening of a calcium channel happens either by a change in membrane potential (voltage-gated calcium channels) or by binding of a certain ligand (ligand-gated calcium channels LGCCs). Neurotransmitters, ions as well as molecules can act as ligands. Besides, calcium influx through these channels from the outside of the cell, calcium can also be released from internal stores (store-operated channels SOCs). For example the inositol 1,4,5-triphosphate (IP3) receptor, which is a calcium channel and is localized to the membrane of the endoplasmatic reticulum (Newton et al. 1994). Upon binding of its ligand IP3 the channel opens and the stored calcium flows into the cytosol along its concentration gradient (Berridge 1991; Morrissette et al. 1993; Sitsapesan et al. 1994). Based on the strict regulation system of the calcium concentration LGCCs are present in every cell type. Neurons and muscles are additionally equipped with VGCCs.

1.3 Voltage-dependent calcium channels

In case of voltage-dependent calcium channels (VGCCs) a certain change in membrane potential is needed to open the ion permeable pore. In the inactive state neurons stay at their resting potential which is in general between -60 to -80 mV (Clapham 1995; Bear et al. 2007). The quarternary structure of a VGCC consists of 4 to 5 subunits: an α_1-subunit, a β-subunit, an associated α_2- and δ-subunit and only in some cases a γ-subunit (Figure 1). The α_1-subunit is

the biggest and the pore forming subunit. It is divided into four homologous repeats each containing six transmembrane domains. Linkers between the fifth and sixth domain of every repeat shape the inner pore wall. The small membranous loop (green square) of these linkers carries specific glutamate groups responsible for ion selectivity (Tanabe et al. 1987; Catterall 2000). The fourth transmembrane domains are multiply positively charged and serve as the voltage sensor. Despite changes in kinetics and activity, expression of the α_1-subunit can be sufficient to create a functional VGCC (Perez-Reyes et al. 1989; Laverda et al. 1991; Singer et al. 1991; Doering & Zamponi 2003). The therefore so called auxiliary subunits β, $\alpha_2\delta$ and γ define the specific properties of the channels. Intracellularly, the β-subunit interacts with the α_1-subunit through the α-interaction domain (AID) at the loop between repeat I and II (Pragnell et al. 1994). The protein consists of a guanylate kinase domain and a conserved SH3 domain (Buraei & Yang 2010). It may play a crucial role in transporting the channel protein from the ER to its integration site and in regulation of voltage-dependent activity as well as inactivation of the channel (Dolphin 2003; Richards et al. 2004; Chen et al. 2004; Van Petegem et al. 2004; Fang & Colecraft 2011). The extracellularly located α_2- and δ- subunits are two single peptides associated by disulfide bonds. During translation only one polypeptide chain emerges which is cleaved subsequently (Ellis et al. 1988; De Jongh et al. 1990, Jay et al. 1991; Gurnett et al. 1996; Calderon-Rivera et al. 2012). It is suggested that the $\alpha_2\delta$-subunit functions in targeting and stabilizing the VGCCs in the membrane of neurons because of the GPI-anchor of the δ-subunit (Davies et al. 2010). Furthermore, it could be shown that kinetics of VGCCs are altered in $\alpha_2\delta$- knockdowns and knockouts (Sipos et al. 2000; Obermair et al. 2005; Tuluc et al. 2008; Obermair 2008; Fuller-Bicer et al. 2009). The γ-subunit is a glycoprotein and consists of four transmembrane domains (Jay et al. 1990, Chen et al. 2007). It takes part in skeletal muscle interaction and in stabilization of the inactivated state of the channel (Freise et al. 2000; Androchnache et al. 2007). Besides its function in muscle membranes it could be shown that γ-subunits influence calcium channel mRNA (Ahlijanian et al. 1990; Caterrall 2000; Moss et al. 2002; Kang & Campbell 2003; Ferron et al. 2008; Campiglio & Flucher). Ca^{2+}-Calmodulin interacts with the α_1-subunit via the IQ motif (King et al. 2007).

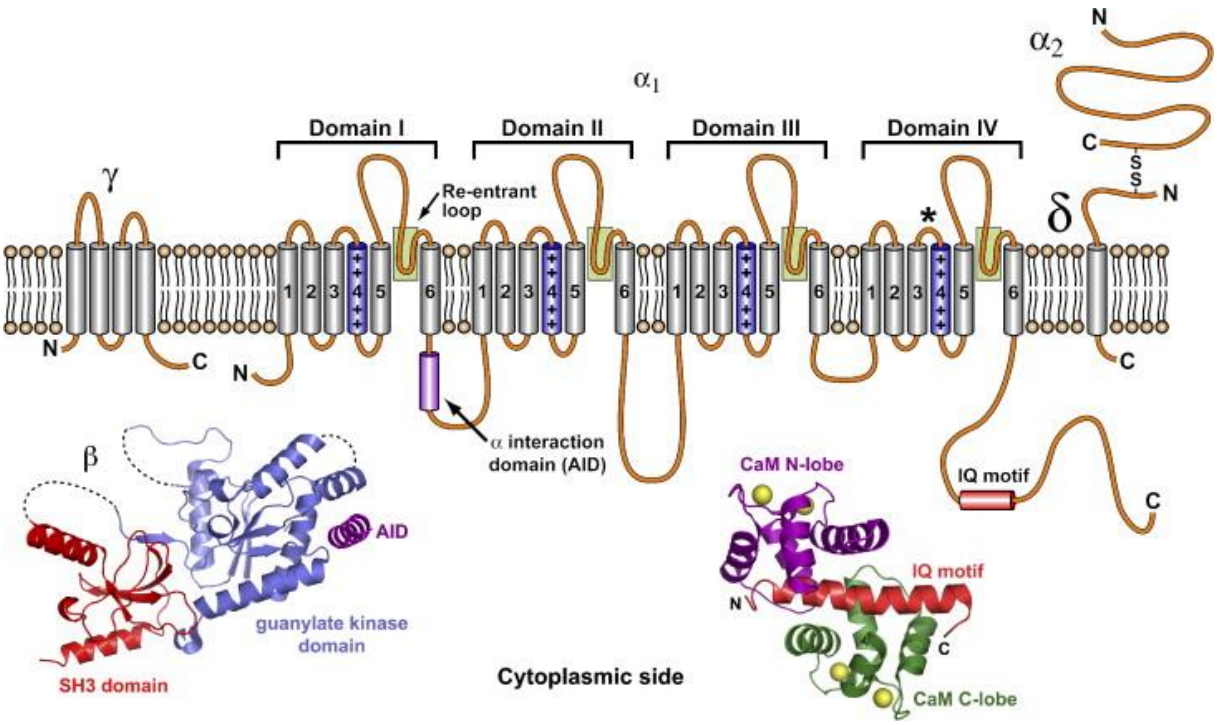

Figure 1: **Quarternary structure of a voltage-gated calcium channel.** The 5 subunits α_1, $\alpha_2\delta$, β and γ are shown at the neuronal membrane. The pore forming α_1 –subunit consists of four homologous repeats each subdivided into six transmembrane domains (TMD). The re-entrant loop (green square) between TMD 5 and 6 forms the inner pore wall and determines the ion selectivity. Every fourth TMD of each repeat carries the voltage sensor. The γ-subunit is located in the membrane as well as the GPI-anchor of the $\alpha_2\delta$-subunit. Crystalline structures of the β-subunit and the Ca^{2+}-Calmodulin are known (Van Petegem et al. 2004, 2005). Both proteins interact with the α_1-subunit at certain sites: the β-subunit at the α-interaction domain (AID) and Ca^{2+}-Calmodulin at the IQ motif. Figure from King 2007.

In vertebrates 10 genes encode for the α_1-subunits of VGCCs which are subdivided into three families: Ca_V1, Ca_V2 and Ca_V3 (Dolphin 2009). These 10 channels are classified by their activation voltages, current kinetics, and pharmacological profiles (Table 1). Whereas low-voltage activated (LVA) channels open at hyperpolarized membrane potentials, high-voltage activated (HVA) channels require a higher depolarization of the membrane to open the pore (Tsien et al. 1988).

Table 1: Vertebrate calcium channel classification (Dolphin 2009)

Activation	α_1-gene IUP name/SU	Type of current	Main localization
HVA	$Ca_V1.1/\alpha1S$	L	Skeletal muscle
	$Ca_V1.2/\alpha1C$		Cardiac, smooth muscle, neuronal
	$Ca_V1.3/\alpha1D$		Sinoatrial node, cochlear hair cells, dendrites
	$Ca_V1.4/\alpha1F$		Retina
	$Ca_V2.1/\alpha1A$	P/Q	Neuronal (presynaptic)
	$Ca_V2.2/\alpha1B$	N	Neuronal (presynaptic)
	$Ca_V2.3/\alpha1E$	R	Neuronal
LVA	$Ca_V3.1/\alpha1G$	T	Neuronal, cardiac
	$Ca_V3.2/\alpha1H$		Neuronal and other tissues
	$Ca_V3.3/\alpha1I$		Neuronal

The Ca_V1 family has the distinction of activating at higher voltages (HVA) mediating long lasting currents (L-type) which among others could be measured in skeletal muscles and in neuronal somatodendritic regions (Reuter 1983; Nowycky et al. 1985; Hounsgaard & Mintz 1988; Heckmann et al. 2003; Carlin et al. 2009). Furthermore $Ca_V1.3$ L-type channels mediate graded transmitter release in inner hair cells (Platzer et al. 2000; Brandt et al. 2003) and also take part in hormone release, gene expression regulation and synaptic integration (Bean 1989; Milani et al. 1990). Four different types of currents are facilitated by the Ca_V2 family, which are also HVA channels. P/Q and R currents are characterized by pharmacological properties while N-type currents show intermediate speeds of activation and inactivation. P/Q- and N-type currents play major roles in transmitter release at several synapses (Dunlap et al. 1995; Catterall 2000; Reid et al. 2003) whereas R-type currents play an important role in synaptic plasticity (Dietrich et al. 2003). Channels of the third family Ca_V3 activate at lower voltages (LVA) and show transient currents (Carbone & Lux 1984; Nowycky et al. 1985). They contribute to neuronal pacemaker activity and synaptic integration in dendrites (Contreras 2006; Steriade 2006; Cain & Snutch 2010; Crandall et al. 2010; Isope et al. 2010). The old letter nomenclature was replaced by a classification in sub numbers regarding pharmacological sensitivities called “International Union of Pharmacology” (IUP) (Catterall et al. 2005).

1.4 *Drosophila* larval motoneurons

To investigate properties and functions of calcium channels the *Drosophila* nervous system serves as a useful model because of lower channel diversity and precise genetic tools. Motoneurons receive input from interneurons of the central pattern generator (Kiehn & Kullander 2004; Marder et al. 2005; Grillner et al. 2005). With their inherent membrane properties they actively form motor output (Kiehn 1991; Kiehn et al. 2000; Heckmann et al. 2003). To understand locomotion in these animals we aim to reveal the precise location and function of calcium channels. 32 motoneurons located in each hemisegment of the ventral nerve cord (VNC) of third instar larvae innervate 30 body wall muscles in the abdominal segments A2-A7. A1 and A8 own fewer muscles and the thoracic segments T1-T3 additionally hold mouthpart controlling muscles (Campos-Ortega & Hartenstein; 1985 Bate 1992; Landgraf et al. 1997; Schmid et al. 1999). Motoneurons form synaptic terminals, also called boutons, at larval crawling muscles which differ in size and shape. Large synaptic boutons of motoneurons that mediate fast neuromuscular transmission are called type I and are subdivided into Ib ("big" 3-6 µm) and Is ("small" 2-4 µm). Type II terminals generate smaller boutons of 1-2 µm (Johansen et al. 1989; Antwood et al. 1993; Budnik 1996). Only muscle 12 additionally receives type III boutons (Gorczyca et al. 1993; Jia et al. 1993). For this study we focused on the motoneurons RP2 and aCC as well as RP3. Named after their shape and localization in the embryo RP stands for "Raw Prawn" (M. Bate & C. S. Goodman) and aCC for "anterior corner cell" (du Lac et al. 1986; Sink and Whitington 1992; Broadie et al. 1993). MN1-Ib is the third instar larva name of the aCC motoneuron and it derives from the lineage of the neuroblast NB1-1. It innervates only the larval crawling muscle 1. NB4-2 is the origin of RP2, which is called MNISN-Is and it innervates the larval muscles 1, 2, 3, 4, 8, 10, 18, 19 and 20 (Figure 2). RP3 derives from NB3-1, is also called MN6/7-Ib, and innervates muscles 6 and 7 (Thomas et al. 1984; Broadus et al. 1995; Doe et al. 1988 a+b; Patel et al. 1989; Udolph et al. 1995; Chu-LaGraff et al. 1995; Bossing et al. 1996; Landgraf et al. 1997; Hoang & Chiba 2001; Choi et al. 2004). The two motoneurons aCC and RP2 are well characterized and have been subject to many studies (Thomas et al. 1984; Sink and Whitington 1991; Halpern et al. 1991; Broadie et al. 1993; Bate & Broadie 1995; Worrell & Levine 2008; Schaefer et al. 2010; Srinivasan et al. 2012). For imaging of neuromuscular terminals we used the type Ib-boutons on muscle 6 and 7. Those boutons are easily identifiable and accessible (Chiba & Rose 1998; Halpern et al. 1991; Sink & Whittington 1991).

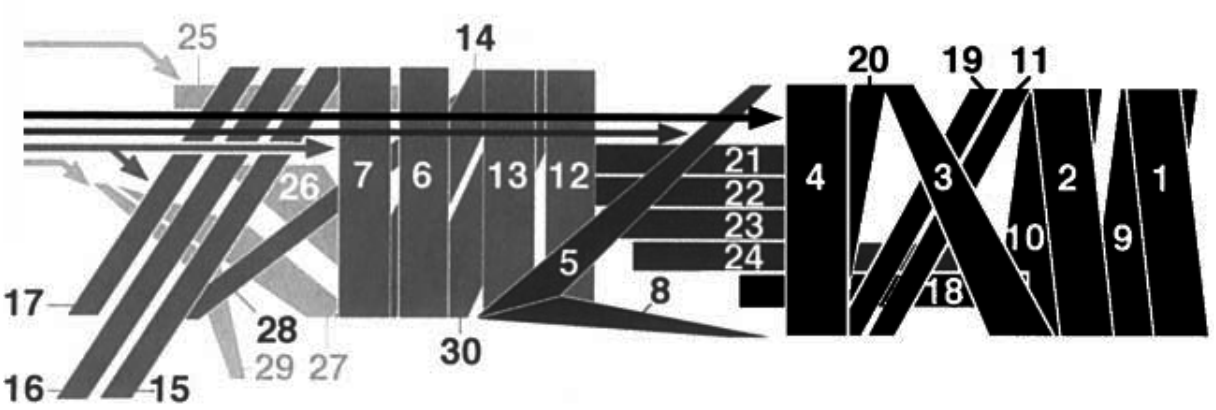

Figure 2: **One hemi-segment of larval body wall muscles.** Whereas muscle one is the most dorsal muscle, muscle 6 and 7 are the biggest ones and lay, close to M 6+7 of the other hemisegment, in the middle of the ventral line (Hoang & Chiba 2001).

1.5 Voltage-dependent calcium channels in *Drosophila*

In contrast to the 10 genes for α_1 subunits of VGCCs the *Drosophila* genome presents only three genes, one homolog to each of the three vertebrate channel families Ca_V1, Ca_V2 and Ca_V3. Regarding channel properties and sequence similarity the *Drosophila* channels are named after the vertebrate genes (old letter nomenclature) with the highest conformity (Table 2). The Ca_v1 homologue DmCa1D is a high-voltage activated channel and mediates L-type currents in somatodendritic regions of larval motoneurons (Worrell & Levine 2008). Furthermore, DmCa1D is the VGCC in *Drosophila* muscles responsible for graded Ca^{2+} potentials to initiate muscle contraction (Ren et al. 1998; Hara et al. 2015). The DmCa1A channel, also called Cacophony, is required for vesicle exocytosis at presynapses (Kawasaki et al. 2002; Hou et al. 2008). It's also involved in synaptic growth and regulation of NMJs (Rieckhof et al. 2003; Xing et al. 2005). In studies investigating the adult flight motoneuron, MN5, it could be shown that DmCa1A mediates at least two different somatodendritic currents, one high-voltage and one low-voltage activated one (Ryglewski et al. 2012). LVA T-type currents could be measured in MN5 playing a role in regulation of DmCa1A HVA- and LVA-currents (Ryglewski et al. 2012). In adult projection neurons Ca_V3-type calcium channels play a role in regulation of excitability (Iniguez et al. 2013). Despite the fact that *Drosophila* has only three genes for VGCCs there is a great range of localizations and properties resulting in different functions. Isoform diversity is drastically increased by interactions with different accessory subunits, and post-transcriptional processes like RNA-editing and alternative splicing (Zheng et al. 1995; Littleton & Ganetzky 2000; Lipscombe et al. 2002). It is still not fully understood how this is regulated and accomplished.

Table 2: Voltage-dependent calcium channels in *Drosophila*

Vertebrate α_1-gene	***Drosophila* α_1-gene**	**Activation**	**Type of current**	**Motoneuron localization**
$Ca_v1.3/\alpha1D$	DmCa1D	HVA	L-type	Soma, dendrites, axon, NMJ (Worrell & Levine 2008; Klein (2013 MA))
$Ca_v2.1/\alpha1A$	DmCa1A; Cacophony	HVA/LVA	N-type T-type	NMJ, somatodendritic region (Kawasaki et al. 2000; Ryglewski et al. 2012)
$Ca_v3.1/\alpha1G$	Dmα1G	LVA	T-type	Somatodendritic region (Ryglewski et al. 2012)

1.6 DmCa1D calcium channel

The DmCa1D channel was first characterized and named by its sensitivity towards dihydropyridines (DHP) "*Drosophila melanogaster* calcium channel α_1-subunit DHP-sensitive" (Zheng et al.1995; Eberl et al. 1998). DmCa1D is homologous to vertebrate L-type channels and is highly expressed in the nervous system and muscle throughout development (Zheng et al. 1995). In larval crawling muscles DmCa1D mediates the dihydropyridine sensitive current (Ren et al. 1998). Furthermore, DmCa1D is responsible for the somatodendritic voltage-dependent Ca^{2+} current in larval motoneurons aCC and RP2 (Worrell & Levine 2008). A stop codon after the fourth transmembrane domain of the fourth repeat prevents transcription of the published null mutant allele *X10*. Homozygous null mutant animals die in late embryonic stages (Eberl et al. 1998). To investigate the function of the DmCa1D channel we combined genetic and pharmacological tools with immunocytochemistry and opto- and electrophysiological recordings.

1.7 Voltage-dependent Ca^{2+} channels at the *Drosophila* presynapse

Multiple studies suggest that at least three different calcium channels exist at the *Drosophila* NMJ (Kawasaki et al. 2002; Kuromi et al. 2004; Hou et al. 2008; Kuromi et al. 2010): A PLTXII sensitive channel mediating fast synaptic transmission, a second PLTXII sensitive channel which showed delayed release, and a La^{3+} sensitive channel facilitating endocytosis. To initiate exocytosis of transmitter-filled vesicles at the presynapse calcium influx through VGCCs is essential. In vertebrates, this is mediated by P/Q- and N-type Ca_V2 calcium channels (Dolphin

2009). In *Drosophila*, the PLTXII sensitive Ca_V2 homolog DmCa1A localizes to presynaptic terminals (Bodi et al. 1995; Kawasaki 2000, 2002, 2004; Kuromi et al. 2004; Hou et al. 2008; Ryglewski et al. 2012) and co-localizes with the CAZ-protein Bruchpilot (Brp) and synaptic vesicles at active zones (Kittel et al. 2006a) mediating exocytosis. In a temperature sensitive mutant cac^{TS2}, synaptic transmission is terminated and animals are paralyzed after reaching 38 °C (Kawasaki et al. 2000). To enable sustained transmitter release and to conserve the presynaptic membrane structure endocytosis and recycling of fused vesicle membrane has to take place (Wu et al. 2014). Despite the automatic coupling of the exo- and endocytic machineries (Haucke et al. 2011) studies claim an important role of calcium even in endocytosis in vertebrates as well as in invertebrates (Heuser & Reese 1973; Gad et al. 1998; Guatimosim et al. 1998; Klingauf et al. 1998; Marks & McMahon 1998; Cousin & Robinson 1998, 2000; Neale et al. 1999; Sankaranarayanan and Ryan 2001). In certain central synapses of the vertebrate brain (Calyx of Held) and in *Drosophila* neuromuscular junctions Ca^{2+} -dependent endocytosis (Kuromi et al. 2004) could be shown. At the *Drosophila* NMJ they claim a VGCC sensitive to La^{3+} to be responsible for this calcium influx and excluded DmCa1A from this task. To name the endocytic channel is still an open question. In 2009 a study asserts that calcium hemi-channels named flower located at the synaptic vesicle membrane fuse to functional channels upon exocytosis in the presynaptic membrane (Yao et al. 2009). This mechanism couldn't be confirmed for other synapses. In my previous work I could show DmCa1D localization at the *Drosophila* NMJ presynapse which makes the channel a candidate for Ca^{2+}-mediated endocytosis.

1.8 Synaptic vesicle cycle

To pass information from one neuron to another an electrical signal arriving at the presynapse is translated into a chemical signal as neurotransmitter-filled synaptic vesicles, which undergo exocytosis for the transmitters to pass the synaptic cleft (Katz 1969). One 40 – 50 nm sized synaptic vesicle equals one quantal size (Rizzoli & Betz 2005). About 1500-2000 neurotransmitter molecules per vesicle are then recognized by postsynaptic receptors (Katz & Miledi 1965; Katz 1971; Zhai & Bellen 2004; Südhof 1995, 2004; Takamori et al. 2006). The fused SV membrane has to be retrieved again via endocytosis. For one thing the structure of the presynapse has to be conserved, for another thing SV proteins, which are located in the presynaptic membrane after endocytosis, have to be removed and recycled in the terminal. The amount of SVs in the synapse is limited and the cell body, which is the place of protein

synthesis, is too far away to facilitate fast neurotransmission (Murthy & De Camilli 2003; Galli & Haucke 2004; Dittman & Ryan 2009). The recycling of an SV from exocytosis to being ready for release takes about 40 to 60 s (Südhof 1995; Galli & Haucke 2001). Depending on the amount of SVs needed they are retrieved from three different SV pools (Rizzoli & Betz 2005). First the readily-releasable pool (RRP), which is represented by docked and primed vesicles at the active zones. These SVs are immediately ready to undergo exocytosis upon a Ca^{2+} signal, but they deplete rapidly during high frequency stimulation. Second, the recycling pool (RP), which delivers SVs during moderate stimulation. Synaptic vesicles of the RP are distributed all over the terminal. Third, the reserve pool (RSP) containing the majority of SVs builds a depot needed for sustained release (Ikeda & Bekkers 2009; Kim & Ryan 2010). For the *Drosophila* NMJ a total number of SVs was estimated to be about 84,000 (Delgado et al. 2000; Kidokoro et al. 2004). Around 200 SVs should be ready to release, 7,000 – 16,000 in the RP and 62,000 SVs in the RSP (Kuromi & Kidokoro 2005). In comparison to that the vertebrate calyx of Held (Held 1893) contains around 77,000 – 188,000 SVs (Satzler et al. 2002; de Lange et al. 2003) in total, 1500 SVs in the RRP and 20,000 to 40,000 SVs (de Lange et al. 2003; Yamashita et al. 2005) in the RP (Sakaba & Neher 2001; Neher & Sakaba 2008; Neher 2010).

1.9 Exocytosis

Exocytosis of transmitter filled SVs takes place at specific sites of the presynapse called active zones (AZs) (Couteaux & Pecot-Dechavassine 1970; Landis 1988). In electron microscopy (EM) those AZs are associated with an electron dense cytoskeletal matrix – cytomatrix at the active zone (CAZ) (Dresbach et al 2001; Harlow et al. 2001) – which contains highly specialized components (Schoch & Gundelfinger 2006) for example: ELKS family proteins like Bruchpilot (Brp), Liprin, GIT family proteins, Rab interacting molecules (RIMs), RIM binding proteins and (M)Unc 13 (Wojcik & Brose 2007; Spangler & Hoogenraad 2007; Wang et al. 2009; Mittelstaedt et al. 2010; Hida & Ohtsuka 2010; Liu et al. 2011; Haucke et al. 2011; Südhof 2012; Ehmann et al. 2014; Peled et al. 2014). The CAZ-associated protein Bruchpilot is essential for T-bar formation, which are electron dense projections in EM where VGCCs and SVs are clustered (Kittel 2006 a; Hallermann et al. 2010). The protein itself has an elongated structure and is part of the T-bar at the center of active zones (Fouquet et al. 2009). In Brp null mutants VGCC clustering is disturbed (Ohtsuka et al. 2002; Kittel et al. 2006 a+b; Maglione & Sigrist 2013). RIM binding proteins bind Ca^{2+} channels to AZs and interact with Bruchpilot (Liu et al. 2011). To dock and finally fuse SVs with the presynaptic membrane formation of the

SNARE (soluble NSF attachment protein receptor proteins) complex is crucial (Jahn & Scheller 2006; Südhof & Rothman 2009). It consists of the synaptic vesicle protein Synaptobrevin (VAMP2) and the two plasma membrane proteins Syntaxin and SNAP-25 (synaptosome-associated protein) (Mohrmann et al. 2010; van den Bogaart et al. 2010). Formation of the SNARE complex is controlled, among others, by Unc 13 (Südhof & Rothman 2009). An essential step for SV fusion with the presynaptic membrane is Ca^{2+} influx through VGCCs (Katz & Miledi 1969; Neher & Sakaba 2008). The DmCa1A channel which is clustered with SVs at the T-bars of AZs mediates this influx (Kawasaki et al. 2000; Kuromi et al. 2004; Kittel et al. 2006 a). Ca^{2+} is then sensed by the SV protein Synaptotagmin which in turn acts on the SNARE complex (Martens & McMahon 2008; Hui et al. 2009; Hua et al. 2011). For this, the Ca^{2+} concentration has to achieve 10-100 µM but the intracellular Ca^{2+} concentration lies below 100 nM (Augustine 2001). To reach this high concentration without affecting other processes in the cell Ca^{2+} levels are elevated only in small areas (~tens of nanometers) called micro domains (Adler et al. 1991; Heidelberger et al. 1994; Schneggenburger & Neher 2000; Gundelfinger et al. 2003). These micro domains exist only in close proximity to DmCa1A channels and SVs, thereby sustaining only for milliseconds (Meinrenken et al. 2003). By fusion of SVs with the presynaptic membrane the latter is expanded. To maintain structure and functionality of the presynapse SV membrane has to be retrieved and recycled by a process called endocytosis.

1.10 Endocytosis

The retrieval of fused vesicle membrane, the endocytosis, takes place at the periactive zone of synaptic terminals surrounding active zones (Marie et al. 2004). There are three different endocytic mechanisms postulated (Kononenko et al. 2013; Zhou et al. 2014). The fastest mechanism happens in 50–100 ms at the periactive zone and is formally known as ‘ultrafast endocytosis. Upon one stimulus via the light-sensitive protein channelrhodopsin formation of large membrane invaginations have been observed in *C. elegans* and in mouse neurons (Watanabe et al. 2013a+b). A process of endocytosis which does not include full collapse of a SV is called ‘kiss-and-run’ and takes less than 1 s from pore opening over transmitter release to SV retrieval (Ceccarelli et al. 1973; Ceccarelli & Hurlbut 1980; Alabi & Tsien 2013). These two fast processes seem to compensate presynaptic membrane elongation really quickly to enable transmission (Zhou et al. 2014). The most important mechanism may be the clathrin and dynamin mediated endocytosis (Miller & Heuser 1984; Granseth et al. 2006; Ferguson et al. 2007). Disruption of these 2 proteins was done in several organism and caused severe defects

in endocytosis (König & Ideka; 1996; Galli & Haucke 2004; Ferguson et al. 2007; Heerssen et al. 2008; Kasprowicz et al. 2008). After full collapse of a SV its retrieval at the periactive zone takes around 10-20 s, which is rather slow in comparison to the other two processes (Smith et al. 2008; Neher 2010). The first step in this mechanism is bending of the membrane in which proteins containing an F-BAR (FCH domain-bin-amphiphysin-Rvs) like FCHo-proteins, amphiphysin, endophilin, syndapin and epsin are involved (McMahon & Gallop 2005; Koh et al. 2007; Pechstein et al. 2010; Henne et al. 2010). Then, a clathin coat assembles along the bended membrane whereby clathrin triskelia build pentagonal and hexagonal disposals (Kirchhausen 2000; Murthy & De Camilli 2003; Jung & Haucke 2007; Dittman & Ryan 2009; Doherty & McMahon 2009). The fission of the invagination is then accomplished by the GTPase dynamin which is a mechanochemical enzyme (Slepnev & De Camilli 2000; Ferguson et al. 2009; Rao et al. 2010). Dynamin is recruited by proteins holding an SH3 domain as: intersectin (Marie et al. 2004; Koh et al. 2004, Pechstein et al. 2010), amphiphysin (Shupliakov et al. 1997), endophilin (Schmitd et al. 1999; Ringstad et al. 1999; Dickman et al. 2005) and syndapin (Qualmann et al. 1999). Such clathrin coated membrane structures occur close to active zones as well as at more lateral sites (Gad et al. 1998; Teng et al. 1999).

1.11 Coupling of exocytosis and endocytosis

Several studies indicate that exocytosis of transmitter filled vesicles and the following endocytosis of the SV membrane is tightly coupled (Haucke et al. 2011). Therefore, specialized scaffolding proteins of the CAZ seem to interact with multidomain endocytic scaffolding proteins to clear the release site after exocytosis to enable further SVs to get docked and primed for release (Gundelfinger et al. 2003). How coupling of exocytosis and endocytosis is accomplished mechanistically is the topic of many studies and still not understood (Haucke et al. 2011). Nonetheless, an activity-dependent regulator of endocytosis may be Ca^{2+} (Gad et al. 1998; Deak et al. 2004). At several synapses it could be shown that endocytosis is Ca^{2+} dependent (Ceccarelli & Hurlbut 1980; Thomas et al. 1990; Smith & Neher 1997; Gad et al. 1998; Naele et al. 1999; Kuromi & Kidokoro 2002; Kuromi et al. 2004; Wu et al. 2007; Xu et al. 2008; Hosoi et al. 2009). Whereas exocytosis is triggered at 10-100 µM Ca^{2+} the concentration needed for endocytosis is much lower and endocytosis is even abolished above 1 µM Ca^{2+} (von Gersdorff & Matthews 1994; Marks & McMahon 1998; Cousin & Robinson 2000). In *Drosophila* the exocytosis mediating VGCC DmCa1A is well characterized (Kawasaki et al. 2000, 2002, 2004; Hou et al. 2008). However, it is still not clear how Ca^{2+}

influx responsible for endocytosis is facilitated. Former studies claimed a second VGCC to be localized at the periactive zone of synaptic terminals (Kuromi et al. 2004, 2010).

1.12 Hypothesis

Amongst all the claims from different studies regarding calcium channels at the *Drosophila* NMJ only one is commonly shared: The VGCC DmCa1A (Cacophony) is necessary and sufficient for fast synaptic transmission (Kawasaki 2002; Hou et al. 2008). It seems to be undisputed that other calcium channels exist at the presynapse but identification above pharmacological properties remain an open question (Kuromi et al. 2004; Hou et al. 2008; Kuromi et al 2010). A regulatory role of Ca^{2+} influx in endocytosis could be shown in several synapses (Ceccarelli & Hurlbut 1980; Thomas et al. 1990; Smith & Neher 1997; Gad et al. 1998; Naele et al. 1999; Kuromi & Kidokoro 2002; Kuromi et al. 2004; Wu et al. 2007; Xu et al. 2008; Hosoi et al. 2009). The responsible channel is suggested to localize to the periactive zone of synaptic terminals causing a much less increase in Ca^{2+} concentration than needed for exocytosis (von Gersdorff & Matthews 1994; Marks & McMahon 1998; Cousin & Robinson 2000). With a specific antibody we could show presynaptic localization of the HVA L-type voltage-gated calcium channel DmCa1D at the *Drosophila* NMJ. Combining this with data of former studies we now claim that Ca^{2+} influx through DmCa1D calcium channels plays a role in clathrin-mediated SV endocytosis. To accomplish this task DmCa1D channels have to localize in close proximity to the endocytic machinery at the periactive zone, which surrounds active zones (Figure 3). Therefore, calcium influx through two different channels (DmCa1A and DmCa1D) control exocytosis and endocytosis separately.

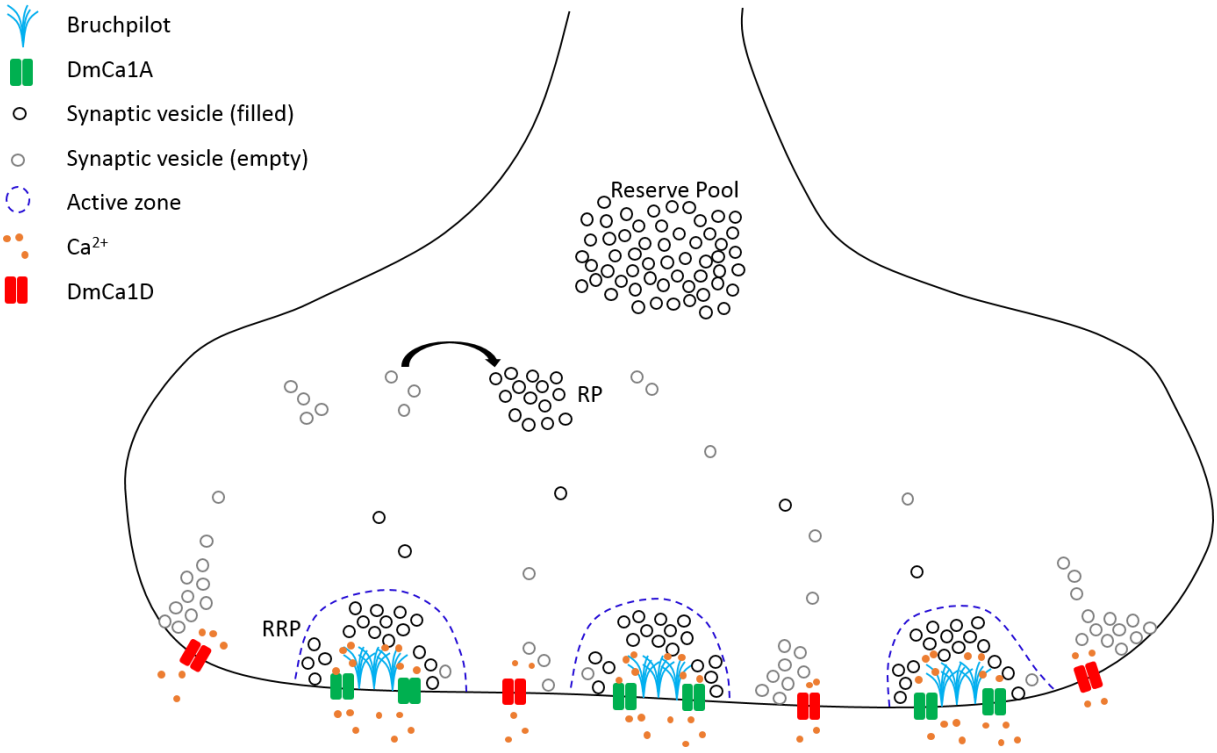

Figure 3: **Hypothetic scheme of the *Drosophila* larval NMJ.** Active zones containing Bruchpilot, DmCa1A channels and SVs of the readily releasable pool (RRP). Exocytosis takes place upon Ca^{2+} influx through DmCa1A. DmCa1D channels localize to the periactive zone of the terminal mediating Ca^{2+} influx which regulated endocytosis. Retrieved SVs are recycled and pass the recycling pool (RCP). The reserve pool builds a large storage of SVs.

1.13 Aim of the study

According to our hypothesis we made the following predictions:

1) DmCa1D localizes to the periactive zone of terminals and not to active zones
2) Presynaptic calcium influx is reduced if DmCa1D is pharmacologically blocked
3) DmCa1D knockdown or knockout in motoneurons will increase synaptic depression during repetitive stimulation
4) Pharmacological blockade of DmCa1D causes a reduction in synaptic vesicle endocytosis rates
5) DmCa1D does not contribute significantly to exocytosis, which is mediated by DmCa1A

To determine the subsynaptic localization of DmCa1D at synaptic terminals we used immunocytochemistry and confocal microscopy. With a specific antibody against the DmCa1D channel and several antibodies against proteins localized to different compartments at the presynapse we tried to differentiate between active and periactive zone. At high stimulation frequencies many synapses show synaptic depression but reach a steady state of synaptic vesicle

release, a balance between SV release and resupply, after 5 to 10 stimuli (Haucke et al. 2011). During high-frequency conditions clearance of release sites seems to be the release limiting cause rather than the number of available SVs (Dittman & Regehr 1998; Neher 2010). High-frequency stimulation typically consists out of tetanic bursts with ~100 stimuli per second (Bear et al. 2007). To analyze the impact of DmCa1D on depression we measured evoked postsynaptic potentials (EPSPs) in larval crawling muscles. In RNAi knockdown and MARCM knockout terminals we expect increased depression during repetitive stimulation protocols. To directly show that loss of DmCa1D reduces SVs retrieval we measured endocytosis with the fluorescent dye FM1-43 (Betz & Bewick 1992). The dye is taken up into synaptic terminals during membrane retrieval and the fluorescence states the endocytosis rate. The trivalent cation lanthanum (La^{3+}) serves as a pharmacological blocker to eliminate DmCa1D calcium influx (Cauvin et al. 1983). Under blocking conditions endocytosis rates at synaptic terminals should be reduced while exocytosis remains unaffected. Furthermore, we expressed the calcium indicator Syp-GCaMP3 in larval motoneurons where it localizes to SVs to show presynaptic calcium influx through DmCa1D upon membrane depolarization. Again, the pharmacological blocker lanthanum was applied to prevent calcium influx through DmCa1D channels. To proof that DmCa1D does not contribute to exocytosis, which is mediated by DmCa1A, is difficult because the channel localizes to all compartments of larval motoneurons and also to the crawling muscles. First we used the postsynaptic calcium indicator GCaMP3, which localizes closely to postsynaptic glutamate receptors and recognizes calcium influx through glutamate receptors only.

2 Material and methods

2.1 *Drosophila melanogaster*

2.1.1 Breeding

Fly food 1 liter:

116.11 g glucose

54.89 g cornmeal

10.56 g agarose

29.02 g yeast

→ Boil at 90 °C for 1 hour, cook for another hour at 85°C. After cooling to 66 °C , the following ingredients are added:

12.2 ml 10 % tegosept

0.56 g ascorbic acid

Fly strains (Table 3) are kept on a yeast-cornmeal-syrup-agar diet in 2 cm Ø standard plastic vials with foam plugs at 25 °C under a 12 hours light/dark cycle. Backups and temperature-sensitive fly lines are reared at 18 °C.

2.1.2 Fly lines

Table 3: *Drosophila* stock list

	Origin/Bloomington	**Genotype**
TRiP lines	35786	y^1 v^1;; P{UAS-GFP.VALIUM10}attP2
	33413	y^1 sc^* v^1;; P{TRiP.HMS00294}attP2
MARCM	42725	P{hsFLP}1, y^1 w^* P{UAS-mCD8::GFP.L}Ptp4E^{LL4}; P{tubPGAL80}LL10 P{neoFRT}40A; P{tubP-GAL4}LL7
	25141+5759	b^1Ca-α1D^{X10} pr^1 cn^1 wx^{wxt} bw^1/sna^{Sco} P{neoFRT}40A; ry^{506}
	25141/5759	b^1 Ca-α1D^{X10} P {neoFRTry+}40A / CyO P{ActGFP}JMR1
DmCa1D null	25141	b^1 Caα1DX10 pr1 cn1 wxwxt bw1/CyO, P{ActGFP}JMR1
	4275	b^1 Ca-α1D^{X7} pr^1 cn^1 wx^{wxt} bw^1/CyO, P{ActGFP}JMR1

Balancer	4533	w^{*}; In(2LR)$noc^{4L}Sco^{rv9R}$, b^{1}/CyO, P{ActGFP}JMR1
	9493	w^{*}; CyO/In(2LR)bw^{V1}, ds^{33k} dp^{ov1} b^{1} bw^{V1}; CxD/TM6B, Tb^{1}
GAL4	S. Sanyal BIOGEN-Idec, Cambridge, USA	w*; RN2-GAL4, UAS-mCD8GFP/CyO ; Act<Stop>GAL4, UAS-FLP
	458	P{GawB}elavC155
	S. Sanyal BIOGEN-Idec, Cambridge, USA	;;D42-GAL4,Cha-GAL80
	S. Sanyal BIOGEN-Idec, Cambridge, USA	;OK37-1-GAL4
Control	3605	w^{1118}
	1	Canton Spezial
DmCa1A	8579	P{GawB}$elav^{C155}$ cac^{HC129} sd^{1} f^{1}/FM7i, P{ActGFP}JMR3
	8581/8582	w*; P{UAS-cac1-EGFP}422A ; P{UAS-cac1-EGFP}786C
GCaMP	Isacoff lab	;;MHC-CD8-GCaMP3-Sh
	Fiala lab	;UAS-syp-GCaMP3/CyO

2.2 Immunocytochemistry

2.2.1 Larval dissection

Dissection was done in 4 cm Ø petri dishes filled with Sylgard-silicone (Dow Corning GmbH, Wiesbaden). Third instar larvae were fixed dorsally with pins in head and abdomen. Covering with saline follows a cut along the dorsal midline till the mandibles. Cuticula was fixed with pins and internal organs were carefully removed.

Saline in mM: NaCl 128; KCl 2; $MgCl_2$ 4; $CaCl_2$ 1,8; HEPES 5; Sucrose 35 → pH 7,24 (NaOH) 300-310 mOsmol

2.2.2 Fixation

Fixation was done at room temperature for 45 min with 4 % paraformaldehyde (PFA) in PBS (Sigma, Germany), which was solved at 56 °C for 1 hour. Two times rinsing with PBS was followed by 1 hour of PBS washing. Improved permeability of the tissue was ensured by 6 x 30 min incubation with 0.5 % Triton X (TX, Sigma, Germany) in PBS.

2.2.3 Antibody incubation

Primary antibodies (Table 4) were diluted in 0.3 % TX in PBS and incubated at 4 °C on a shaker for 1 night. 5 % bovine serum albumin (BSA) was added if DmCa1D antibody was in use. After

at least 8 x 30 min PBS washing, samples were incubated in secondary antibodies (Table 5) at 4 °C on a shaker for 1 night.

2.2.4 Shortened antibody incubation

After fixation, samples were treated with 0.5 % Triton X for 3 x 20 min. Primary antibodies (Table 4) were diluted in 0.3 % TX in PBS and incubated at room temperature on a shaker for 2 hours. After a vigorous washout with 3 x 20 min PBS secondary antibodies (Table 5) incubated for 1 hour at room temperature.

Table 4: Primary antibodies

Antigen	Host	Dilution	Origin	Antigen description
DmCa1D	goat	1:100	Santa Cruz Biotechnology, Santa Cruz, CA, USA N-type Ca^{2+} CPα1B (L-17) sc-32083	*Drosophila* L-type VGCC
GFP	rabbit	1:200	Thermo Fisher Scientific A-11122	Ectopically expressed green fluorescent protein
Bruchpilot	mouse	1:200	Developmental Studies Hybridoma Bank Nc82	*Drosophila* presynaptic CAZ-protein (T-bar, active zone)
Fasciclin II	mouse	1:200	Developmental Studies Hybridoma Bank 1D4	*Drosophila* presynaptic cell adhesion molecule (periactive zone)
Synaptotagmin	mouse	1:100	Developmental Studies Hybridoma Bank 3H2 2D7	*Drosophila* synaptic vesicle protein (presynaptic marker)
Endophilin	guinea pig	1:500	Bellen lab Verstreken et al. 2002	*Drosophila* endocytotic protein (periactive zone)
HRP	goat	1:200	Dianova (Jackson Immunoresearch) 132-005-021	Horseradish peroxidase, antibody binds to neuronal membranes

Table 5: Secondary antibodies

Antigen	Host	Dilution	Origin	Fluorophore
Goat	donkey	1:400	Dianova (Jackson Immunoresearch)	Cy2, Cy3, Cy5
Mouse	donkey	1:400	Thermo Fisher Scientific (Invitrogen)	AF 488, AF 555, AF 647
Rabbit	donkey	1:400	Thermo Fisher Scientific (Invitrogen)	AF 488

Guinea pig	donkey	1:400	Thermo Fisher Scientific (Invitrogen)	AF 488

2.2.5 Embedding

Secondary antibodies were washed out with 6 x 30 min PBS following treatment with increasing series of EtOH: 50 %, 70 %, 90 % and 100 %. Dehydrated samples were embedded in methylsalicylate (Fagron, Netherlands). To increase the space between slide and coverslip a 100 µm metal plate with a hole (Ø 1 cm) was glued between 2 coverslips. Coverslips were sealed with nail polish and samples were stored at 4 °C.

2.2.6 Confocal microscopy

Scanning was done at the Leica TCS SP8 confocal microscope with the software LAS AF (Leica application suite Advanced Fluorescence). Fluorescent dyes Cy2® and Alexa Fluor® 488 were excited with the argon laser at 488 nm and detected with a photomultiplier at 500-550 nm. The diode laser excited at 561 nm Cy3® and Alexa Fluor® 555, whereas detection was at 570-620 nm. Excitation of Cy5® and Alexa Fluor® 647 happened at 633 nm, detection at 645-700 nm. For weak signals we used a hybrid detector (HyD) which is more sensitive towards photons, thereby increasing the signal. With a 40x oil immersion objective (NA 1.4) and additional digital zoom we obtained 1024x1024 pixel images. For image processing we used the Leica software LAS AF 2.3.5 and Fiji (www.fiji.sc).

2.3 MARCM

The published null mutation of the DmCa1D channel *DmCa1D*^{X10} is embryonically lethal. Consequently, electrophysiological and immunohistological investigations of motoneurons are impossible. To address this we created mosaic null mutants with the MARCM-technique (mosaic analysis with a repressible cell marker) (Wu et al. 2006). The goal hereby is to obtain single specific cells, which are homozygous null mutant in an otherwise heterozygous animal. At first, we had to do a series of genetic crosses and screening to bring the constructs needed for the technique into one animal (2.3.1). After verification of the FRT-construct in the screened flylines via PCR (2.3.2) the final cross was set up (2.3.3). All cells in F1 animals are heterozygous for the null mutation on one sister chromatid and for the protein GAL80 on the other, each closely located behind the FRT (flippase recognition target) site (Figure 4). GAL80 inhibits GAL4, which prevents expression of UAS-GFP to label the cell. If the flippase is now activated in the G2 phase of the cell cycle after DNA replication by heat shock (hs-FLP), heterologous recombination at the FRT sites between two sister-chromatids is induced. Cleaved

parts of GAL80 and the mutation exchange places, resulting in two heterologous sister chromatid pairs. During mitosis one chromatid of each pair is pulled into respectively two cells. The cell containing both copies of the null mutation is now able to express GFP, thereby being labeled. In the other cell GAL4 is inhibited by two copies of GAL80. The heat shock has to be precisely timed in development during division of the mother ganglion cell of motoneurons aCC and RP2 (2.3.3).

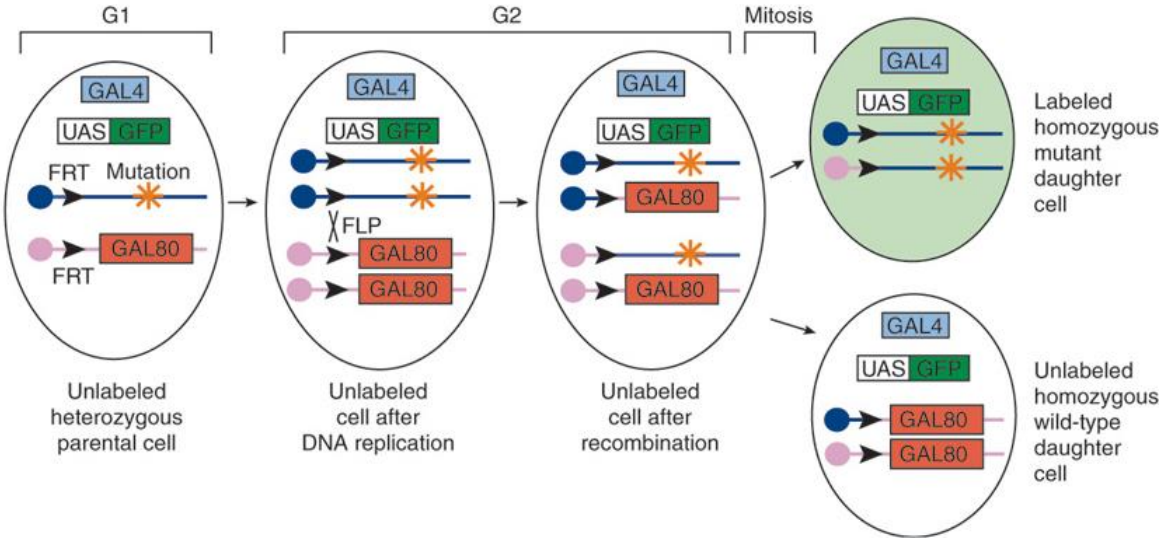

Figure 4: **Heterologous recombination during mitosis using MARCM.** In G1 all cells are heterozygous for the mutation and for the GAL4 inhibitor GAL80. After DNA replication heat shock is induced in G2 phase to activate the flippase which targets to the FRT sites. The cleaved parts of each sister chromatid exchange places, resulting in two heterologous sister chromatid pairs. During mitosis two chromatids, both containing the mutation, are pulled into one cell. The same happens with the two chromatids containing GAL80. The homozygous mutant cell is now able to express GFP via GAL4 (Wu et al. 2006).

2.3.1 MARCM flies

To generate null mutant mosaics we first had to bring the known DmCa1D null mutation *DmCa1D*^{X10} in front of the FRT 40A site by screening for a natural cross–over in female flies with the genotype: $\frac{+}{+}$; $\frac{\text{b1 1DX10 pr1 cn1 wxwxt bw1}}{\text{sna[ScO] \{FRT40A ry+\}}}$; $\frac{\text{ry}-}{\text{ry}-}$.

The desired result would be: $\frac{+}{\text{Y}}$; $\frac{\text{b1 1DX10 pr1 \{FRT40A ry+\}}}{\text{CyO,Act}-\text{GFP}}$; $\frac{\text{ry}-}{\text{ry}-}$, so the 1D$^{\text{X10}}$ (35E5-6) and the sna[Sco] (35D2), which are at close proximity, exchanged places. The estimated recombination rate between these two loci is around 4 %. For more detailed information, see appendix (6.1).

2.3.2 PCR

A cross with each male fly screened for wildtype eye color (FRT with ry+) and the loss of Scutoid (sna^{Sco}) was set up. One fly of each F1 generation was taken for DNA extraction.

2.3.2.1 DNA extraction

Squishing buffer: 10 mM Tris-Cl pH 8.2, 1mM EDTA, 25 mM NaCl

Proteinase K: 0.2 mg/ml (Invitrogen™)

A pipette tip filled with 50 µl squishing buffer containing Proteinase K was used to mash a single fly in a tube for 5-10 seconds. After that the squishing buffer was expelled into the tube. Incubation of the preparation was done for 30 minutes in a 36 °C water bath. For Proteinase K inactivation the temperature was raised to 95 °C for 2 minutes. Sample could be stored at 4 °C for several months.

2.3.2.2 Thermocycling

First, the ThermoPol buffer and dNTPs are defreezed on ice. The thermocycler was turned on and preheated to 95 °C (lid to 105 °C). Samples (Table 6) were prepared on ice before transferring them into the thermocycler and starting DNA amplification (Table 7). To amplify the FRT-site we used published primers (made by Sigma Aldrich), which should result in a 687 bp replicate (Sulkowski et al. 2011).

Table 6: Reaction setup

Component	Volume	Final conc.	Description
10x ThermoPol Reaction Buffer	1 µl	1x	New England BioLabs B9004S
10 mM dNTPs	0.2 µl	200 µ	KAPABiosystems KK1017
10 µM fwd Primer	0.2 µl	0.2 µM	5’ to 3’ CACCTGCAAAAGGTCAGACA 58.4 °C salt adjusted melting temperature
10 µM rev Primer	0.2 µl	0.2 µM	5’ to 3’ CCTGACGGACCATTGATACC 60.5 °C salt adjusted melting temperature
Taq DNA Polymerase	0.05 µl	1.25 units/50 µl	New England BioLabs M0267S
Template DNA	1 µl	< 1000 ng	see DNA extraction
Nuclease-free water	7.35 µl		

Table 7: Thermo-cycling conditions

Process	Temp	Time	Extra
1.Initial denaturation	95 °C	300 s	
2.Denaturation	95 °C	30 s	
3.Annealing	58 °C	60 s	temp gradient possible
4.Extension	68 °C	180 s	30 cycles
5.Final Extension	68 °C	300 s	
6.Pause	4 °C	till processing	

2.3.2.3 Gel electrophoresis

To separate the expected 687 bp replicate we prepared 0.7 % agarose in TBE buffer (0.1 M Tris base, 0.1 M Boric acid, 2 mM EDTA, pH 8) and boiled it. After cooling 2 drops of ethidium bromide (Carl Roth HP47.1 - liquid dropper bottle 250 µg/ml) per 50 ml gel were added and the gel was poured with a 3 mm pocket comb. For visualization of the lanes we added 2 µl Gel loading dye purple (6x) no SDS (New England BioLabs B7025) to each 10 µl sample before loading the pockets. 2-Log DNA Ladder (0.1-10.0 kb) (New England BioLabs N3200S) was used as molecular weight standard (1µg/lane). The gel was run at 70 V for 1-2 hours in a BioRad gel chamber with a BioRad PowerPac HC power supply. The Doc-Print II Imaging System (Vilber Lourmat) was utilized to record the ethidium bromide marked DNA bands. Analyzing and image processing was done with Adobe Photoshop CS5 and Corel Draw XVII.

2.3.3 Heat shock induced heterologous recombination

The null mutant FRT line was crossed to a line containing a heat shock-activated flippase, Tub-GAL80 FRT at the site 40A, UAS-GFP and Tub-GAL4.

$$\frac{hsFLP-GFP}{hsFLP-GFP};\frac{\{FRT40A\ ry+\}\ tub-Gal80}{\{FRT40A\ ry+\}\ tub-Gal80};\frac{tub-Gal4}{tub-Gal4}\mathbf{X}\frac{+}{+};\frac{b1\ 1DX10\ pr1\ \{FRT40A\ ry+\}}{Cy1\ cn1\ dplvl\ pr1-GFP};\frac{ry-}{+}$$

To create null mutant aCC and RP2 motoneurons this cross was set up 48 hours before egg laying with ~50 females and ~20 males. They were transferred into an egg laying chamber (Figure 5), which was placed on an agar plate. To increase the amount of eggs a syringe was used as egg laying chamber. Once the flies were inside, the available room was reduced by further inserting the plunger. This forced the females onto the agar plate, which triggered increased egg laying. After one hour egg laying agar plates were incubated for hours at 25°C to reach the time point of birth of motoneurons aCC and RP2. To induce the heterologous recombination eggs were heat shocked at 34 °C for 30 minutes. All embryos were collected and transferred on fly food for four days at 25 °C or eight days at 18 °C to reach the third larval stage.

Agar plate recipe:

200 ml red grape juice

6g sucrose

3g agarose (1.5 %)

- ➔ Bring to a boil in the microwave
- ➔ Let it cool to 65 °C

3 ml 100% ethanol

1.5 ml glacial acetic acid

- ➔ Pour into petri dishes (4 cm Ø)
- ➔ After cooling store in the fridge

Figure 5: **Egg laying chamber** syringe with inserted plunger on an agar plate.

2.4 Muscle recordings

To investigate the function of the DmCa1D channel we used an RNAi knockdown to reduce the amount of protein. We drove expression of a short hairpin RNAi construct (HMS00294) from the Transgenic RNAi Project (TRiP) stocks (Ni et al .2008; Perkins et al. 2015) in larval motoneurons aCC and RP2. The hairpin construct has been inserted at an AttP-site with a VALIUM vector (Vermillion-AttP-Loxp-Intron-UAS-MCS) into the third chromosome (Ni et al. 2009). UAS-mCD8::GFP was co-expressed with the knockdown, therefore affected terminals were labeled with GFP. As a control the same vector VALIUM was inserted at the same site into the third chromosome in a vermillion (v^1) and yellow (y^1) background but without the hairpin construct (Ni et al. 2008). If GAL4 is under control of the even-skipped promotor like RRA-GAL4, expression takes place in larval motoneurons aCC and RP2. To obtain a strong knockdown effect in only few aCC and RP2 motoneurons we used the even weaker RN2-GAL4 driver, which is also under control of the even-skipped promotor (Fujioka et al. 2003).

Furthermore, a UAS-FLP, which is activated in only few random aCC and RP2 cells by RN2-GAL4 cuts out a stop-codon in the Act-GAL4, which is flanked by two FRT-sites (Hartwig et al. 2008; line courtesy Dr. S. Sanyal, BIOGEN-Idec, Cambridge, MA, USA). This enables the strong driver Act-GAL4 to express the RNAi construct and GFP to label knockdown affected cells and results in a mosaic pattern of motoneurons in the VNC. We received a knockdown strength of about 70 % in Ca^{2+} current recordings during patch clamp from RP2 somas (Kadas et al. in preparation). In general, RNAi knockdowns produce long double-stranded RNAs (300-600 bp), which are cleaved by Dicer2 into multiple 21 bp long siRNAs binding to the target mRNA (Elbashir et al. 2001; Dietzl et al. 2007; Ni et al. 2008, 2009, 2011). Here, we used a short hairpin construct (70-90 bp) to generate a single 21 bp siRNA to specifically target the mRNA of the DmCa1D channel (Chang et al. 2006; Haley et al. 2008).

Knockdown
w*; RN2-GAL4, UAS-mCD8GFP/CyO ; Act<Stop>GAL4, UAS-FLP **X** y^1 sc^* v^1;; P{TRiP.HMS00294}attP2

Control
w*; RN2-GAL4, UAS-mCD8GFP/CyO ; Act<Stop>GAL4, UAS-FLP **X** y^1 v^1;; P{UAS-GFP.VALIUM10}attP2

Because a knockdown doesn't have to result in a complete absence of the protein, we tested a knockout of the DmCa1D channel, *DmCa1D*^{X10}. The null mutation is embryonically lethal if homozygous, therefore the only way to investigate a knockout was by using the MARCM method (2.3). Here, we could generate few homozygous null mutant cells, labeled with GFP, in an otherwise heterozygous animal (Wu et al. 2006). Control experiments were measured in non-GFP-labeled terminals of heterozygous flies.

Table 8: Electrophysiological setup

Microscope	BX51WI	Olympus (Japan)
Micromanipulator	HS-2A Headstage (x0.1 LU gain)	Molecular devices Axon Instruments (USA)
Stimulator	Isolated Pulse Stimulator Model 2100	A-M Systems (USA)
Differential Amplifier (stimulation)	Differential AC Amplifier Model 1700	A-M Systems (USA)
Amplifier (recording)	AxoClamp 2B	Molecular devices Axon Instruments (USA)
Digitizer	Axon Digidata 1550	Molecular devices Axon Instruments (USA)

Electrode puller	Flaming/Brown Puller Model P-97	Sutter Instrument Company (USA)

Borosilicate glass microelectrodes with filament (OD 1 mm, ID 0.5 mm; Molecular devices Sutter Instrument USA) were pulled with the settings: heat 495, pull strength 55, velocity 75, delay 80 and air pressure 400, to generate measuring electrodes. For suction electrodes the following settings were used: heat 462, pull strength 0, velocity 30, time 250 and air pressure 500. This program was looped 3 times till pulling was possible.

Third instar larvae with a DmCa1D-knockdown (RNAi) and -knockout (MARCM) with the respective controls were dissected as described above 2.2.1. To measure evoked postsynaptic potentials (EPSPs) on a setup (Table 8) a sharp glass electrode filled with 2M KAc was inserted into larval crawling muscles, which are innervated by aCC (1) and RP2 (1, 2, 3, 4, 9, 10, 18, 19, 20) (Hoang & Chiba 2001; Choi et al. 2004). The respective nerve was sucked up with a saline filled suction glass electrode after the tip was carefully shortened to increase the opening (Figure 6).

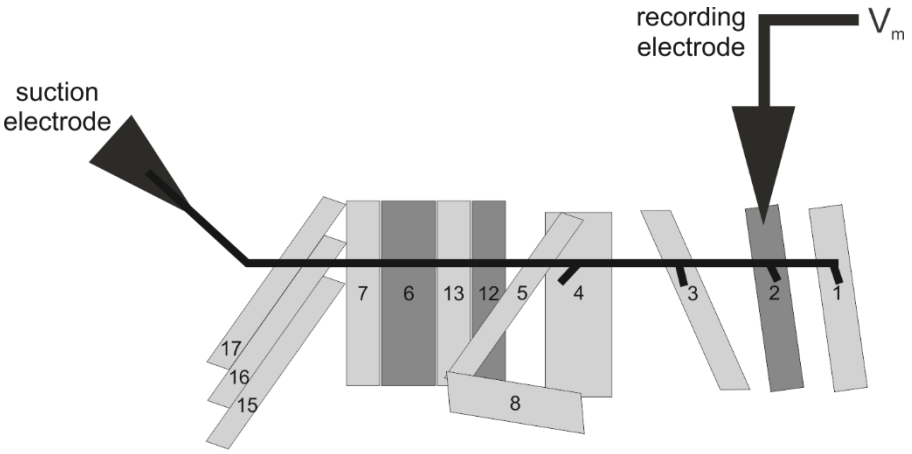

Figure 6: **Scheme of the experimental procedure of extracellular stimulation.** Third instar larvae are dissected to expose larval crawling muscles 1-30. The nerve bundle branching into abdominal segment 2 or 3 is soaked into a suction electrode to stimulate the terminals. A sharp glass electrode containing 2M KAc was placed into the respective muscle recording evoked postsynaptic potentials.

The nerve was stimulated with a frequency of 5 Hz and 2-4 V. In each sample the required voltage for one muscle contraction was doubled for the measurements. 30 s before and after a 5 Hz train a single PSP was evoked to get a control amplitude without short-term plasticity. EPSPs were recorded using AxoClamp 10.2. Recordings with a membrane potential of at least 40 mV were chosen for analysis with Clampfit 10.2. Figure 7 shows a recording example of the EPSPs from a 5 Hz stimuli train. The decrease in EPSP amplitude is synaptic depression. To

increase the effect of depression we lowered the standard saline calcium concentration (1.8mM) to 1mM Ca^{2+}. Concentrations even lower showed interferences of the membrane potential.

1 mM Ca^{2+} saline: NaCl 128 mM; KCl 2 mM; $MgCl_2$ 4 mM; $CaCl_2$ 1 mM; HEPES 5 mM; Sucrose 37 mM → pH 7,24 (NaOH) 300-310 mOsmol

Statistical analysis was done using SPSS 23. Data have been tested for normal distribution with a Shapiro-Wilk test. Normally distributed data were analyzed using a T-test with independent samples. Significance level was set at $p \leq 0.05$ (*), highly significant levels at $p \leq 0.005$ (**) and $p \leq 0.001$ (***).

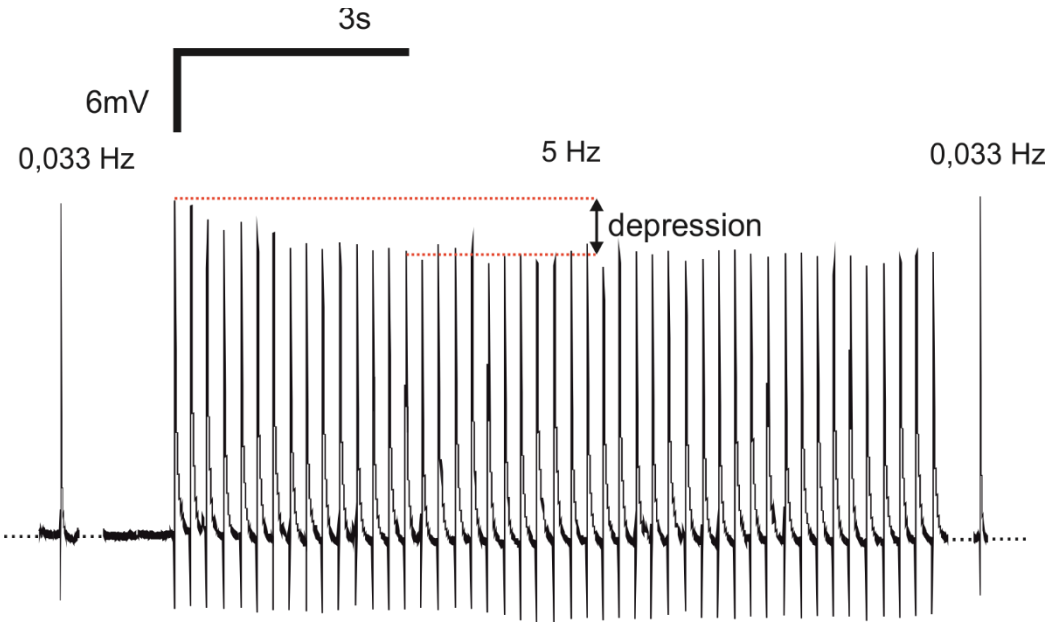

Figure 7: **Depression in a recording example of evoked postsynaptic potentials (EPSPs).** Upon stimulation frequency of 5 Hz amplitudes of EPSPs decrease rapidly until they reach a steady state. The difference in amplitude from beginning to steady state level is depression.

2.5 FM1-43 uptake

To test the role of DmCa1D in synaptic endocytosis we used the amphiphilic dye FM1-43. With its lipophilic tail FM1-43 integrates into the lipid bilayer membrane. (Betz et al. 1992, Betz & Bewick 1992, Ramaswami 1994). The positive charged head group prevents the dye from membrane permeation by keeping it in solution. The two aromatic rings and the linking double-bond bridge determine the excitation and emission wavelength. More double-bonds result in longer wavelengths. The used FM1-43 has an excitation wavelength of 502 nm and an emission wavelength of 626 nm (Figure 8). The protonated form of the fluorophore when solved in water

has a reduced quantum yield, therefore only dye integrated into the membrane shows strong fluorescence (Betz et al. 1996, Cochilla et al. 1999).

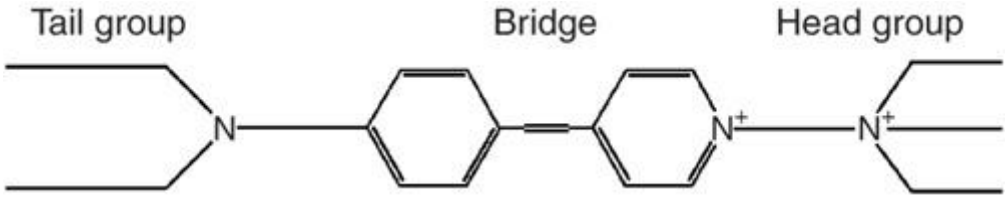

Figure 8: **Structure of the ampiphilic dye FM1-43.** The lipophilic tail integrates into the presynaptic membrane whereas the positive charged head group keeps the protein in solution thereby preventing it to pass the membrane. The two aromatic rings and the linking double-bond determine the excitation wavelength (Gaffield & Betz 2007).

The staining procedure during synaptic transmission is shown in Figure 9. The styryl dye is in bath solution surrounding the presynaptic membrane and subsequently integrates into it (Figure 9a). When exocytosis of transmitter filled synaptic vesicles takes place the membrane of the vesicles has to be recycled afterwards. During this recycling process the dye is incorporated into vesicles either by kiss and run retrieval or via clathrin-mediated endocytosis after a full collapse. After a vigorous washout, dye uptake can be determined by measuring fluorescence intensity. Loaded dye can be released again by inducing exocytosis (Figure 9b). During kiss and run and a full collapse of synaptic vesicles the dye diffuses in the membrane or dissolves into the aqueous bath solution (Kavalali & Jorgensen 2014).

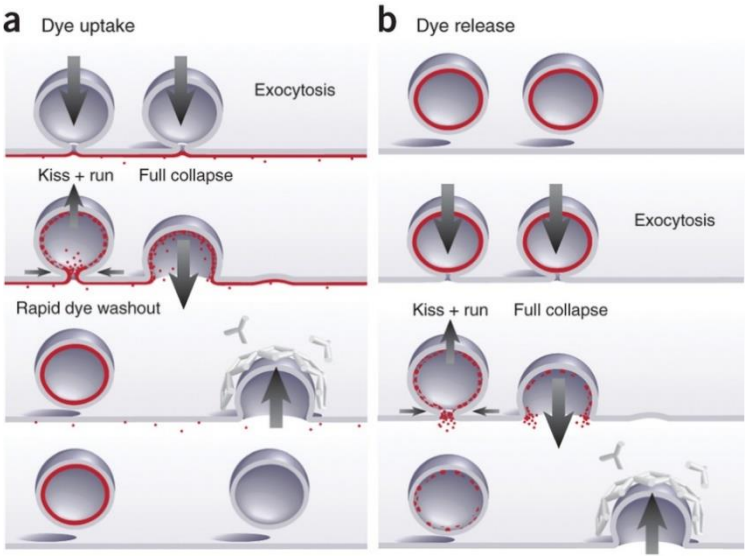

Figure 9: **Uptake and release of FM1-43.** (a) Exocytosis is induced during bath application of FM1-43. FM1-43 is taken up into terminals by membrane retrieval. After washout of the dye fluorescence can be measured. (b) Release of the dye is accomplished through inducing exocytosis. After washout of released dye remaining fluorescent can be measured (Kavalali & Jorgensen 2014).

To separate the role of DmCa1D in endocytosis of synaptic vesicles we used the inorganic pharmacological blocker lanthanum (La^{3+}). In former studies it was used at concentrations of 40 µM to reduce endocytosis at the periactive zone at neuromuscular synaptic terminals of *Drosophila* third instar larvae without knowing the target of La^{3+} (Kuromi et al. 2004, 2010). To find out the optimal concentration of lanthanum we first tested the blocker during intracellular muscle recordings. Because the DmCa1D channel is widely spread in larval crawling muscles of *Drosophila* EPSPs should diminish in addition of the blocker. At a concentration of 1µmol lanthanum in 1mM Ca^{2+} saline EPSPs were completely eliminated (appendix 6.2).

Statistical analysis was done using SPSS 23. Data have been tested for normal distribution with a Shapiro-Wilk Test. Normally distributed data were analyzed using a T-test with independent samples. Data are represented in bars and error bars indicate standard deviation. A Mann-Whitney U test was accomplished with not normally distributed data. Illustration was done in box plots (25-75 % quartile). Whiskers exhibit 1.5 times the interquartile range at maximum (1.5xIQR) (Tukey 1977). Significance level was set at $p \leq 0.05$ (*), highly significant levels at $p \leq 0.005$ (**) and $p \leq 0.001$ (***).

2.5.1 High potassium

Table 9: Saline composition

	0 Ca^{2+} saline	20 mM K^+ saline	90 mM K^+ saline
NaCl (mM)	128	110	40
KCl (mM)	2	20	90
$MgCl_2$ (mM)	4	4	4
$CaCl_2$ (mM)	0	1.8	1.8
HEPES (mM)	5	5	5
Sucrose (mM)	38	35	35

→ pH 7,24 (NaOH) 300-310 mOsmol

Third instar larvae of the wildtype strain Canton S were dissected in 0 Ca^{2+} saline (Table 9) to prevent exocytosis of synaptic vesicles. Saline was replaced by high K^+ saline (20 mM or 90 mM) in addition of 4 µM FM1-43. After 1 minute incubation sample was washed with 0 Ca^{2+} saline for 5 minutes. When lanthanum was used 1 µM La^{3+} in 0 Ca^{2+} saline was incubated for 5 minutes before replacing high K^+ saline (20 mM or 90 mM) containing 4 µM FM1-43 and 1 µM La^{3+}. Loaded boutons of muscles 6 and 7 (RP3) in the abdominal segments A2 or A3 were

recorded with a Hamamatsu digital camera C4742-95 and the image acquisition software Simple PCI. To measure the unload event of the dye vesicle exocytosis was induced again by high K^+ saline (90 mM) for 5 minutes. After a 5 minutes wash with 0 Ca^{2+} saline the same boutons, but unloaded, were recorded again. Mean grey analysis of FM1-43 uptake was done with Fiji.

2.5.2 Stimulation protocol – 5 Hz

Because high potassium solutions initiate immense activity of all neurons we stimulated single motoneurons extracellularly with a suction electrode. To reproduce the protocol used for intracellular muscle recordings (2.4) with FM1-43 we stimulated the nerve, which projects onto muscles 6 and 7 in the abdominal segments A2 or A3, with a frequency of 5 Hz (Figure 10). Furthermore the same saline with a calcium concentration of 1mM was used. The experiment was first done with 4 µM FM1-43. To reduce the amount of dye uptake the concentration was reduced to 1 µM FM1-43. Third instar larvae were dissected in 0 Ca^{2+} saline to prevent exocytosis following endocytosis. Additional 5 minutes of incubation with 1 µM La^{3+} in 0 Ca^{2+} saline were done when lanthanum was added. To get visible loading we stimulated with 5 Hz in 1mM Ca^{2+} saline with 4µM or 1 µM FM1-43 and 1 µM La^{3+} under blocking conditions for 5 minutes. After 5 minutes washing with 0 Ca^{2+} saline images were taken. To release the dye from the terminals preparations were incubated in 60 mM K^+ saline for 5 minutes followed by a 5 minutes 0 Ca^{2+} saline washout. Mean grey analysis of FM1-43 uptake was done with Fiji.

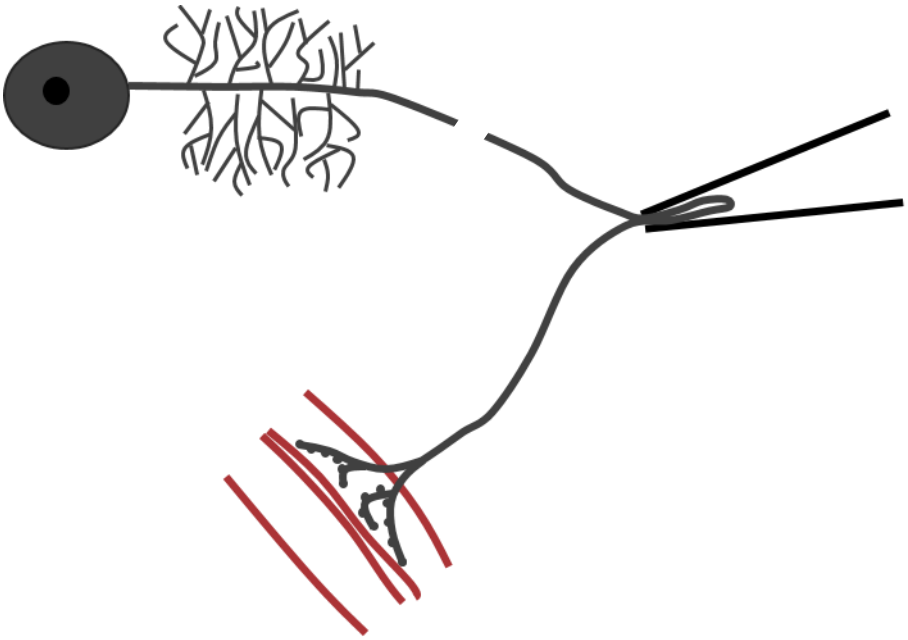

Figure 10: **Stimulation of a larval motoneuron axon via a suction electrode.** Axons were cut to prevent movement. Nerve projecting onto muscles 6 and 7 of the abdominal segements A2 or A3 is soaked into the electrode. Stimulation leads to FM1-43 uptake into terminals.

2.5.3 Stimulation protocol – crawling bursts

Besides stimulation protocols with high potassium and 5Hz we wanted to achieve more physiological conditions. Therefore we stimulated the axons forming boutons on muscle 6 and 7 (RP3) in the abdominal segments A2 or A3 with a crawling-like pattern. It consists of a 120 Hz burst for 0.25 seconds following a 1 second intraburst pause to the next 120 Hz burst for 0.25 seconds. We used normal saline (1.8 mM Ca^{2+}), 4 µM FM1-43 and for blocking solution 1 µM La^{3+}. After a stimulus train of 1 minute, which equals to 50 bursts, we reduced the stimulation to 20 bursts and to 5 bursts. To remove residual dye we washed 5 minutes with 0 Ca^{2+} saline. For dye release preparations were incubated for 5 minutes in 60 mM K^{+} saline followed by a 5 minutes 0 Ca^{2+} saline washout. Mean grey analysis of FM1-43 uptake was done with Fiji.

2.6 Synaptic Ca^{2+} Imaging with GCaMP3

To measure Ca^{2+} influx into the presynapse we used the genetically encoded fluorescent Ca^{2+} indicator GCaMP (Nakai et al. 2001). The fluorescent protein consists out of a circularly permuted enhanced GFP (cpEGFP) (Baird et al. 1999) which is connected to the Ca^{2+} binding protein calmodulin (CaM) at the N-terminus and to the CaM-binding peptide M13 (fragment of myosin light chain kinase) at the C-terminus (Figure 11) (Crivici & Ikura 1995). In Ca^{2+} free environment cpGFP is protonated, leading to poor fluorescence. Upon binding of Ca^{2+} to CaM

the interaction of CaM and M13 induces a conformational change in the cpGFP which closes the protonating water pathway. The following rapid de-protonation results in a much brighter fluorescence of the chromophore. By now there are many different improved forms of GCaMP available. These include enhanced folding, faster kinetics and better fluorescent characteristics (Tian et al. 2009; Akerboom et al. 2009, 2012; Chen et al. 2013). Here we used constructs containing GCaMP3 (Tian et al. 2009) coupled to specific synaptic targets.

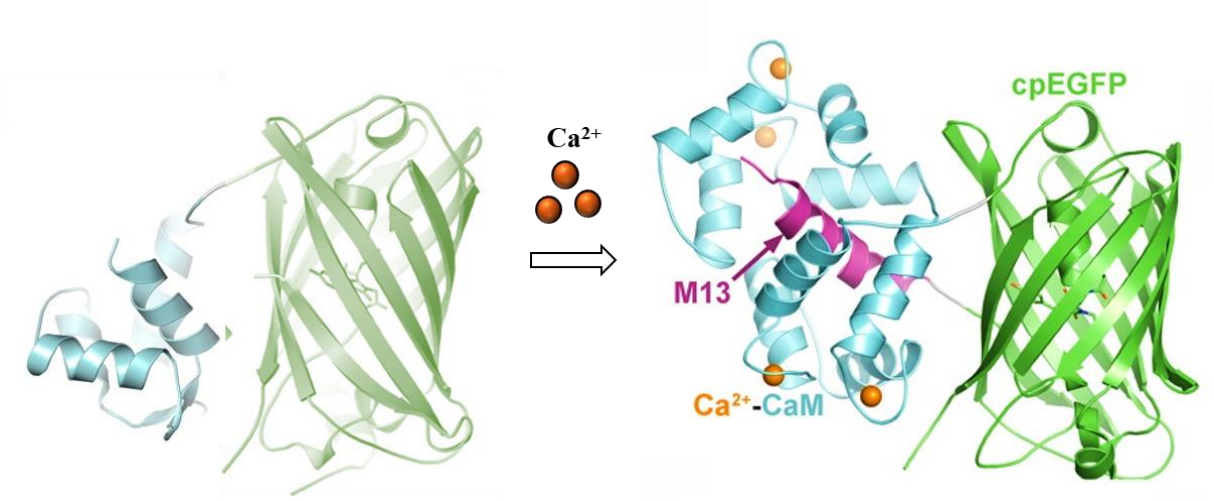

Figure 11: **GCaMP structure:** GCaMP consists out of a circularly permuted enhanced GFP (cpEGFP), Ca^{2+} Calmodulin (CaM) and the CaM interacting peptide M13 (myosin light chain kinase). On the left GCaMP is in a protonated form and shows only poor fluorescence. Upon binding of calcium M13 interacts with CaM causing a conformational change. cpEGFP is going to be deprotonated resulting in a much brighter fluorescent signal (altered from Akerboom et al. 2009).

2.6.1 Presynaptic GCaMP3

In 2015, André Fiala's lab created a UAS-construct to express GCaMP3 coupled to a rat synaptophysin (Dreosti et al. 2009; Li et al. 2011; Pech et al. 2015). *Drosophila* does not have a synaptophysin homolog so a rat-synaptophysin, which binds to SVs, is ectopically expressed in larval motoneurons (Leube 1995). The rat synaptophysin also localizes to SVs in *Drosophila* (Figure 12). Upon membrane depolarization voltage-dependent calcium channels open and Ca^{2+} flows into the terminal, which is visualized by the SV-bound GCaMP3. To mention here is that SVs are present in the different pools all over the terminal. We drove expression of the SypGCaMP3 construct under control of the motoneuron driver OK3-71. Third instar larvae were dissected as in 2.2.1. Stimulation was done like in 2.5.2 with a suction electrode to induce synaptic activity which causes presynaptic Ca^{2+} influx. Stimulation protocol was the following: Starting with 5 action potentials, 10 second pause, 10 actions potentials, 10 second pause and 20 action potentials. The frequency of 120 Hz correlates to the interburst pattern during larval crawling (2.5.3). Ca^{2+} induced fluorescence change was recorded with a Hamamatsu digital

camera C4742-95 and the image acquisition software Simple PCI 6. To block DmCa1D channels we incubated samples with 1µM La^{3+} for 3 minutes. Analysis of ΔF/F was done using Simple PCI 6.

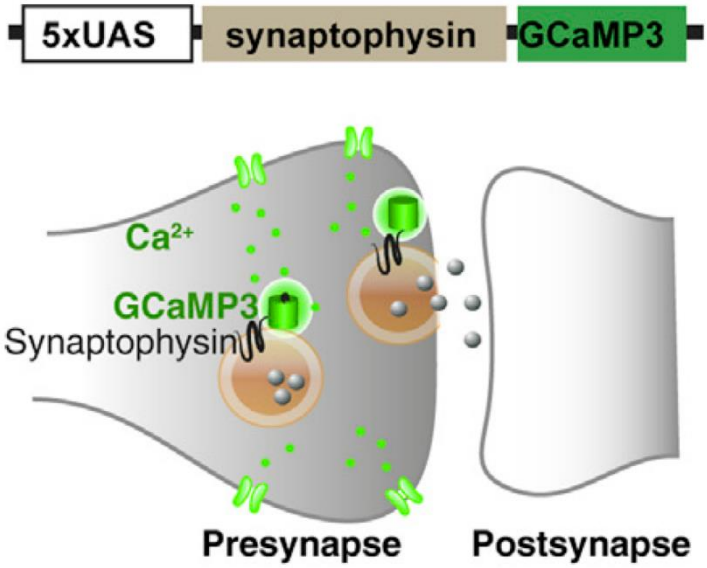

Figure 12: **GCaMP3 targeted to synaptophysin.** Ectopically expressed rat synaptophysin localizes to synaptic vesicles. GCaMP3 is linked to the synaptophysin cytosolic C terminus. Upon Ca^{2+} influx into the presynaptic terminal GCaMP3 binds to Ca^{2+} and undergoes a conformational change which leads to increased fluorescence (Pech et al. 2015).

2.6.2 Postsynaptic GCaMP3

To measure synaptic transmission we used a postsynaptically expressed GCaMP3 (Peled & Isacoff 2011, 2014). Under control of the myosin heavy chain (MHC) promotor GCaMP3 is expressed in larval crawling muscles (Chiba et al. 1995). The fluorescent protein (Figure 13) is coupled to the integral membrane protein CD8 at the N-terminus and the PDZ interaction domain of the potassium channel Shaker (Sh) at the C-terminus (Zito et al. 1999). Through the interaction of the PDZ domain with the PDZ protein disc large (Dlg) the construct is localized to the subsynaptic reticulum of muscles surrounding boutons and anchored in the membrane by the protein CD8 (Zito et al. 1997; Tejedor et al. 1997). The localization of the Ca^{2+} reporter should facilitate detection of Ca^{2+} influx exclusively through postsynaptic glutamate receptors (GluRs) (Chang et al. 1994; Guerrero et al. 2005). Third instar larvae were dissected as in 2.2.1. Stimulation was done like in 2.5.2 with a suction electrode to induce synaptic transmission leading to postsynaptic Ca^{2+} influx through GluRs. We stimulated with 1 action potential every 10 seconds to prevent synaptic plasticity. Ca^{2+} induced fluorescence change was recorded with a Hamamatsu digital camera C4742-95 and the image acquisition software Simple PCI 6. To

block DmCa1D channels we incubated the samples with 1µM La^{3+} for 3 minutes. Analysis of ΔF/F was done using Simple PCI 6.

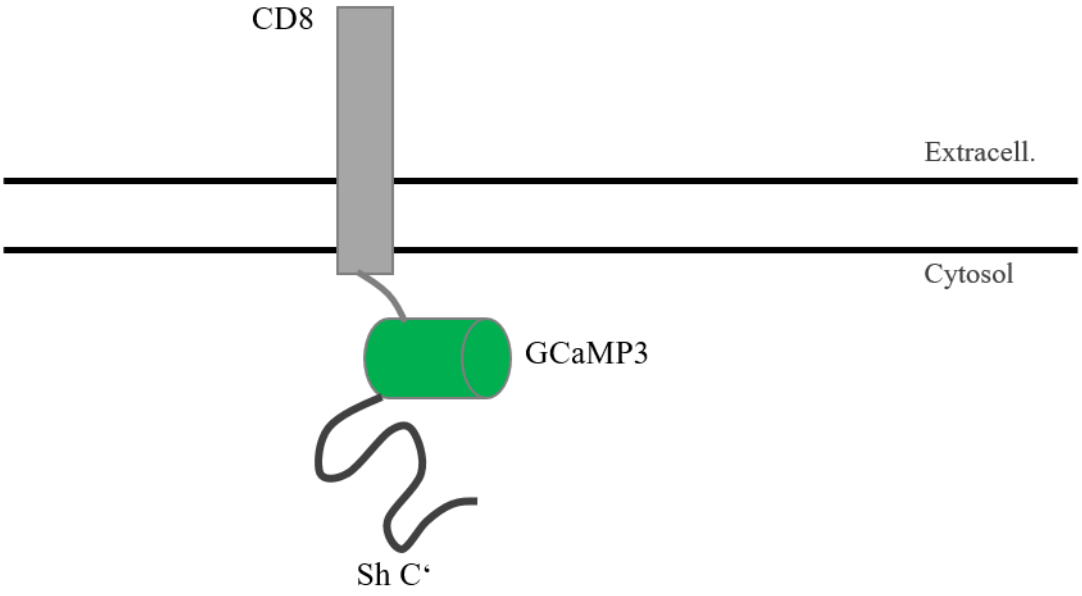

Figure 13: **Postsynaptic GCaMP3 construct MHC-CD8-SynapGCaMP3-Sh.** GCaMP3 is coupled to the membrane anchor protein CD8 and to the PDZ domain of the K^+ channel Shaker. The PDZ domain interacts with the PDZ protein disc large which localizes to the subsynaptic reticulum surrounding boutons. Expression in muscle is driven by the promotor myosin heavy chain (MHC) (adapted from Guerrero et al. 2005).

To test if the MHC-CD8-SynapGCaMP3-Sh construct does also recognize Ca^{2+} influx through postsynaptic DmCa1D channels we directly injected current into larval crawling muscle 6 with a sharp glass electrode. This will prevent Ca^{2+} influx through postsynaptic glutamate receptors but will lead to opening of voltage-gated DmCa1D channels localized to the muscle membrane.

Table 10: Electrophysiological setup

Microscope	Axioskop 2 FS plus	Zeiss (Germany)
Micromanipulator	HS-2A Headstage (x0.1 LU gain)	Molecular devices Axon Instruments (USA)
Amplifier	Axopatch 200B	Molecular devices Axon Instruments (USA)
Digitizer	Digidata 1322A	Molecular devices Axon Instruments (USA)
Electrode puller	Flaming/Brown Puller Model P-97	Sutter Instrument Company (USA)

Borosilicate glass microelectrodes with filament (OD 1 mm, ID 0.5 mm; Molecular devices Sutter Instrument USA) were pulled in an electrode puller with the settings: heat 495, pull strength 55, velocity 75, delay 80 and air pressure 400, to generate sharp electrodes.

Third instar larvae of the wildtype strain Canton S were dissected as described above 2.2.1. To stimulate muscle 6 on a setup (Table 10) we inserted a sharp glass electrode filled with 2M KAc into the larval crawling muscle. Samples yielding a membrane potential above -60 mV were discarded. Every 10 seconds a short current pulse of 2 nA was injected into muscle 6, using the Axopatch amplifier, while Ca^{2+} induced changes in fluorescence were imaged with a Hamamatsu digital camera C4742-95 and the image acquisition software Simple PCI 6. ΔF/F was analyzed using Simple PCI 6.

Normal saline: NaCl 128 mM; KCl 2 mM; $MgCl_2$ 4 mM; $CaCl_2$ 1.8 mM; HEPES 5 mM; Sucrose 37 mM → pH 7,24 (NaOH) 300-310 mOsmol

3 Results

To investigate the DmCa1D channel we used the well characterized larval motoneurons aCC and RP2 as well as the terminals on muscle 6 and 7 formed by MN6/7-Ib (RP3). An RP2 motoneuron consists out of four main compartments (Figure 14): the soma containing the nucleus (1) the primary neurite from which the dendritic tree emerges (2) and then the axon (3) that projects onto the larval crawling muscles, thereby forming synaptic terminals (4).

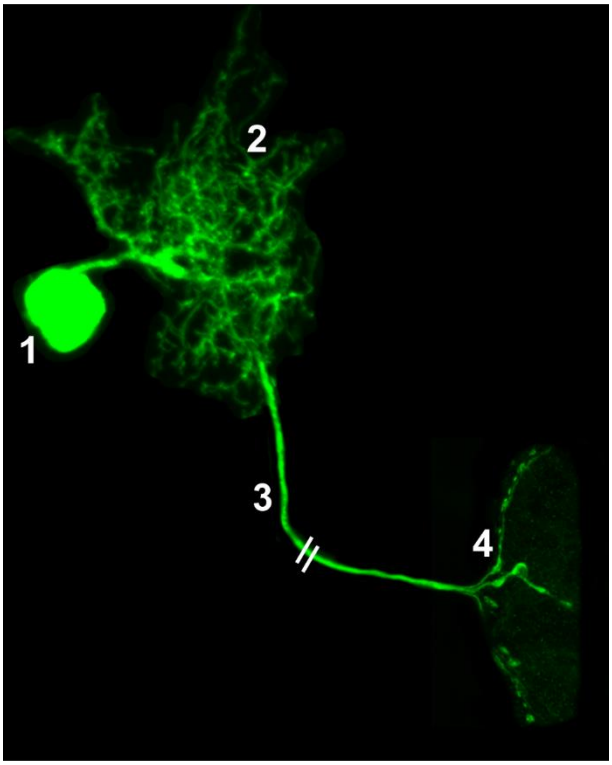

Figure 14: **Compartments of a GFP positive larval RP2 motoneuron with modified scales.** Starting from the soma (1) embedded in the VNC, the primary neurite shows a great dendritic tree (2). The axon (3) then projects onto a larval crawling muscle, thereby forming neuromuscular synaptic terminals (4).

3.1 Proof of DmCa1D antibody specificity

In my previous work I studied DmCa1D localization in *Drosophila* larval motoneurons aCC and RP2. Former studies could indirectly proof presence of DmCa1D in those neurons by patch clamp experiments. A hypomorphic mutant DmCa1D^{AR66} and an RNAi-knockdown of the protein resulted in a significant reduction of somatodendritic L-type current (Worrell & Levine 2008). The localization of DmCa1D channels in motoneurons was determined by immunocytochemistry. A human pan α-N-type Ca^{2+} α-1B polyclonal antibody was published to recognize DmCa1A channels in *Drosophila* (Astorga et al. 2012). We showed specificity of that antibody for DmCa1D channels by multiple means: First, immunocytochemistry

experiments showed antibody staining in the sarcomeric structure of larval crawling muscles (Figure 15B) and already hinted towards the DmCa1D channel, which mediates Ca^{2+} influx in *Drosophila* muscles (Ren et al. 1998; Eberl et al. 1998). Second, the western blots: Proof of antibody specificity was brought forward with a western blot of adult brain homogenate. Figure 15A shows western blot results with the potential DmCa1D antibody and an α-GFP antibody. Since embryonic tissue generated too much unspecific binding, we used a homogenate of 10 adult brains per lane. Because of embryonic lethality of DmCa1D null mutants (*DmCa1D*^{X10}) we were forced to circumvent that proof of principle. Sequence analysis of the antibody yielded the three VGCCs in *Drosophila*: DmCa1A, DmCa1D, and Dmα1G as possible binding proteins (Santa Cruz Biotechnology, Santa Cruz USA). In wildtype control flies from the strain Canton S (lane 1) a single band at around 275 kDa appeared, which corresponds to the predicted weight of DmCa1D of 276.4 kDa (Zheng et al., 1995). To exclude DmCa1A as recognition target of the antibody we used DmCa1A null mutants *cac*^{HC129} and pan-neuronally expressed (elav^{C155}-Gal4) the cloned splice variant cac1 of DmCa1A (Kawasaki et al. 2002) with an enhanced-GFP tag (UAS-cac1-eGFP). This tag can be recognized by an α-GFP antibody (lane 2 and 4). When incubated with the α-DmCa1D antibody, the same single band, as in the control, at around 275 kDa appeared (lane 2). Application of an α-GFP antibody on the same sample resulted in a broad signal between 205-240 kDa (lane 4), which does not occur in Canton S controls (lane 5). Therefore, DmCa1A clearly yields a band at a different size than the one detected with the α-DmCa1D antibody. In case of the Dmα1G channel we used the published null mutant *ΔDmα1G*, since homozygous flies reach adulthood (Ryglewski et al. 2012). Again, in animals without any 1G protein, the DmCa1D antibody detected one single band at 275 kDa, thus showing that the antibody does not detect Dmα1G channels. Third, we did immunocytochemistry in larval motoneuron somas of genetic mosaics expressing DmCa1D RNAi knockdown or *DmCa1D*^{X10} MARCM knockout (Figure 16). We expressed the short hairpin RNAi-construct under control of the RN2-GAL4,UAS-FLP driver (D-F). RNAi expressing cells are also GFP positive. RP2 and aCC motoneurons, which do not express RNAi and GFP, served as internal controls. As additional control for potential effects of GFP on DmCa1D expression, RN2-GAL4,UAS-FLP was crossed to w^{1118}. In the control, one out of three MN somata is labeled with GFP (A-C), but they all show similar DmCa1D staining intensities (B). By contrast, in genetic mosaics, RNAi and GFP expressing MNs (D-F) show a weaker DmCa1D signal in comparison to internal non-GFP labeled control motoneurons (E). We used the MARCM technique to generate homozygous *DmCa1D*^{X10} null mutant motoneurons in heterozygous animals (G-I). Homozygous null mutant motoneurons are GFP

positive (H). GFP negative motoneurons served as internal controls (I). In comparison to internal control motoneurons, The GFP positive null mutant motoneuron show no DmCa1D staining in the soma (G-I). These results proof that the human pan α-N-type Ca^{2+} α-1B polyclonal antibody specifically recognizes DmCa1D channels in *Drosophila*.

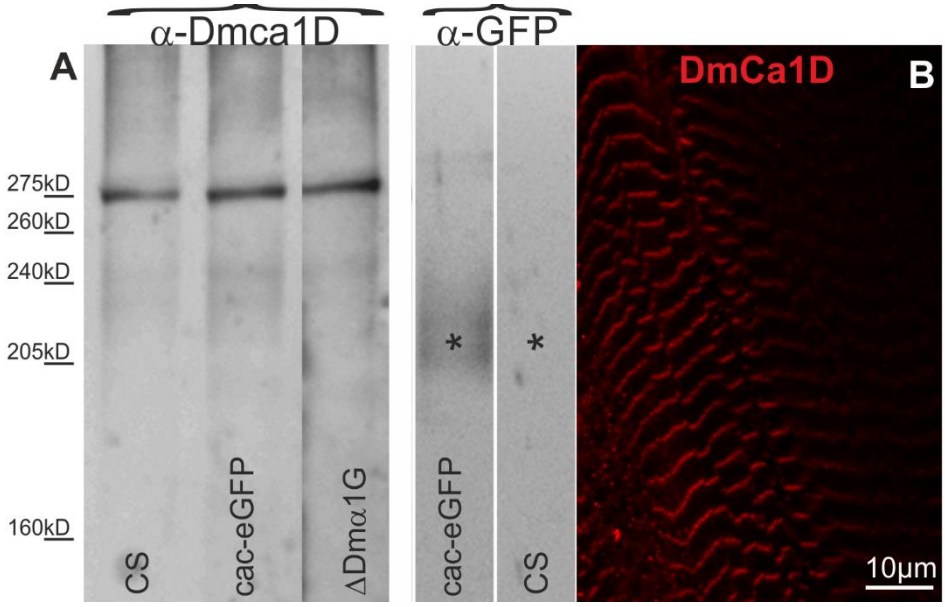

Figure 15: **Proof of α-DmCa1D antibody specificity in western blot and immunocytochemistry of muscle.** Each pocket was loaded with a homogenate of 10 brains. **A** Western blotting with α-DmCa1D of Canton S controls, DmCa1A (Cac) null mutants with pan-neuronal expression of cac1-eGFP and *Dmα1G* null mutants show a single band at around 275 kDa, which corresponds to the predicted weight of the DmCa1D channel (276.4 kDa, Zheng et al. 1995). Western blotting with α-GFP of DmCa1A (Cac) null mutants with pan-neuronal expression of cac1-eGFP shows a broad signal at around 220 kDa, which is not present in Canton S controls. The predicted size of cac1-eGFP is 239 kDa (Kawasaki et al. 2002). **B** Immunostaining of larval body wall muscle with the DmCa1D antibody labels the sarcomeric structure of the muscle.

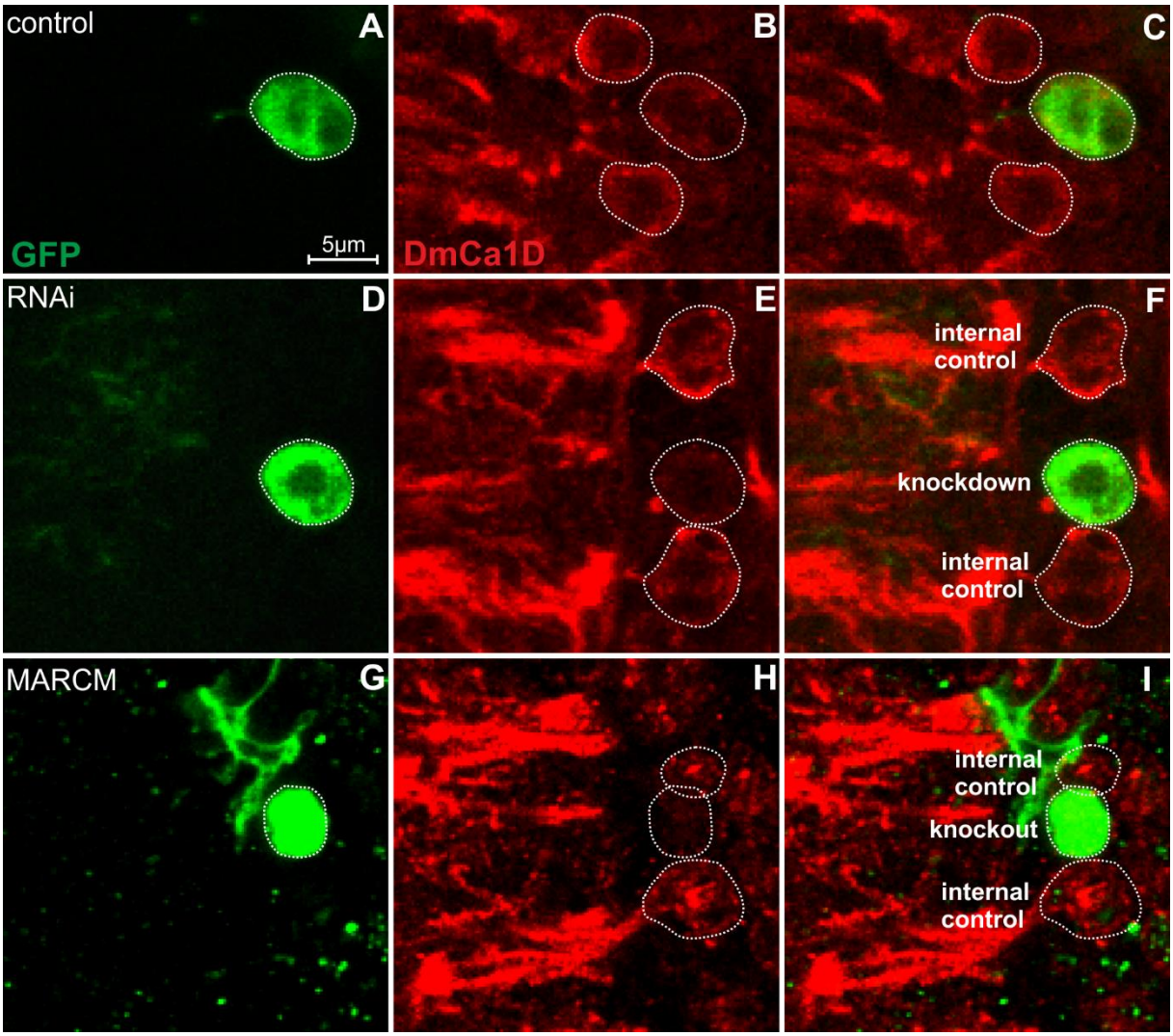

Figure 16: **Reduced DmCa1D staining in larval motoneurons expressing DmCa1D RNAi knockdown and no DmCa1D staining in DmCa1D MARCM knockout larval motoneurons.** Double-staining of the larval ventral nerve cord (VNC) with α-GFP (green) and α-DmCa1D (red). Single sections. **A-C** GFP is expressed under control of RN2-GAL4,UAS-FLP as control. Magnification of three motoneurons stained with α-GFP and α-DmCa1D. The three MNs show similar DmCa1D staining intensities **D-F** Larval motoneurons (RN2-GAL4,UAS-FLP) expressing DmCa1D-RNAi knockdown and GFP. DmCa1D staining is reduced in the RNAi and GFP positive MN. **G-I** DmCa1D MARCM knockout positive motoneurons are GFP-labeled. The DmCa1D knockout and GFP positive MN shows no DmCa1D staining in comparison to internal controls.

Immunocytochemistry with the α-DmCa1D antibody revealed DmCa1D localization in aCC and RP2 motoneurons. In Figure 17 the ventral nerve cord (VNC) of a third instar larva is stained with α-GFP (green), α -Bruchpilot (blue) and α- DmCa1D (red). GFP is expressed under control of the larval motoneuron driver RRA-GAL4. The active zone marker Bruchpilot labels every synapse in the neuropil. DmCa1D localizes to the somata of larval motoneurons aCC and RP2 (Figure 17C). DmCa1D label can be seen in tracts and commissures within the VNC, thus indicating axonal localization. In addition to that, motoneuron axons emerging from the VNC in bundles show DmCa1D staining (arrowhead Figure 17C). Presence of the DmCa1D in

motoneuron axons could either be caused by functional L-type calcium channels in the axonal membrane, or alternatively, by DmCa1D channel transport along the axon to synaptic terminals.

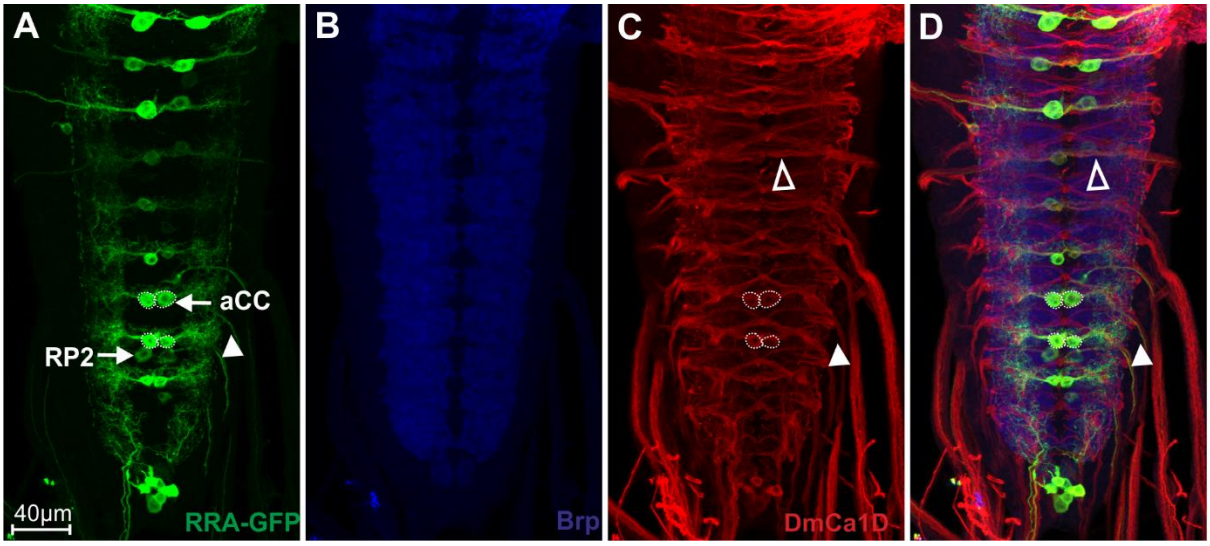

Figure 17: **α-DmCa1D staining in larval aCC and RP2 motoneurons to somata and axons.** VNC of the larval genotype RRA-GAL4-GFP stained with α-GFP (green), α-Bruchpilot (blue) and α-DmCa1D (red). Projection of 25 slices. **A** GFP is labeled in larval motoneurons aCC and RP2 including soma, dendrites and axons. **B** The active zone marker Bruchpilot stains every synapse of the neuropil. **C** DmCa1D staining reveals motoneuron somata (dotted circles) and axons (arrowheads). Tracts and commisures within the VNC are also labeled (empty arrowheads). **D** Overlay of all three stainings.

These possibilities were further analyzed by Ca^{2+} imaging experiments. In collaboration with Dr. Carsten Duch, we showed activity dependent Ca^{2+} influx into motoneuron axons, thus indicating functional DmCa1D channels in the axonal membrane. Initiating single action potentials in a GCaMP6f (Chen et al. 2013) expressing RP2 motoneuron by extracellular stimulation of the nerve with a suction electrode causes axonal Ca^{2+} influx. A single action potential is sufficient to increase the axonal Ca^{2+} concentration by 4 % (Figure 18), the intra-axonal calcium responses increase with the number of action potentials at a stimulation frequency of 80 Hz, and it saturates at 5 action potentials at about 10% increase (Figure 18). These data clearly demonstrate that DmCa1D channels localize to the axonal membrane of motoneurons and mediate Ca^{2+} influx into axons upon single action potentials. The function of axonal DmCa1D channels is discussed in 4.1.

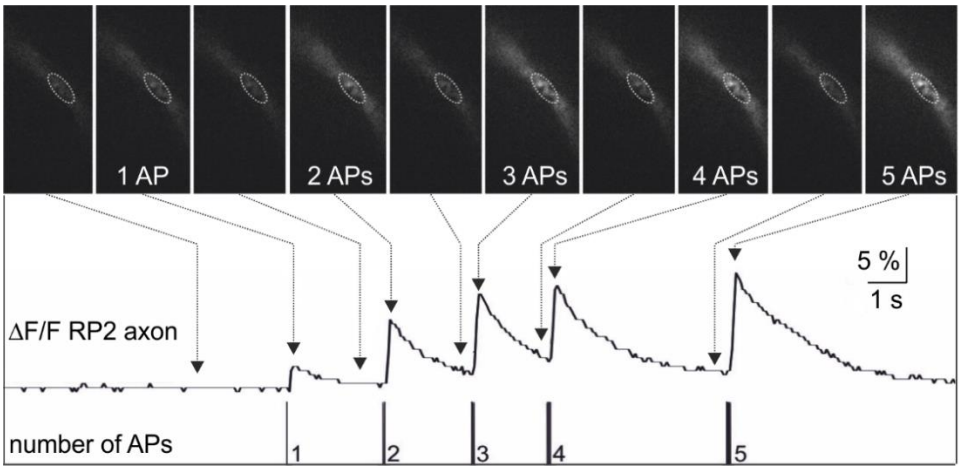

Figure 18: **Action potential-induced calcium signals in an RP2 motoneuron axon.** The upper row shows Ca^{2+} imaging of an axon stimulated with action potentials (1-5 APs). Mean grey was measured in the encircled areas. The more action potentials, the more increases ΔF/F (Ref. Carsten Duch).

Selective enlargements of the DmCa1D staining in the VNC indicated additional DmCa1D channel localization to dendrites of aCC and RP2 motoneurons (Figure 19). DmCa1D doesn't localize to the entire dendritic tree, but appears to be clustered to patches of dendritic membrane regions. The dendritic function of DmCa1D in *Drosophila* motoneurons was further studied in collaboration with Drs. Kadas, Ryglewski, Worrell, and Duch. We found that dendritic DmCa1D channels amplify synaptic drive to motoneuron dendrites, a function that is reminiscent to that of dendritic L-type calcium channels in vertebrate spinal motoneurons (Heckmann et al. 2003). A respective manuscript is in preparation, but given the large number of contributing authors, this thesis will focus on the axonal and presynaptic function of Dmca1D channels.

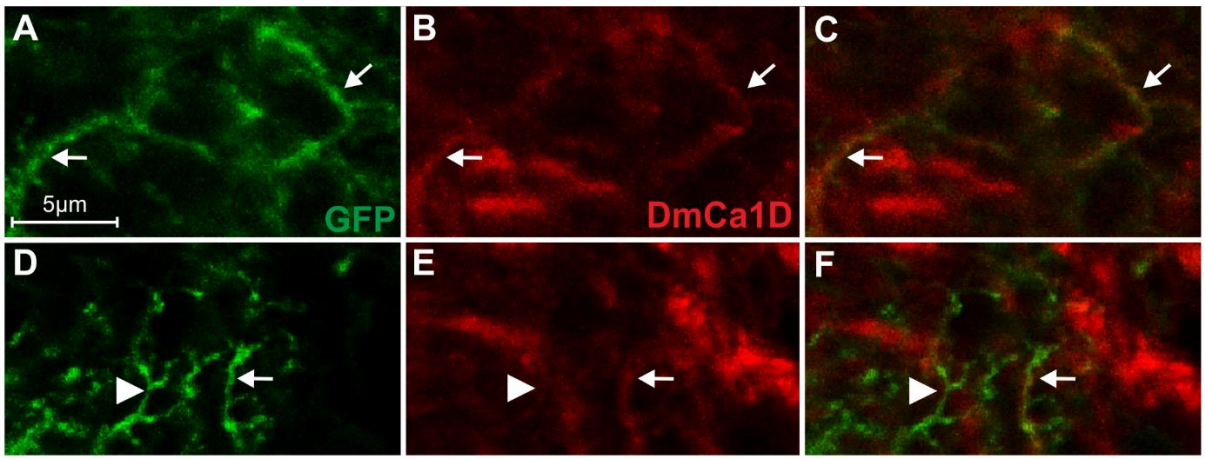

Figure 19: **DmCa1D shows clustered localization to dendrites of larval aCC and RP2 motoneurons.** RRA-GAL4-GFP larval ventral nerve cord (VNC) with magnification of two dendritic trees **A-C** and **D-F**, stained with α-GFP (green) and α-DmCa1D (red). Single sections. In **A** and **D** GFP labels dendrites of larval motoneurons. **B** and **E** DmCa1D staining is present in certain dendritic branches (arrows) but also lacks in many aborizations (arrowhead). **C** and **F** Overlay of the two stainings shows overlap of GFP and DmCa1D, indicated by arrows.

3.2 Presynaptic localization of DmCa1D

By following DmCa1D staining along the axon we discovered the channel at presynaptic terminals on larval crawling muscles (Figure 20). Because of DmCa1D label in the axon, at terminals and in muscles it is hard to distinguish the different compartments.

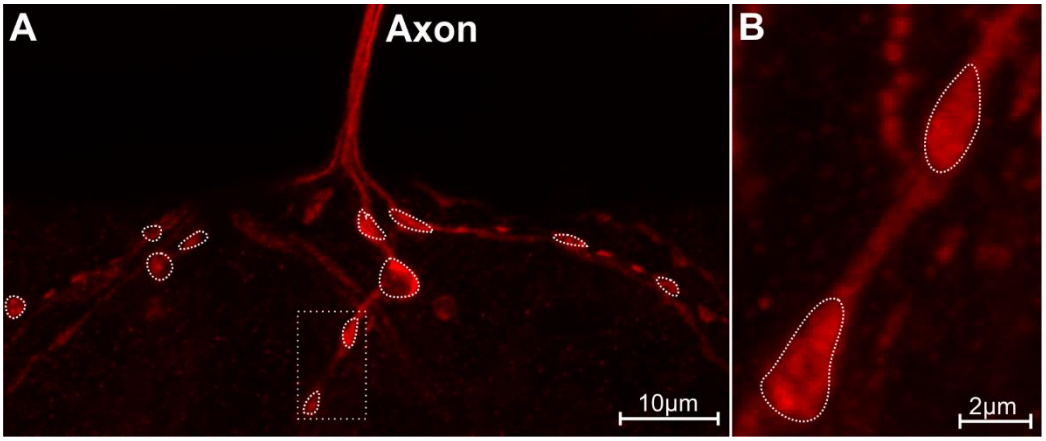

Figure 20: **DmCa1D seems to localize at synaptic terminals of larval aCC and RP2 motoneurons. A** The axon projects onto a larval crawling muscle thereby forming synaptic terminals (encircled). **B** Magnification of the dotted square in **A** shows DmCa1D antibody label at the presynapse of synaptic terminals.

To proof that DmCa1D channels localize to synaptic terminals, we co-labeled DmCa1D with synaptic markers: The vesicle-bound protein Synaptotagmin and the active zone marker Bruchpilot (Figure 21). Synaptic vesicles (SVs) accompanied by Synaptotagmin are situated throughout the entire terminal in the reserve and recycling pool, at active zones ready to release and at the periactive zone undergoing endocytosis. Because the antibodies against Bruchpilot and Synaptotagmin share the same host (mouse), a tagged Bruchpilot-short construct served as active zone marker in co-stainings. The construct is a short part of the Bruchpilot protein, which localizes naturally at the active zone to endogenous Bruchpilot proteins. It also carries an mStrawberry-tag, which is visible in red wavelength (Schmid et al. 2008; Fouquet et al. 2009). Staining of DmCa1D (red) with Synaptotagmin (green) and the tagged Bruchpilot-short (blue) construct show that DmCa1D localizes to presynaptic terminals. Synaptotagmin occasionally co-localizes with Bruchpilot (Figure 21C+E) and DmCa1D (Figure 21E+K). Because Synaptotagmin is a vesicle bound protein, it localizes to active and periactive zones. Vesicles undergo exocytosis at active zones labeled by Bruchpilot and they are retrieved at the periactive zone.

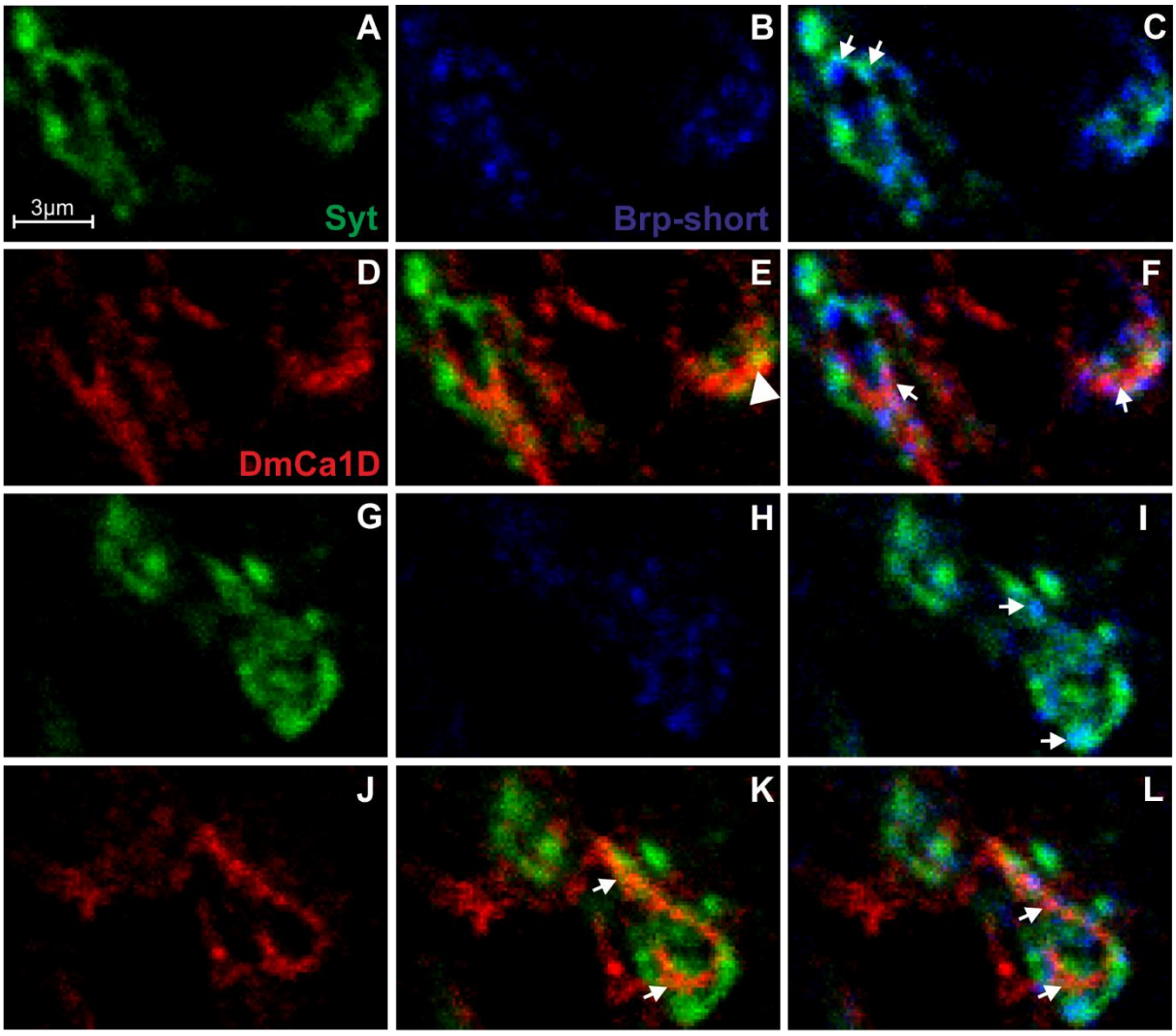

Figure 21: **DmCa1D channels localize to synaptic terminals of larval aCC and RP2 motoneurons.** Triple staining of NMJ boutons with α-Synaptotagmin (green), Bruchpilot-short Strawberry (blue) and α-DmCa1D (red) in single sections. **A-F** and **G-L** show one section respectively with Synaptotagmin (**A+G**), Bruchpilot (**B+H**) and DmCa1D (**D+J**). Arrows in **C** and **I** indicate partially overlapping of Synaptotagmin and Bruchpilot. Synaptotagmin and DmCa1D in **E** and **K** show nearly no co-localization at all (arrows) beside the arrowhead in **E**. All three stainings in **F** and **L** show sparse overlap (arrows in **L**). Arrows in **F** show partial overlap of Bruchpilot and Synaptotagmin.

We could show that DmCa1D channels localize to the presynaptic membrane of synaptic terminals. To further reveal the subsynaptic localization of DmCa1D we used several different antibodies against proteins of specific regions at the presynapse. The T-bar forming CAZ protein Bruchpilot and the SV release-mediating calcium channel DmCa1A (Cacophony) served as active zone markers. Fasciclin II and Endophilin are proteins of the periactive zone. To show DmCa1A localization we used the cac1-eGFP construct (Kawasaki et al. 2002), which is one single splice variant of the protein with an eGFP-tag. Because the antibodies against

Bruchpilot and Fasciclin II share the same host mouse, a tagged Bruchpilot-short construct served as active zone marker in co-stainings.

3.2.1 Active zone

The most famous and commonly used active zone marker in *Drosophila* is the CAZ-associated protein Bruchpilot. As mentioned before (1.8), Bruchpilot is essential for T-bar formation at active zones, which enables coupling of SVs and VGCCs DmCa1A (Kittel et al. 2006 a+b). The antibody nc82 binds to the C-terminus of the Bruchpilot protein (Wagh et al. 2006). Stainings with nc82 (blue) and α-DmCa1D (red) of synaptic boutons (Figure 22) show an alternating pattern of the two proteins (arrows in C and F) at the terminal. Little overlap is indicated by arrowheads in C and F. Images show single slices with ~ 1µm thickness.

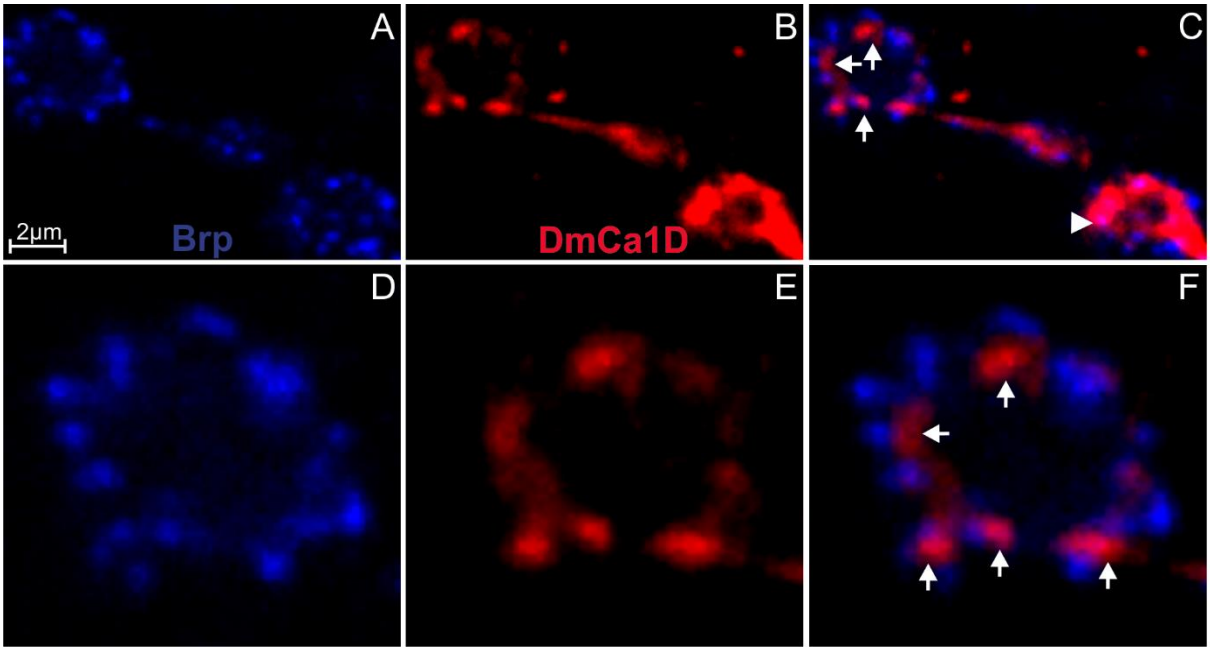

Figure 22: **DmCa1D channels do not localize to the active zone, labeled by Bruchpilot.** Synaptic terminals stained with the known active zone marker Bruchpilot (blue) and DmCa1D (red). **A-C** and **D-F** show single slices. **D-F** Magnification of the left bouton. **A+D** Bruchpilot staining labels active zones of synaptic boutons. **B+E** DmCa1D staining at the terminal. **C+F** Overlay of Bruchpilot and DmCa1D stainings. Bruchpilot and DmCa1D show alternating patterns (arrows). DmCa1D localizes to axon and terminals, thereby also overlaps with Bruchpilot staining (arrowheads).

In the center of T-bar formations at active zones DmCa1A (Cacophony) channels are localized to mediate Ca^{2+} influx which triggers fusion of docked SVs with the presynaptic membrane to release neurotransmitters into the synaptic cleft (Fouquet et al. 2009; Liu et al. 2011; Maglione & Sigrist 2013). Again, we made use of the available UAS-cac1-eGFP construct (Kawasaki et

al. 2002) and drove expression under the pan-neuronal driver elav^{C155} in a null mutant background (*cac*^{HC129}). Live imaging revealed the typical dotted pattern of active zones in synaptic boutons (Figure 23A). DmCa1A (green) and DmCa1D (red) show no co-localization (arrows in Figure 23C) after a shortened immuno-protocol. DmCa1D yields a linear structure along the terminal branch in Figure 23B and C. However, when the immunocytochemistry protocol was performed as in 2.2.3, cac1-eGFP staining intensity decreased and more broad labels appeared instead of typical active zone circles (Figure 23D-F). Nonetheless, DmCa1A and DmCa1D co-stainings yield nearly no overlap (Figure 23F).

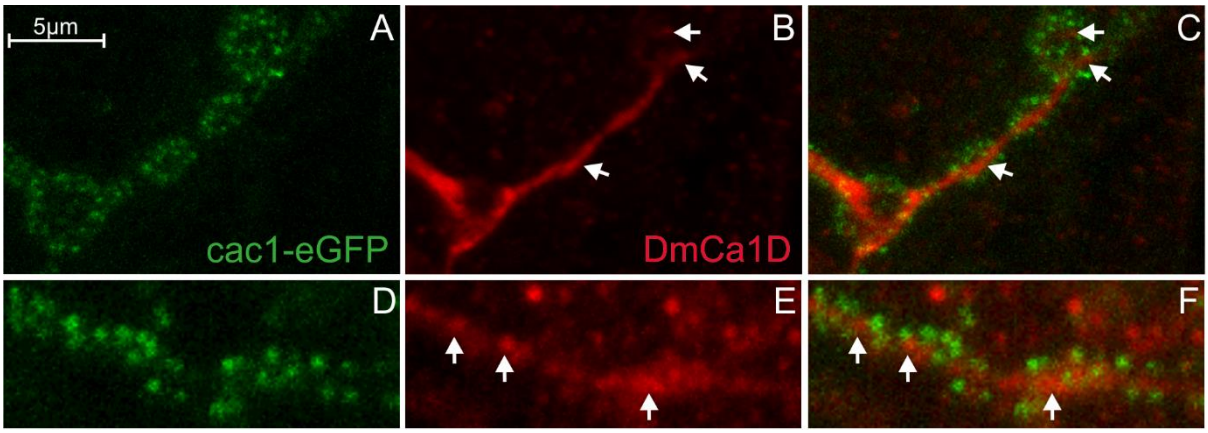

Figure 23: **DmCa1D channels do not localize to the active zone, labeled by DmCa1A.** Synaptic terminals stained with the DmCa1A/Cacophony construct cac1 (green) and DmCa1D (red). **A+D** Cac1-eGFP expressed under a pan-neuronal driver in a DmCa1A null mutant (*cac*^{HC129}) background. **A-C** show cac1-eGFP live and α-DmCa1D staining in a stack of 4 slices. **D-F** demonstrate α-GFP (green) and α-DmCa1D (red) in a stack of 10 slices. In **C** DmCa1D staining is linear-like and follows through all boutons. Arrows show no overlap of GFP and DmCa1D stainings in **C** and **F**.

3.2.2 Periactive zone

The DmCa1D channel doesn't seem to be localized at the highly specialized active zones in synaptic terminals. Hence, it localizes to the AZ surrounding area at synaptic boutons called the periactive zone. We used two published periactive zone markers to reveal DmCa1D localization within the periactive zone: Endophilin and Fasciclin II. Fasciclin II (Fas II) is a homophilic cell adhesion molecule which is localized pre- and postsynaptically and has an important function in synapse growth and stabilization (Harrelson & Goodman 1988; Grenningloh et al. 1991; Schuster et al. 1996). Furthermore, it could be shown that Fas II localizes to the periactive zone. Thereby, it does not substantially co-localize with the endocytic machinery including Dynamin, Endophilin and Dap 160 (Marie et al. 2004). To compare the localizations of Fas II (green) and DmCa1D (red) we did immunocytochemistry together with

α-Bruchpilot (blue) to distinguish the active zone (Figure 24). The overlay of Fas II and Brp in Figure 24C shows an alternating pattern of the two stainings (arrows). DmCa1D and Fas II show distinct localizations (arrows) or overlaps at some sites (Figure 24 arrowheads). This confirms that Fas II does not localize to active zones labeled with Bruchpilot. DmCa1D does not co-localize with Fas II at the periactive zone (Figure 24E).

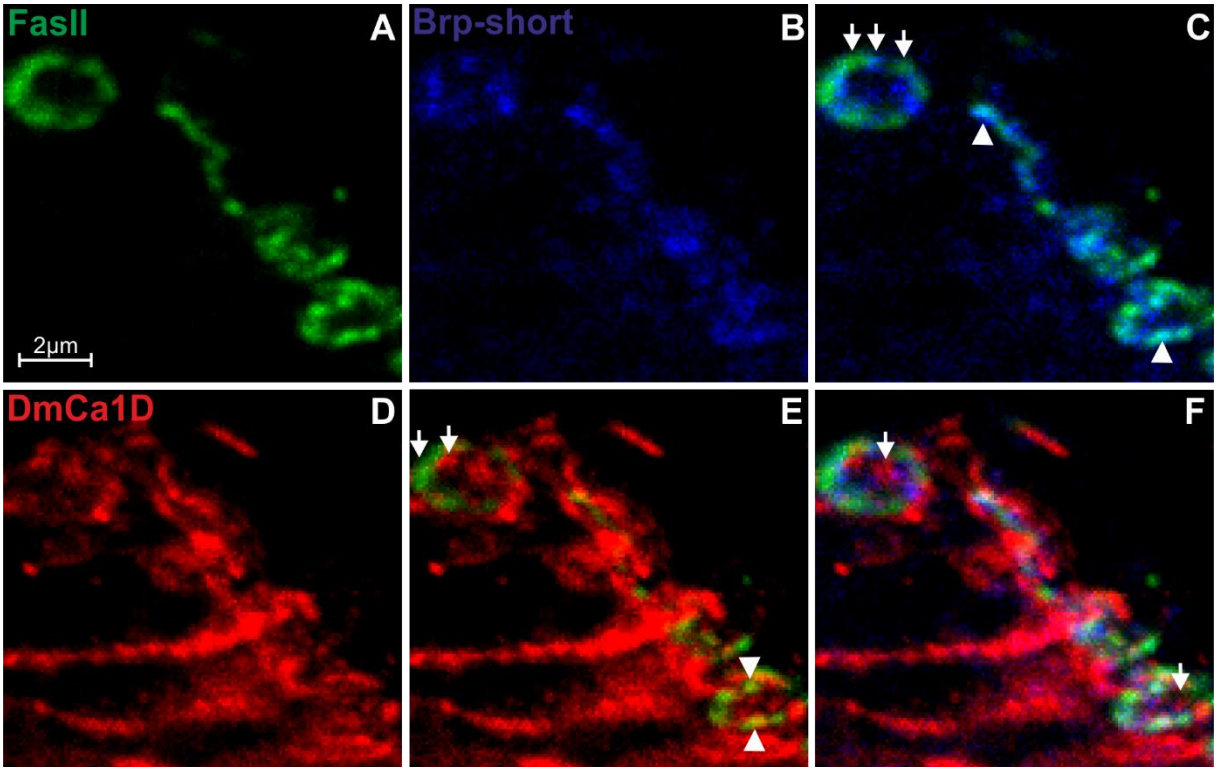

Figure 24: **DmCa1D staining does not co-localize with Fasciclin II at the periactive zone.** Synaptic terminals stained with **(A)** the periactive zone marker Fasciclin II (green), **(B)** the active zone marker Bruchpilot-short (blue) and **(D)** DmCa1D (red). Single slice. In **C** arrows indicate an alternating pattern of α-Bruchpilot and α-Fasciclin II (Fas II) with single sites of little overlap (arrowheads). There is no overlap of DmCa1D and Fas II in **E** indicated by arrows and partial overlap is shown with arrowheads. All three stainings in **F** show mainly distinct localizations (arrows).

In earlier stainings of Fas II (green) and DmCa1D (red) without α-Bruchpilot we observed less background staining regarding DmCa1D (Figure 25). These data reveal Fas II and DmCa1D stainings more accurately and show that the two proteins localize in close proximity to each other with partial overlap at the edges (Figure 25C and F arrowheads). Over time we faced several problems concerning microscope hardware and antibody purity which couldn't be solved so far.

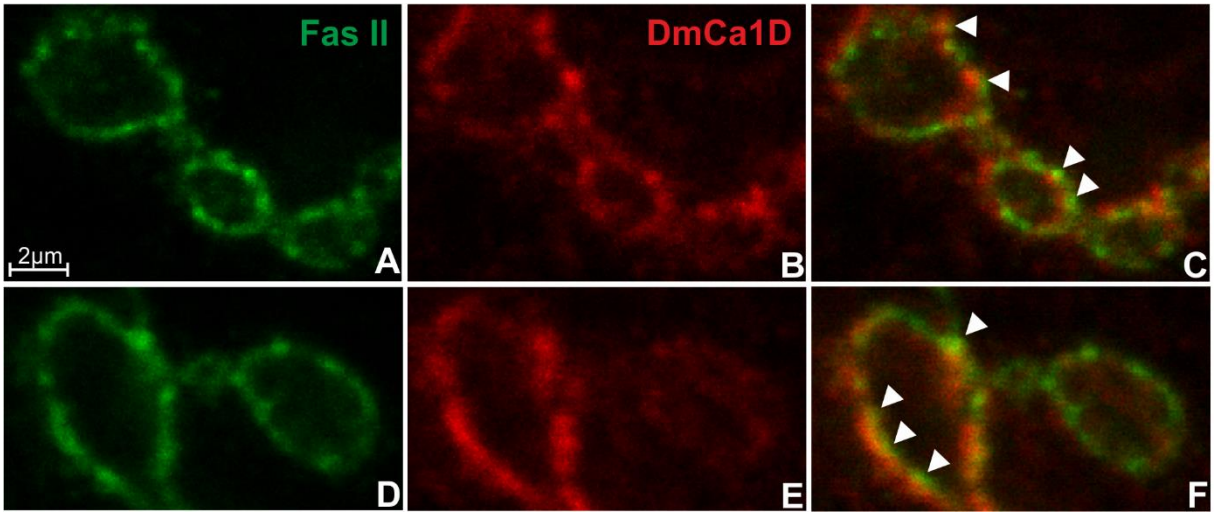

Figure 25: **DmCa1D staining localizes closely to Fasciclin II at the periactive zone.** Double staining of synaptic terminals with α-Fasciclin II (green) and α-DmCa1D (red). **A-C** and **D-F** respectively display different single sections. Fas II staining is shown in **A** and **D** , DmCa1D in **B** and **E**. Merges of both antibodies in **C** and **F** reveal close proximity and partial overlap of Fas II and DmCa1D (arrowheads).

The second periactive zone protein we used as marker is Endophilin. Endophilin is part of the endocytic machinery containing an SH3 and an enzymatic domain (Schmidt et al. 1999). It is involved in membrane bending and it interacts with Dynamin (Micheva et al. 1997; Ringstad et al. 1999; Dickman et al. 2005). Loss of Endophilin leads to elimination of clathrin-mediated endocytosis (Verstreken et al. 2002). An antibody against Endophilin was kindly provided by the Bellen lab (BCM Houston). First, we stained only Endophilin (green) and Bruchpilot (Brp-short construct) (blue) to compare the results with published data (Verstreken et al. 2002; Marie et al. 2004). Stainings of Endophilin and Bruchpilot show no overlap (Figure 26A-C) at synaptic terminals. Endophilin covers the whole periactive zone, and the active zone marker Bruchpilot labels within the gaps of the Endophilin label (Figure 26D-F). This contradicts former studies which showed that Endophilin localizes to specific areas within the periactive zone (Marie et al. 2004).

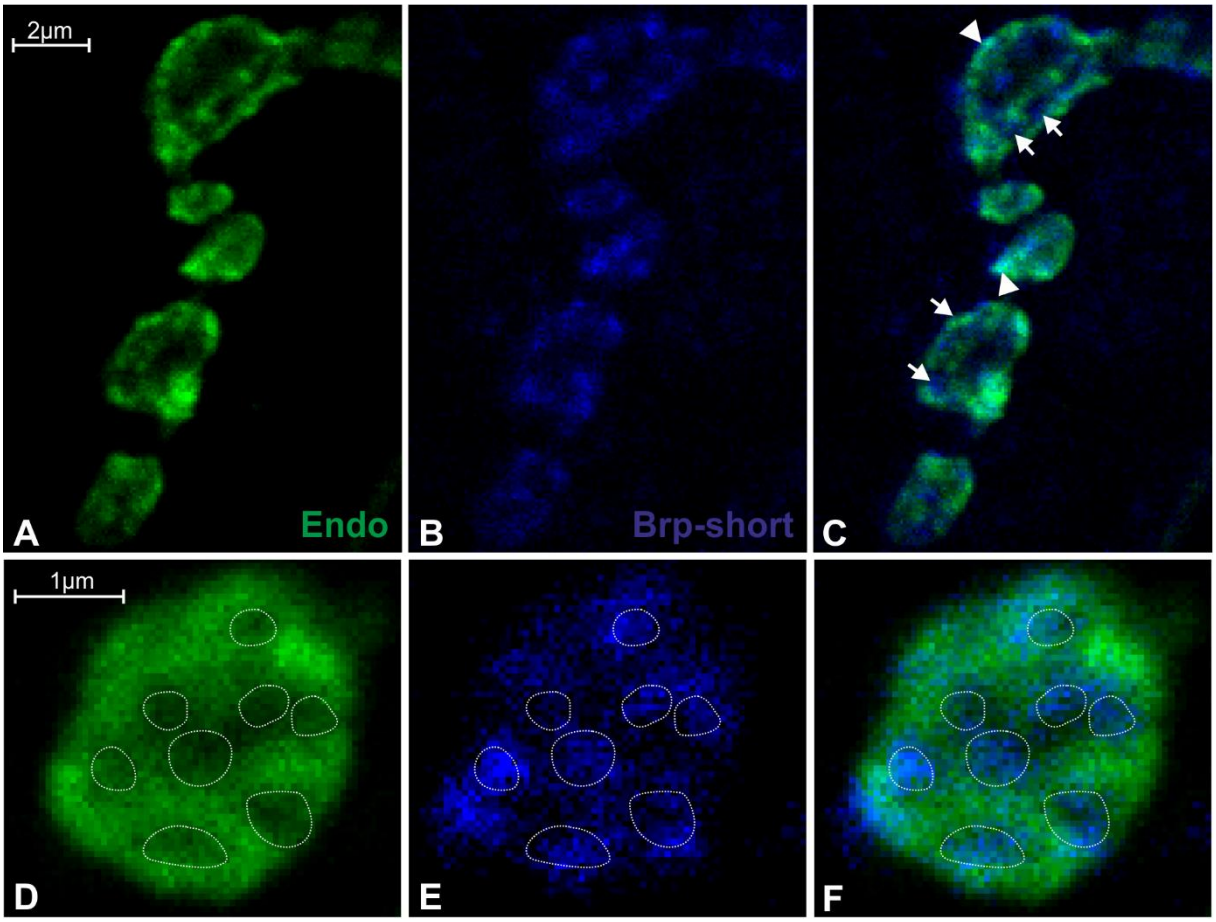

Figure 26: **Endophilin labels the whole periactive zone while Bruchpilot labels active zones.** Periactive zone marker Endophilin (green) and active zone marker Bruchpilot-short (blue) at terminals of the NMJ. **A-C** and **D-F** are different single sections. α-Endophilin staining is shown in **A** and **D**, Bruchpilot staining in **B** and **E**. Arrows in the antibody merge in **C** indicate distinct localizations of Endophilin and Bruchpilot. Arrowheads show partial overlap. Encircled staining-free areas of the Endophilin antibody at the bouton in **D** are filled with Bruchpilot staining (**E and F**).

In Figure 27 we stained Endophilin (green), Bruchpilot (blue) and DmCa1D (red). Again, Endophilin and Bruchpilot show little to no overlap (Figure 27C and I). DmCa1D staining yields much background (Figure 27A-F) which makes it difficult to differentiate between specific and unspecific antibody staining. DmCa1D mainly does not overlap with either Endophilin (E) or Bruchpilot (F) (arrows) except of single overlapping sites (arrowheads). In G-L DmCa1D label is more distinct and shows no overlap with Bruchpilot (L). Endophilin yields a similar staining pattern as DmCa1D (L) with Bruchpilot (I). The overlay of DmCa1D and Endophilin (K) reveals that the similar patterns only overlap at the edges of both antibody labels. Consequently, DmCa1D channels localize to the periactive zone of synaptic terminals in close proximity, with partial overlap, to Endophilin, which is part of the endocytic machinery.

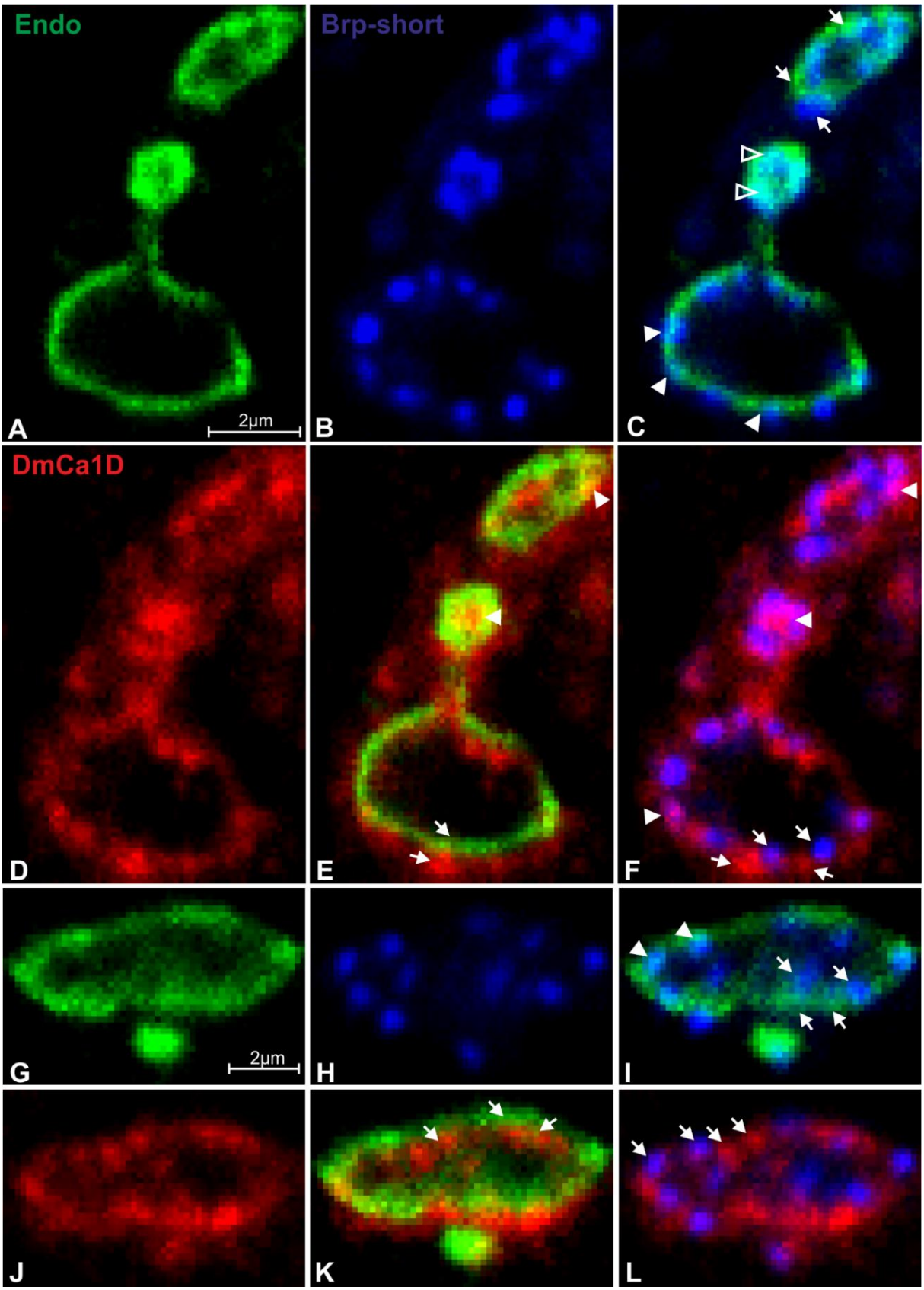

Figure 27: **DmCa1D channels localize to the periactive zone and show partial overlap with Endophilin.** Triple staining of NMJ synaptic boutons with α-Endophilin (green), Bruchpilot-short (blue) and α-DmCa1D (red). **A-F** and **G-L** are two different single sections. Endophilin (Endo) staining is to be seen in **A** and **G**, Bruchpilot-short (Brp-sh) in **B** and **H**, DmCa1D label in **D** and **J**. Merging of Endo and Brp in **C** and **I** shows an alternating pattern of the two antibodies (arrows). Empty arrowheads in **C** indicate co-localization of Endo and Brp-sh. Arrowheads point at partial overlap of Endo and Brp. Merges of Endo and DmCa1D stainings are shown in **E** and **K**. Antibodies

partially overlap (arrowheads) or are distinct to each other (arrows). **F** and **L** picture the merge of Brp-sh and DmCa1D. The two stainings overlap in some areas (arrowheads) but mainly appear distinct (arrows).

3.3 Genetic tools to probe the function of presynaptic DmCa1D channels in motoneuron terminals

To investigate the function of the DmCa1D channel we used different genetic tools available in *Drosophila* as well as pharmacological substances. A strong knockdown of the channel protein was achieved by using RNAi from the TRiP-line collection (Transgenic RNAi Project). To destroy mRNA these constructs use the endogenous way of microRNAs (Ni et al. 2008; 2009). The UAS-short-hairpin construct appeared to show a strong knockdown when expressed under a strong GAL4 driver (Dimitrios Kadas). Because of the embryonic lethality of the DmCa1D null mutant allele *X10* we generated GFP-labeled mosaic null mutants with the MARCM (mosaic analysis with a repressible cell marker) method to test a complete knockout of the channel protein (Eberl et al. 1998). In an otherwise heterozygous null mutant animal we induced a heterologous recombination during specific time points in development to generate single null mutant cells (Wu et al. 2006). In addition to that the anorganic Ca^{2+} antagonist La^{3+} was used in minor concentrations to block Ca^{2+} influx through DmCa1D channels. La^{3+} and Ca^{2+} ions compete for the negatively charged binding sites whereby La^{3+} displaces Ca^{2+} (Cauvin et al. 1983). Former studies used 40 µM lanthanum to block endocytosis. Because we know its target, the DmCa1D channel, we tested the concentration needed to eliminate postsynaptic potentials (Appendix 6.2). At a concentration of 1 µM La^{3+} evoked postsynaptic potentials were abolished.

3.3.1 RNA interference

To test the effect of the DmCa1D calcium channel in synaptic depression we first tested an RNAi-knockdown of the channel using a Transgenic RNAi Project (TRiP) stock (Ni et al .2008; Perkins et al. 2015). The UAS short-hairpin RNAi construct (HMS00294) was crossed to the RN2-flippase line to generate a genetic mosaic with a strong knockdown, driven under the Actin-GAL4 driver in a subset of RP2 and aCC motoneurons (see methods 2.4). Briefly, if GAL4 is under control of the even-skipped promotor RRA-GAL4 the pattern of larval motoneurons looks like in Figure 28A-C. To obtain a strong knockdown effect in only few aCC and RP2 motoneurons we used the even weaker RN2-GAL4 driver, which is also under control of the even-skipped promotor. Furthermore a UAS-FLP, which is activated in only few random aCC and RP2 cells by RN2-GAL4, cuts out a stop-codon flanked by two FRT-sites from Act-GAL4. This enables the strong driver Act-GAL4 to express the hairpin RNAi and GFP to label

knockdown affected cells (Hartwig et al. 2008) resulting in a mosaic pattern of motoneurons in the VNC (Figure 28D-F).

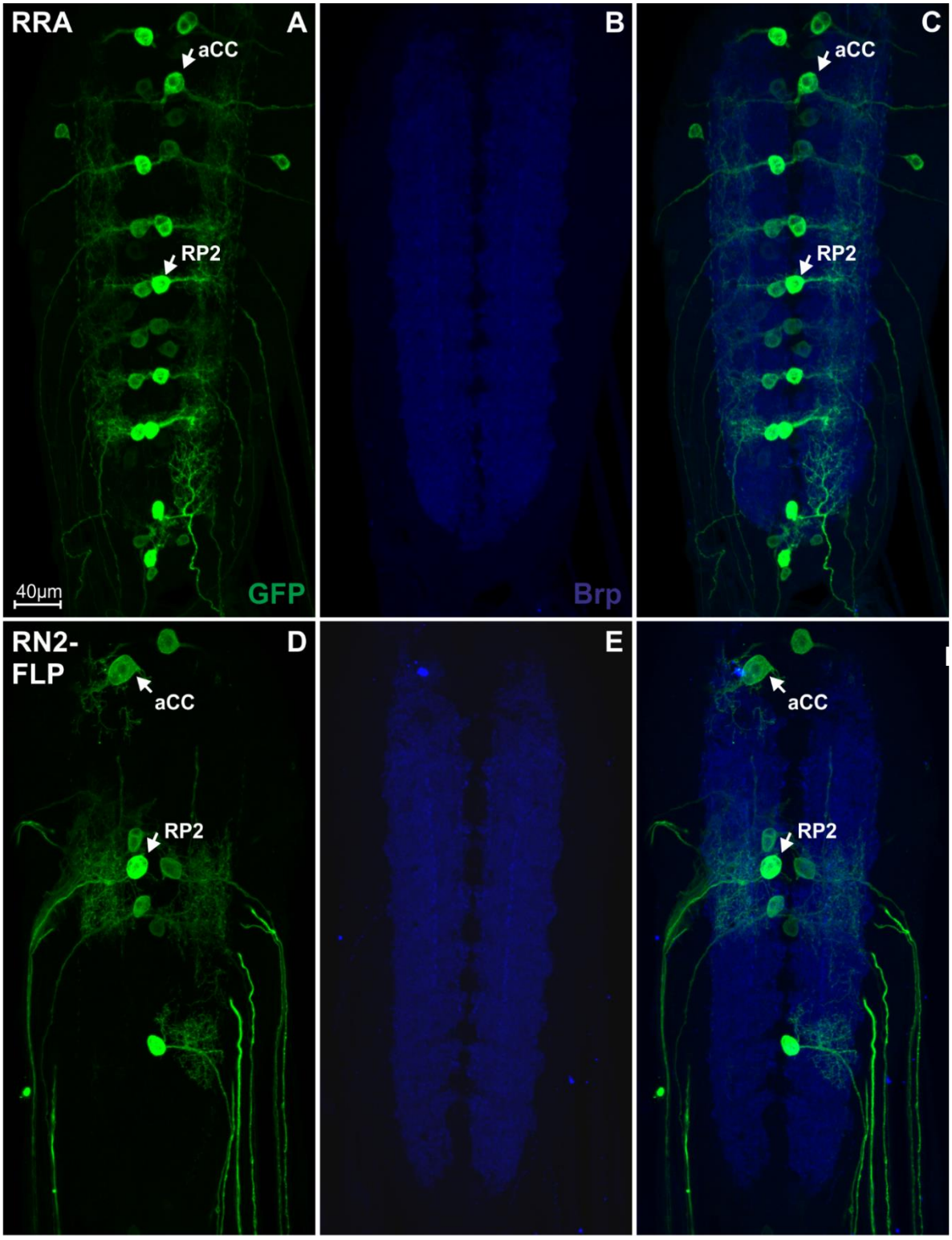

Figure 28: **Genetic mosaic expression pattern of the RN2-GAL4, UAS-FLP driver in larval aCC and RP2 motoneurons.** Ventral nerve cord of third instar larvae labeled with α-GFP (**A+D** green) and α-Bruchpilot (**B+E** blue). **A-C** GFP expression under control of RRA-GAL4 in larval motoneurons aCC and RP2. **D-F** Mosaic expression of GFP with RN2-GAL4, UAS-FLP in only a subset of aCC and RP2 motoneurons.

3.3.1.2 Knockdown-affected synaptic terminals of MNs

We also tested the knockdown efficacy of DmCa1D RNAi directly at neuromuscular junctions of larval crawling muscles by immunocytochemistry (Figure 29). Again, we expressed the short hairpin RNAi-construct under control of the RN2-GAL4,UAS-FLP driver (D-F). Knockdown cells are GFP positive. To unambiguously identify presynaptic terminals we used the active zone marker Bruchpilot. In mosaic control animals and following mosaic RNAi expression we always imaged two nearby Bruchpilot-stained terminals (B, F, J, N), one of each is labeled with GFP and one without (A, E, I, M). The GFP positive terminals originate from RP2 cells which form type Is boutons. The internal control terminal without GFP forms type Ib boutons (Hoang & Chiba 2001). In both terminals of the control (GFP +/-), DmCa1D staining intensities appear equally strong (C). By contrast, following a mosaic RNAi knockdown, the GFP positive terminal reveals little to no DmCa1D signal at all as indicated by arrows (G, K, O). Expression of DmCa1D TRiP RNAi under control of the RN2-GAL4,UAS-FLP driver results in a strong knockdown of the VGCC DmCa1D in synaptic terminals. GFP positive terminals yield reduced Bruchpilot staining in comparison to GFP negative terminals in some of the samples. A quantitative analysis of Bruchpilot staining in Is and Ib boutons was done by Nina Eckl (2016). It could be shown that Bruchpilot staining intensities in Is and Ib boutons in the same plane are indistinguishable. DmCa1D seems to have no effect on the number of Bruchpilot molecules in synaptic terminals.

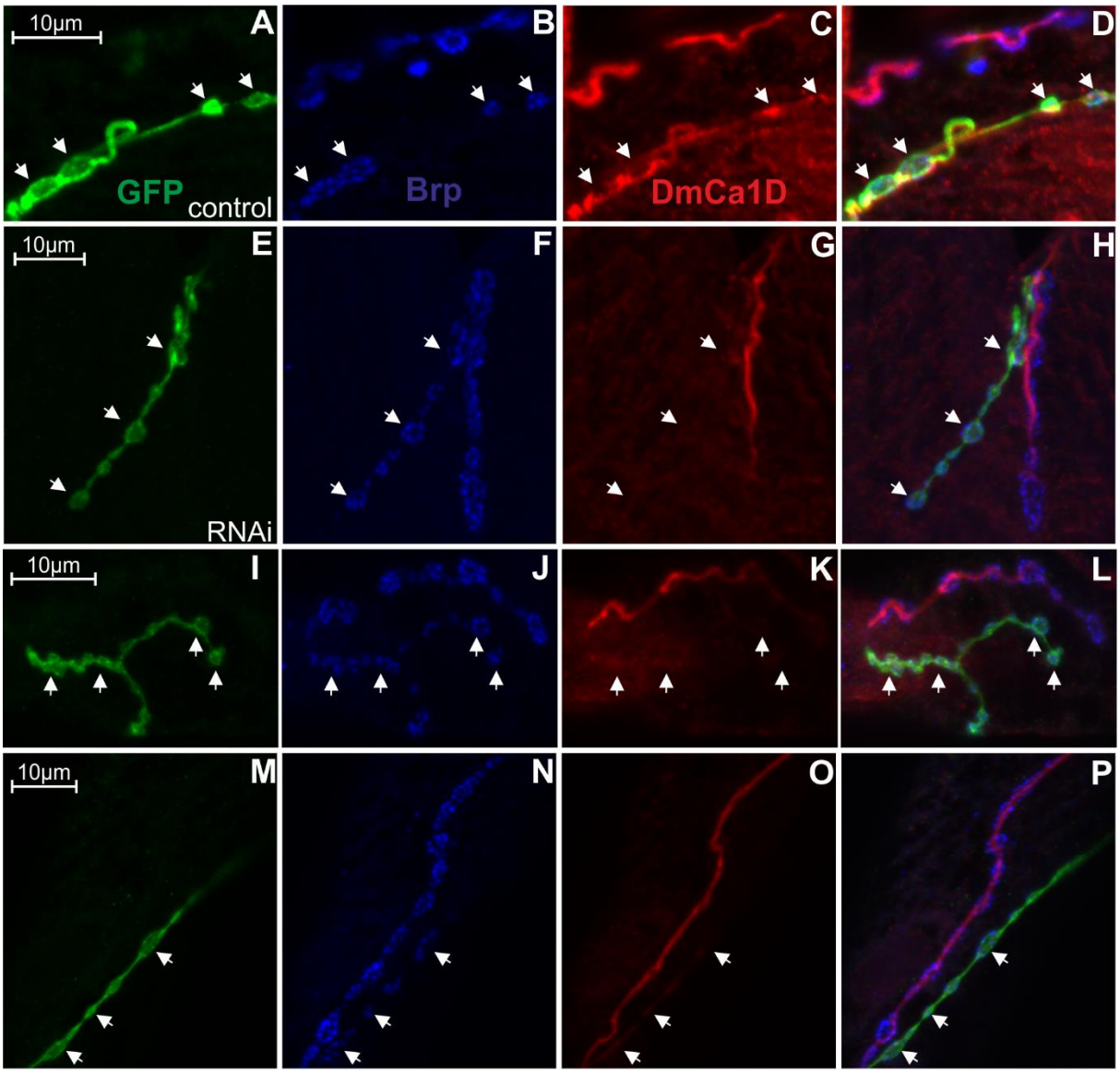

Figure 29: **DmCa1D RNAi knockdown in GFP positive terminals of larval motoneurons shows reduced DmCa1D staining.** Triple staining of presynaptic terminals from two different axons. **A-D**, **E-H**, **I-L** and **M-P** show single sections respectively. α-GFP (green) is expressed under control of RN2-GAL4,UAS-FLP and labels one of two terminals in each section (**A, E, I, M**). **A-D** represent the control RN2-GAL4,UAS-FLP crossed to w^{1118}. **E-H**, **I-L** and **M-P** show RNAi knockdown affected terminals (arrows) which are labeled with GFP (RN2-GAL4,UAS-FLP crossed to HMS00294). In **B, F, J** and **N** both terminals are labeled with the active zone marker Bruchpilot (blue). DmCa1D (red) staining is shown in **C, G, K** and **O**. In RNAi knockdown animals the GFP-labeled terminal (arrows) displays very sparsely to none DmCa1D whereas the other terminal (non-GFP) shows a clear staining. In the control both terminals are labeled with DmCa1D.

3.3.2 MARCM

To investigate the functional consequences of complete loss in motoneurons in genetic mosaics of the DmCa1D channel we used the null mutant *DmCa1D*^{X10}. Because of the fact that the null mutation is homozygous lethal the only way to achieve a viable knockout was by using the MARCM (Mosaic Analysis with a Repressible Cell Marker) technique (Wu et al. 2006). We generated few homozygous null mutant motoneurons in an otherwise heterozygous animal.

Null mutant cells are GFP positive (2.3). Those animals reach larval stages and adulthood which makes knockout affected cells available for electrophysiological and immunocytochemical investigations. To generate MARCMs of larval motoneurons aCC and RP2 the heat shock has to happen during development of these cells in the embryo. A heat shock 2 hours after egg laying for 30 minutes in a 34 °C water bath results in a VNC pattern like in Figure 30. Larval motoneurons are labeled with arrows (A).

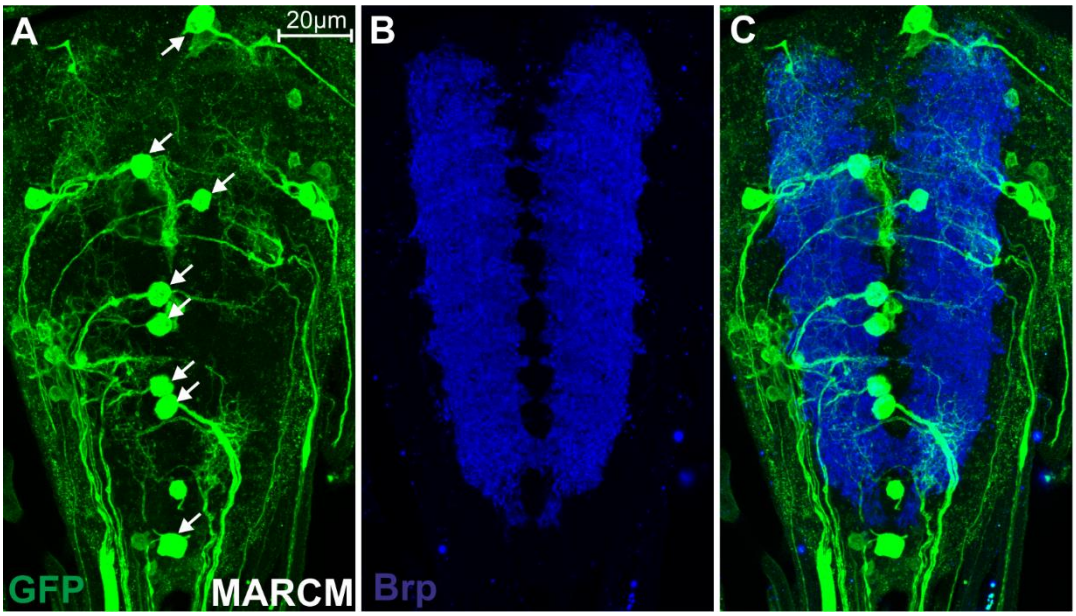

Figure 30: **MARCM positive larval aCC and RP2 motoneurons.** Projection view of 20 slices. **A** α-GFP (green) label indicates *1DX10* positive motoneurons (arrows). Heat shock was induced 2 hours after egg laying for 30 minutes in a 34°C water bath. **B** Neurpil of the ventral nerve cord stained by the active zone protein Bruchpilot (blue). **C** Overlay of GFP and Bruchpilot antibody stainings.

3.3.2.1 MARCM knockout-affected synaptic terminals of MNs

I also looked at synaptic terminals of homozygous null mutant motoneurons on larval crawling muscles (Figure 31). To identify presynaptic terminals we used the active zone marker Bruchpilot. In all samples we acquired two nearby Bruchpilot-stained terminals (B, F, J, N, R) one of each labeled with GFP and one without (A, E, I, M, Q). In the control (RN2-GAL4, UAS-FLP crossed to w^{1118}) both terminals (GFP +/-) are equally stained with DmCa1D (C). Null mutant terminals (G, K, O, S) show no DmCa1D signal (arrows) in comparison to the second non-GFP labeled terminal. This confirmed that I successfully used the MARCM technique to generate genetic mosaics in which only a subset of aCC or RP2 motoneurons is homozygous DmCa1D null mutant in an otherwise heterozygous background.

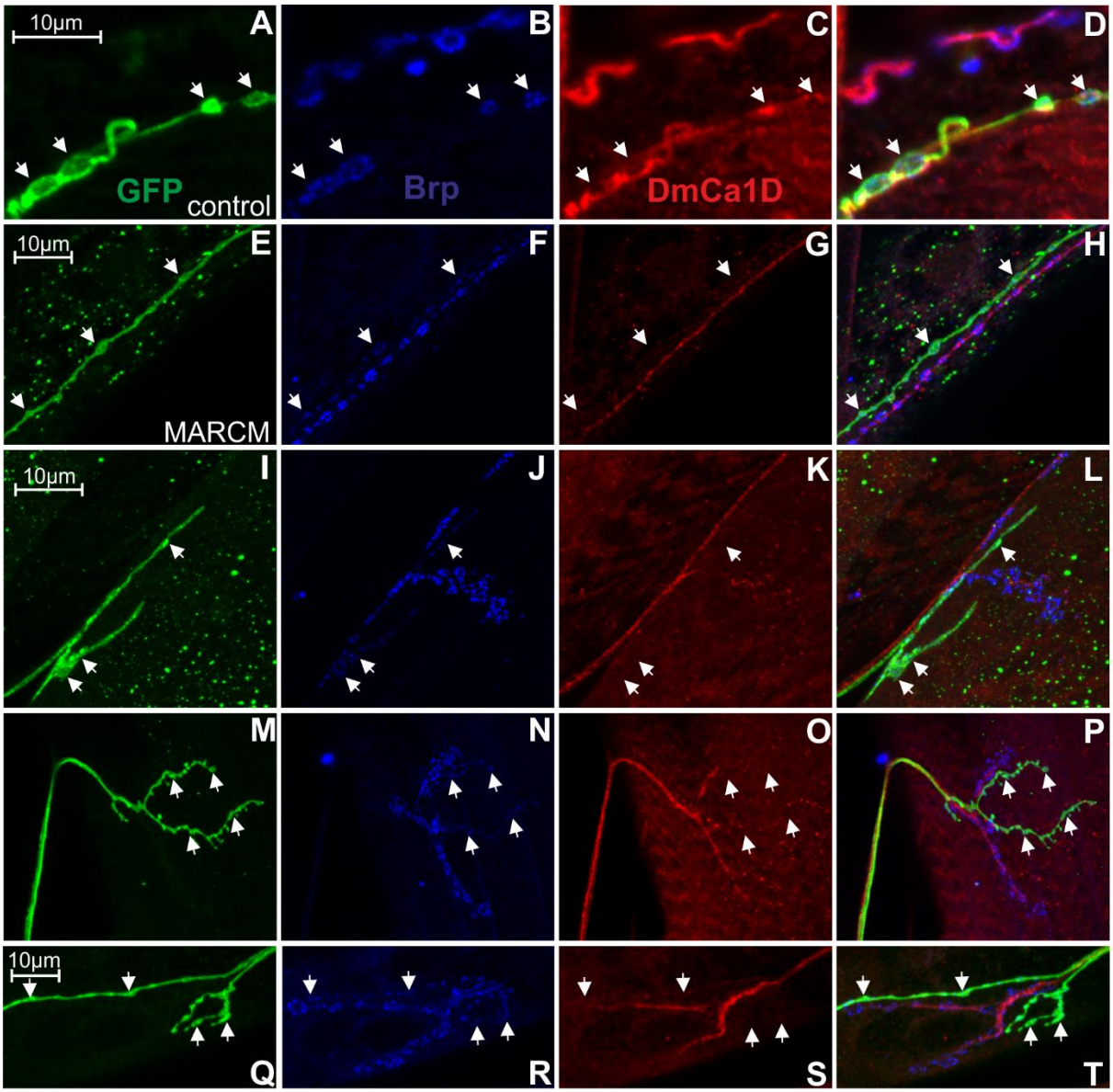

Figure 31: **DmCa1D MARCM knockout at GFP positive terminals of larval motoneurons shows no DmCa1D staining.** Triple staining of presynaptic terminals from two different axons in MARCM positive animals. **A-D**, **E-H**, **I-L**, **M-P** and **Q-T** show single sections respectively. GFP (green) is expressed under the control of RN2-GAL4, UAS-FLP (control) or of Tub-GAL4 in homozygous null mutant (*1DX10*) cells. Only one of two terminals is GFP positive in each section (**A**, **E**, **I**, **M**,**Q**). **A-D** represent the control (RN2-GAL4, UAS-FLP crossed with w1118). **E-H**, **I-L**, **M-P** and **Q-T** show MARCM affected, and therefore 1D null mutant terminals (arrows) which are labeled with GFP. In **B**, **F**, **J**, **N** and **R** both terminals are labeled with the active zone marker Bruchpilot (blue). DmCa1D staining (red) is shown in **C**, **G**, **K**, **O** and **S**. In MARCM knockout positive animals the GFP-labeled terminal (arrows) displays no DmCa1D staining whereas the other terminal (non-GFP) shows clear antibody labeling. In the control both terminals (GFP +/-) are stained with DmCa1D.

3.4 Intracellular muscle recordings

Via immunocytochemistry with the specific DmCa1D antibody I could show the efficacy of the RNAi knockdown and the MARCM knockout in presynaptic terminals of larval motoneurons. I now used these two techniques to reveal the function of DmCa1D at the presynapse. According to our hypothesis that DmCa1D plays a role in synaptic vesicle retrieval via

endocytosis, reduction or loss of DmCa1D would impair the recycling process. Thereby, fewer vesicles should be available for release during repetitive stimulation, thus increasing synaptic depression. To measure synaptic depression during repetitive stimulation from the postsynaptic muscle I recorded evoked post synaptic potentials (EPSPs) from larval crawling muscles.

3.4.1 RNAi knockdown

To evoke post synaptic potentials (EPSPs) we extracellularly stimulated GFP labeled knockdown axons with a frequency of 5 Hz (2.4). A sharp glass electrode was placed into the muscle innervated by the same axon and the membrane potential was recorded in current clamp mode (Figure 32). During repetitive stimulation at 5 Hz, EPSP amplitude decreases over time until a steady state is reached. This short-term plasticity is called synaptic depression. The steady state likely indicates a balance between recycling and release during ongoing stimulation. The first 10 s of each recording, which corresponds to 50 EPSPs, were used for analysis. Synapses affected by the knockdown show a steeper decrease in EPSP amplitude over time until the steady state is reached.

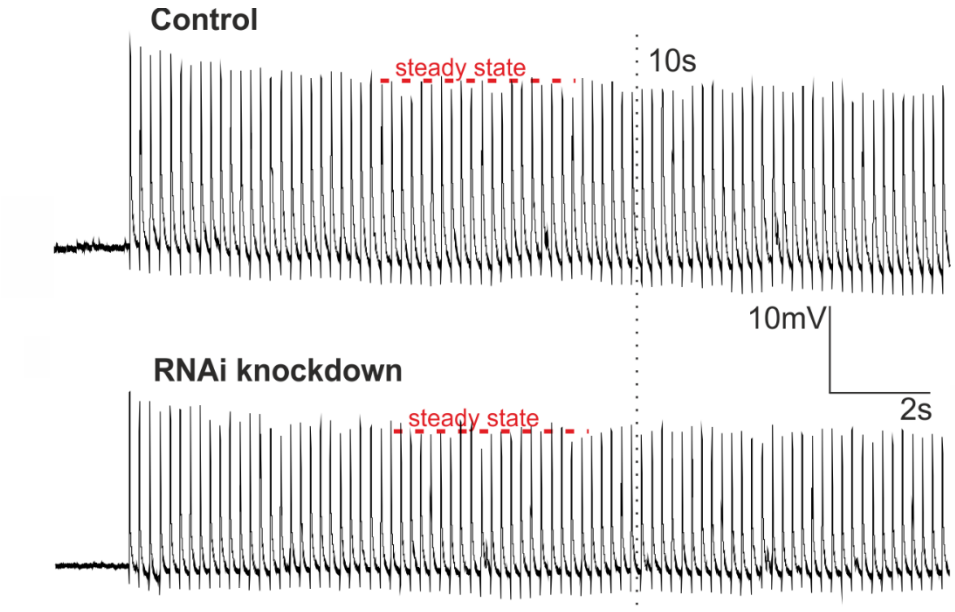

Figure 32: **Synaptic depression is increased in aCC and RP2 motoneurons expressing DmCa1D RNAi knockdown.** Evoked post-synaptic potentials (EPSPs) – recording examples of motoneurons expressing DmCa1D RNAi TRiP-HMS00294 and the respective control. Amplitudes of EPSPs in mV as a function on time in seconds decrease till a steady state is reached. The first 10 seconds of each recording were used for quantitative analysis.

Synaptic depression was measured by the decrease in EPSP amplitude over time. Therefore, EPSP amplitudes were normalized to the first amplitude in recordings from 10 animals. Figure

33 shows fits of 10 control recordings (grey, n=10) and 10 knockdown recordings (light blue, n=10). Data were fitted with a first order exponential standard fit in Clampfit 10.2. After the initial decrease controls reach the steady state at around 85 % of the first EPSP amplitude after 5 seconds during stimulation. The relative EPSP amplitudes of knockdown cells decrease to a steady state level of around 80 % of the first EPSP amplitude after 7 seconds. A statistical analysis was done comparing control and knockdown after the steady state is reached. The normally distributed data show a highly significant difference in a T-test ($p<0.001$).

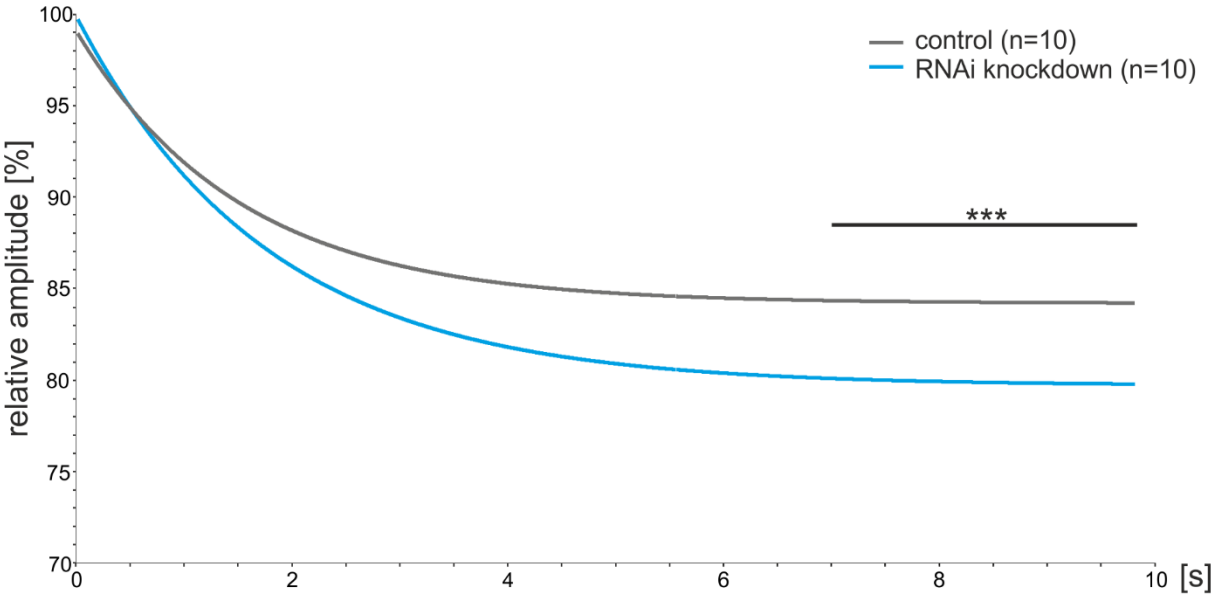

Figure 33: I**ncreased synaptic depression in aCC and RP2 motoneurons expressing DmCa1D RNAi knockdown.** Intracellular recordings of larval crawling muscles innervated by knockdown affected motoneurons with a 5 Hz stimulus protocol. Relative amplitude, normalized to the first amplitude, of evoked postsynaptic potentials (EPSPs) is plotted against time in seconds. Results of RNAi-knockdown motoneurons are shown in light blue (n=10) and the respective control in grey (n=10). Initially, both curves decrease equally. After 1-2 seconds EPSP amplitudes of RNAi knockdown cells decrease even stronger and remain at around 80 %. Control amplitudes stay stable at around 85 %. Statistical analysis with a T-test yields a highly significant difference between control and knockdown after reaching the steady-state (7 s) ($p<0.001$).

3.4.2 MARCM knockout

The same protocol for extracellular stimulation as in 3.5.1 was used in DmCa1D null mutant motoneurons generated by MARCM (Figure 34). GFP positive motoneurons, homozygous for the null mutant allele *DmCa1D*^{X10}, were compared with GFP negative control motoneurons in heterozygous null mutant animals. To measure synaptic depression we analyzed the decrease in EPSP amplitude over time. EPSP amplitudes of 10 knockout and 10 control animals were normalized to the amplitude of the first EPSP. For analysis we used the first 50 EPSPs of each recording. After several seconds of repetitive stimulation a steady state in EPSP amplitude is

reached. In DmCa1D null mutant motoneurons EPSP amplitudes decrease stronger in comparison to respective controls.

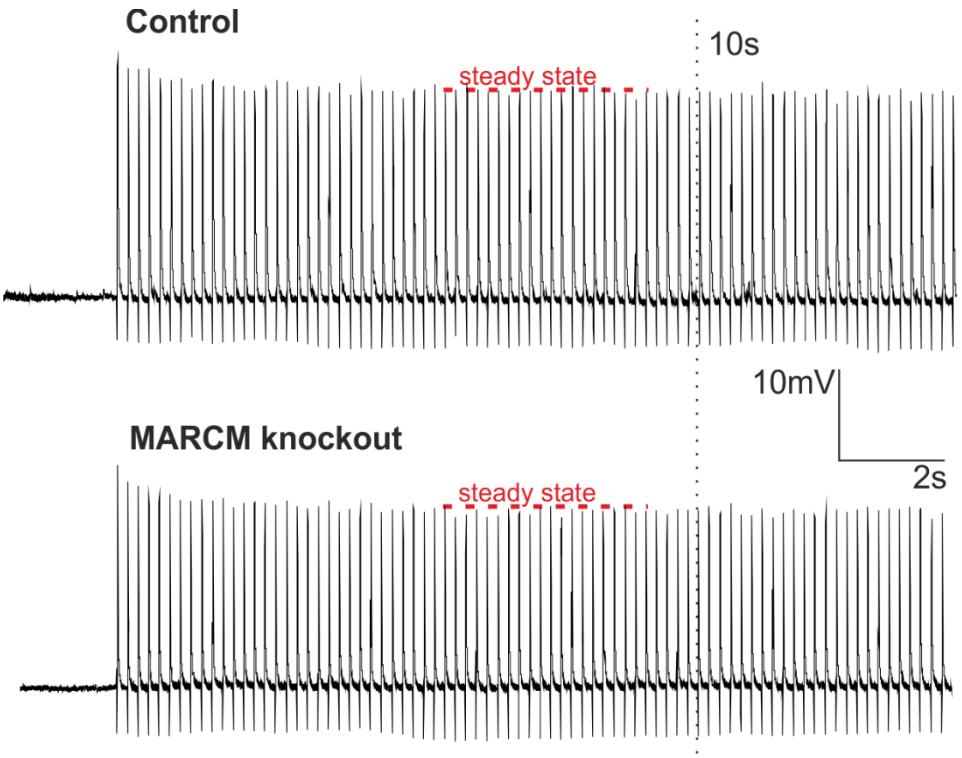

Figure 34: **Synaptic depression is increased in DmCa1D MARCM knockout positive aCC and RP2 motoneurons.** Evoked post-synaptic potentials (EPSPs) – recording examples of DmCa1D MARCM null mutant cells and the respective control. Amplitudes of EPSPs in mV as a function on time in seconds decrease till they reach a steady state. MARCM knockout positive terminals show increased synaptic depression in comparison to controls. The first 10 seconds of each recording were used for quantitative analysis.

EPSP amplitudes were normalized to the first amplitude in recordings from 10 animals, respectively. Results of 10 control recordings (black, n=10) and 10 knockout recordings (blue, n=10) were fitted in Figure 35. Data were fitted with a first order exponential standard fit in Clampfit 10.2. After the initial small decrease controls reach the steady state at around 90 % already after 3 seconds during stimulation. Knockout cells yield a much larger decrease in relative EPSP amplitude and stay stable at around 77 % after 5 seconds. After reaching the steady state level a statistical analysis was done comparing control and knockout. The normally distributed data show a highly significant difference in a T-test ($p<0.001$).

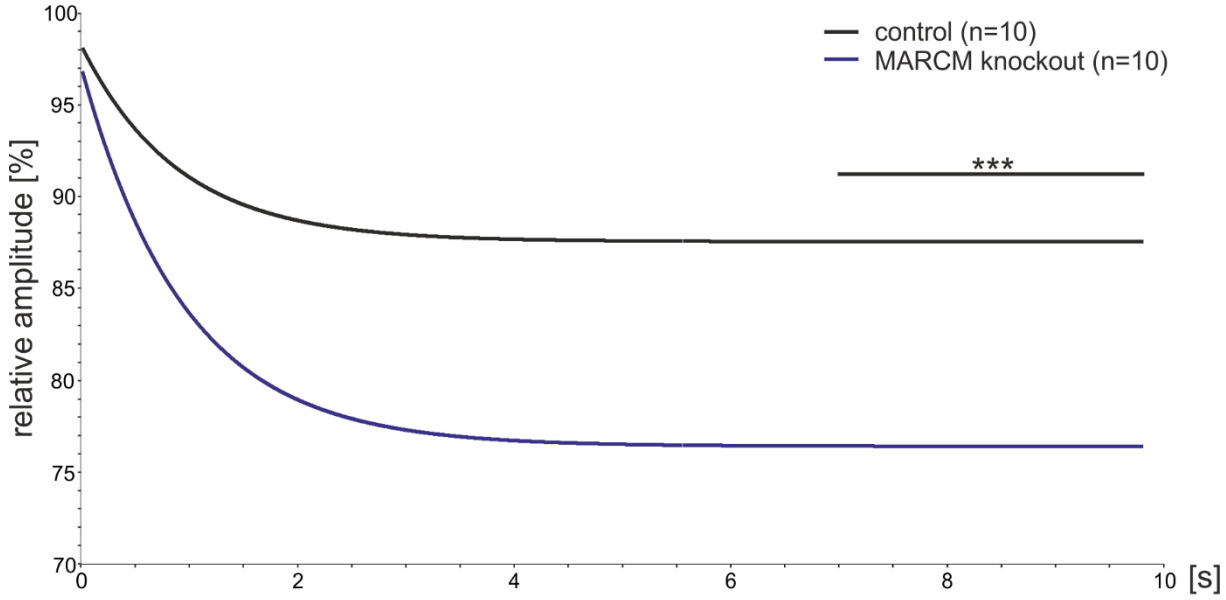

Figure 35: **Quantitative analysis shows increased synaptic depression in DmCa1D MARCM knockout positive aCC and RP2 motoneurons.** Intracellular recordings of larval crawling muscles innervated by MARCM knockout affected motoneurons with a 5 Hz stimulus protocol. Normalized to the first one, relative amplitude (%) of evoked postsynaptic potentials (EPSPs) is plotted against time in seconds. Results of knockout motoneurons are demonstrated in blue (n=10) and the respective control in black (n=10). Immediately with the second EPSP MARCM cells show a much steeper decrease in amplitudes than the respective controls. After 2 seconds controls already remain at around 88 % whereas knockout cells stay stable at around 77 % after 4 seconds of stimulation. Statistical analysis with a T-test yields that the relative amplitudes of control and knockout terminals are highly significant different to each other after reaching the steady-state (7 s) ($p<0.001$).

3.5 FM1-43 measured endocytosis

The effect of increased depression in DmCa1D RNAi knockdown and MARCM knockdown affected motoneurons can be explained by two different scenarios. First, SV recycling could be impaired. Clearance of release sites after exocytosis is essential to dock and prime new transmitter filled SVs. Reduced SV retrieval would block those release sites and fewer vesicles would be able to be released upon the next membrane depolarization, leading to synaptic depression. Second, less synaptic facilitation would lead to a reduction in postsynaptic responses to repetitive stimulation. Directly after a conditioning stimulus inducing exocytosis, the local Ca^{2+} concentration at active zones is increased. These Ca^{2+} microdomains decay rapidly in hundreds of milliseconds. Upon a second stimulus shortly after the first, this Ca^{2+} influx will add up to remaining Ca^{2+}. Thus, more SVs will undergo exocytosis following more transmitters to be released which is synaptic facilitation (Katz & Miledi 1968; Zucker & Regehr 2002; Hallermann et al. 2010). Less residual Ca^{2+} would then lead to increased synaptic depression. To distinguish the impact of DmCa1D on exocytosis and endocytosis we used the fluorescent dye FM1-43, which enables direct measuring of endocytosis (Betz et al. 1992, Betz & Bewick 1992). The styryl dye FM1-43 integrates into lipid bilayer membranes. Built into the

outer presynaptic membrane, the dye is taken up into the presynaptic terminal via endocytosis. After the removal of non-incorporated dye the rate of SV endocytosis is reflected in the fluorescence of FM1-43 in the terminal (Figure 36A). Loaded dye can be released again via exocytosis of SVs. FM1-43 will dissociate from the membrane and will dissolve in the bath solution (B). To induce FM1-43 uptake, SV release has to be evoked. Release can either be induced by activation of all neurons with high extracellular potassium solution or by direct electrical stimulation of the motoneurons under investigation with a suction electrode. The high potassium concentration changes the resting membrane potential to more positive, causing the motoneuron to permanently fire action potentials. With a suction electrode the axon of a motoneuron is sucked up and stimulated extracellularly with a defined frequency (2.4). After washout of the remaining dye from the bath, loaded terminals can be detected by fluorescent imaging (Figure 36A). MN6/7-Ib terminals on muscle 6 and 7 of the abdominal segment 3 are shown as a representative example. To now unload the terminals, exocytosis has to be evoked again via high potassium solution or extracellular stimulation. Washout removes released FM1-43 and the remaining fluorescence in the terminals can be detected (Figure 36B). To disable the function of DmCa1D we added 1 µM of the pharmacological blocker lanthanum (La^{3+}) for 5 minutes in a pre-incubation and during evoked exocytosis. Endocytosis and exocytosis were measured using the following protocol (Figure 36C): First, exocytosis is induced with high K^+ solution or extracellular stimulation. After washout with a Ca^{2+} free saline, fluorescence of loaded terminals is recorded which corresponds to the rate of endocytosis. Exocytosis is induced again followed by a washout with Ca^{2+} free saline. The rate of exocytosis is then defined by recording the remaining fluorescence in the terminals.

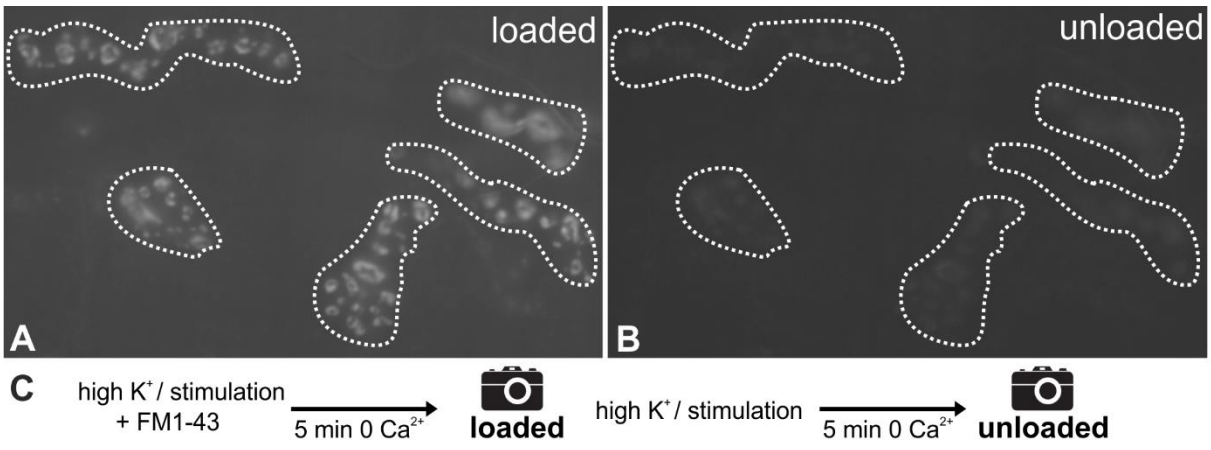

Figure 36: **FM1-43 dye uptake into synaptic terminals of larval crawling muscles.** Larval body wall muscles 6 and 7 in abdominal segment A3. **A** Loaded terminals show bright staining of FM1-43. In respective unloaded terminals in **B** FM1-43 label is strongly reduced. **C** Protocol used to load and unload synaptic terminals with FM1-43.

3.5.1 High potassium induced FM1-43 uptake

To load terminals with the fluorescent dye FM1-43 we used a high potassium solution containing 90 mM K^+ to induce motoneuron firing in control Canton S larvae (Figure 37). Exocytosis of SVs is followed by membrane retrieval by which the dye is incorporated into recycled vesicles. Figure 37A shows loaded terminals of muscles 6 and 7 in the abdominal segment 3. After a second incubation with 90 mM K^+ previously loaded vesicles were released again in an activity dependent manner. Remaining fluorescence of the dye in the terminals was recorded (B). Most of the dye was released, but terminals are still visible, meaning that the same amount of loaded dye molecules was not released again but remained in the terminal. To disable DmCa1D we added 1 µM La^{3+} and imaged the loading (C) and the unloading process of FM1-43 (D) in motoneuron terminals again. Loaded terminals in A and C show similar fluorescent signal likewise unloaded terminals in B and D.

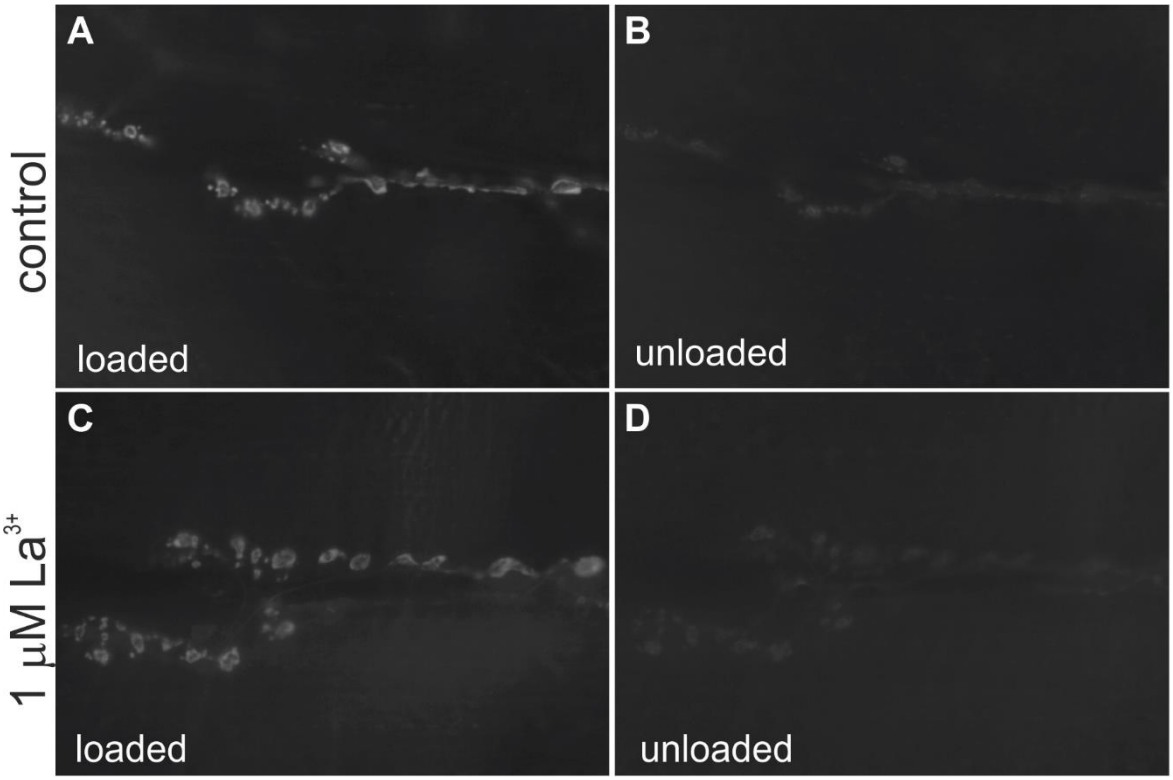

Figure 37: **Saturated loading of synaptic terminals on larval body wall muscle 6 and 7 with 4µM FM1-43. A** and **C** show loaded terminals, **B** and **D** the respective unloaded terminals after dye release. **A** and **B** represent the control dye uptake and release in 90 mM K^+ saline. Terminals are loaded under blocking conditions with added 1 µM La^{3+} in **C** and **D**. Both terminals in **A** and **C** are brightly labeled with FM1-43. Unloaded terminals in **B** and **D** show strongly reduced FM1-43 staining.

Quantification of 9 control terminals and 7 treated with La^{3+} is shown in Figure 38. Upon motoneuron firing fluorescent intensity in synaptic terminals was similar after loading in 90

mM K^+ in controls (median=24.02) and after pharmacological blockade with La^{3+} (median=24.84). Fluorescent intensities showed no significant difference in comparison of controls and in addition of La^{3+} (p=0.512) in a Mann-Whitney U test (MWU). This indicated no differences in synaptic vesicle recycling. Similarly, La^{3+} had no effect on unloading of previously loaded terminals. Mean grey values of controls (median=5.07) and with La^{3+} (median=3.69) show no significant difference (p=0.528). This indicates that pharmacological blockade had no effect on release as evoked by high extracellular K^+.

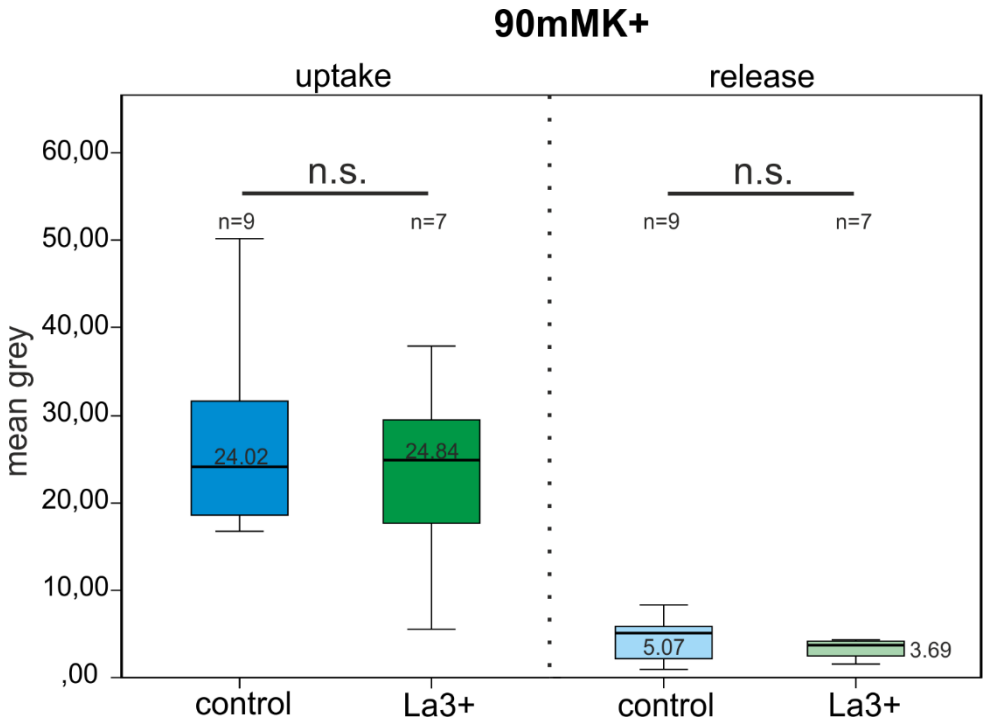

Figure 38: **Addition of La^{3+} shows no statistical difference in FM1-43 uptake and release in 90 mM K^+ solution.** Controls are shown in blue box plots, incubation with La^{3+} is shown in green box plots. Between control dye uptake (median=24.02, n=9) and uptake under blocking conditions (median=24.84, n=7) there is no statistically significant difference in a Mann-Whitney U test (p=0.512). Also, no statistically significant difference (p=0.528, MWU) exists between control dye release (median=5.07, n=9) and release in addition of La^{3+} (median=3.69, n=7).

Incubation with 90 mM K^+ induces a massive uncontrolled activation of all neurons in the nervous system. This led to immense dye uptake into the terminal reaching saturation of SVs in the recycling pool. To reduce dye uptake into synaptic terminals we next used a milder potassium concentration of 20 mM K^+ (Figure 39). Less [K^+] results in less activation of neurons. Less motoneuron firing causes less vesicles to be released and following to be recycled. Less dye is loaded into the terminal, hence the fluorescence signal is weaker. Loaded terminals of a control are shown in A. Individual boutons with much less dye fluorescence

intensity than in Figure 37 can be identified. During a second incubation with 20 mM K^+ the dye was released again from previously loaded terminals. No fluorescent signal in terminals can be detected after dye release, loaded FM1-43 was completely released again (B). If we now add 1 µM La^{3+}, identification of individual boutons is not possible anymore, merely the outlines of whole terminal branches can be recognized (C). In addition of La^{3+} the recycling rate of synaptic vesicles is reduced. Previously loaded terminals are not visible anymore after release induced by the second incubation with 20 mM K^+ and La^{3+} (D). The incorporated dye was completely released.

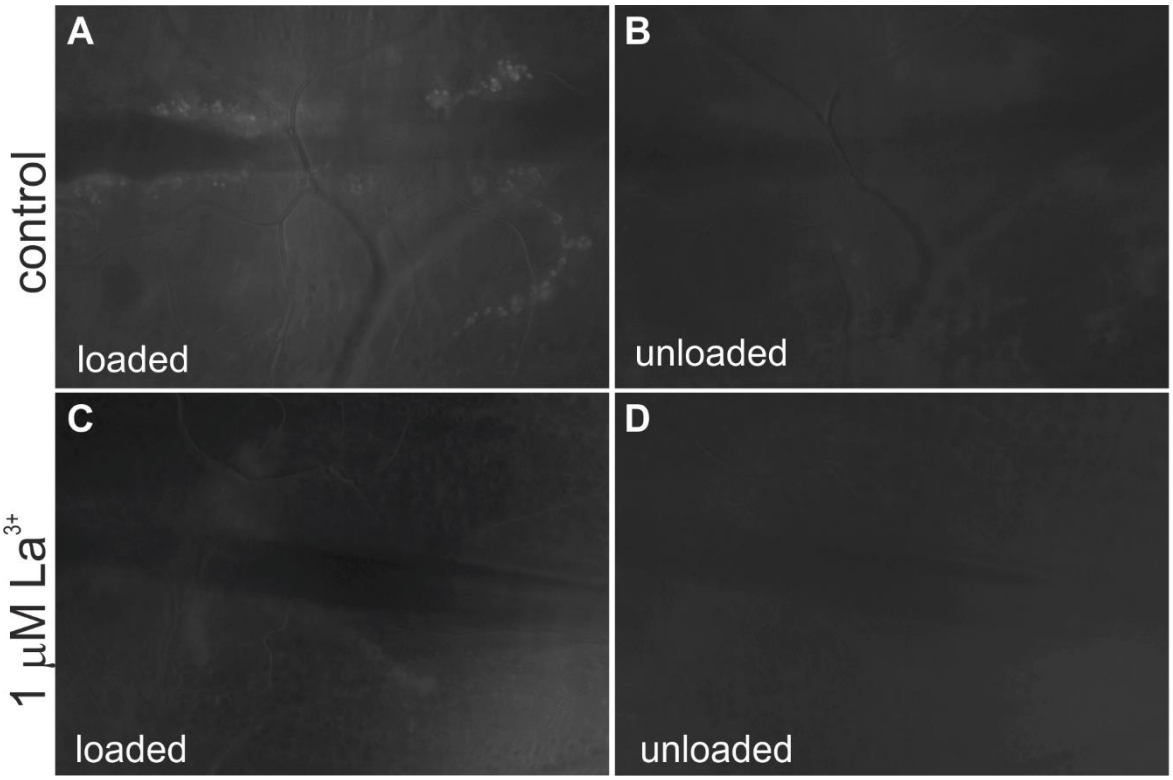

Figure 39: **Non-saturated loading of synaptic terminals on larval body wall muscle 6 and 7 with 4µM FM1-43. A** and **C** show loaded terminals, **B** and **D** the respective unloaded terminals after dye release. **A** and **B** represent the control dye uptake and release in 20 mM K^+ saline. Terminals are loaded under blocking conditions with added 1 µM La^{3+} in **C** and **D**. Terminals in **A** are mildly loaded with dye. In **C** only outlines of the terminal branches are barely visible. Unloaded terminals in **B** and **D** show nearly no FM1-43 staining.

In Figure 40, 10 control terminals and 13 treated with La^{3+} are quantified. Upon motoneuron firing induced with a milder potassium concentration of 20 mM K^+ less vesicles undergo exocytosis following endocytosis. After loading in 20 mM K^+, dye intensities in synaptic terminals in controls (median 6.68) are highly significantly different to each other ($p<0.001$) in a Mann-Whitney U test after a pharmacological blockade with La^{3+} (median 2.30). During a stimulation of all neurons with 20 mM K^+ no saturation of SVs with FM1-43 is reached.

Addition of La^{3+} leads to a weaker fluorescent signal than in controls, which corresponds to a reduction in SV retrieval. By contrast, La^{3+} had no effect on release of previously incorporated dye. Fluorescence signals of controls (median 0.64) and in addition of La^{3+} (median 0.47) show no significant difference (p=1, MWU). The release of FM1-43 induced by 20 mM K^+ is not affected in addition of the pharmacological blocker La^{3+}.

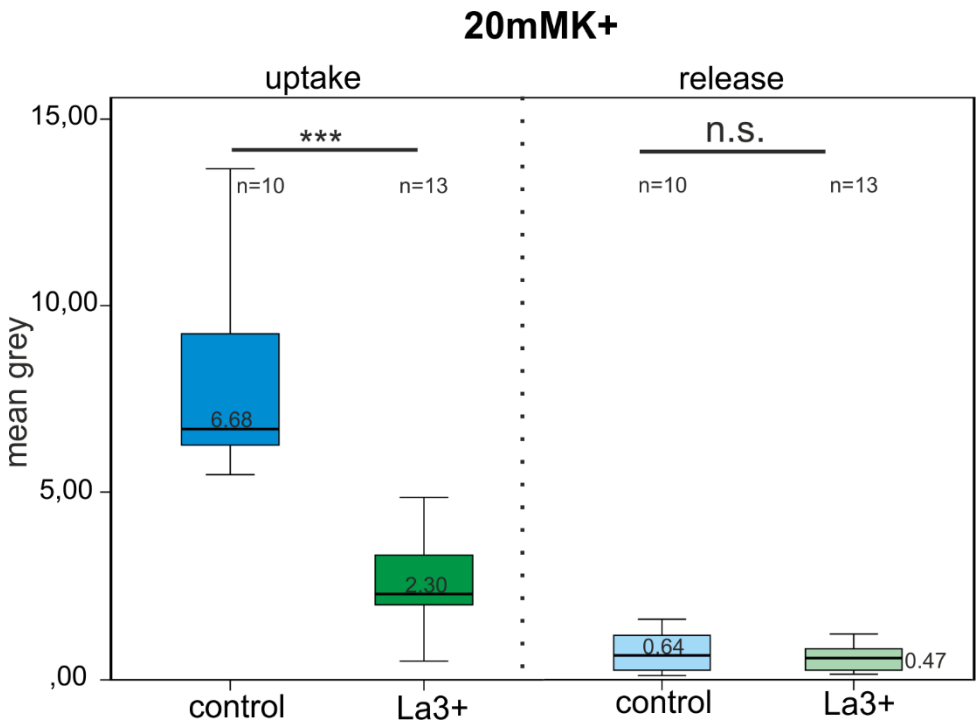

Figure 40: **Addition of La^{3+} shows a highly significant difference in FM1-43 uptake in 20 mM K^+ solution. Release remains unaffected.** Statistical analysis of FM1-43 uptake and release in 20 mM K^+ solution. Controls are shown in blue box plots (n=10), incubation with La^{3+} is shown in green box plots (n=13). Between control dye uptake (median=6.68) and uptake under blocking conditions (median=2.3) there is a statistically highly significant difference (p<0.001) in a Mann-Whitney U test. No statistically significant difference (p=1, MWU) exists between control dye release (median=0.64) and release in addition of La^{3+} (median=0.47).

3.5.2 Stimulation with 5 Hz

Stimulation with high K^+ solutions initiates an uncontrolled activation of all neurons. Therefore, we used extracellular repetitive stimulation with a suction electrode to directly stimulate single motoneurons with a defined frequency of 5 Hz for 5 minutes. With this stimulation we also reproduced the depression protocol in muscle recordings (2.4). During 5 Hz stimulation for 5 minutes with a concentration of 4µM FM1-43 we reached saturation of dye uptake again like with 90 mM K^+. To reduce the amount of incorporated dye we reduced FM1-43 concentration from 4 µM to 1 µM. Quantification of 14 controls and 13 animals under blocking condition is shown in Figure 41. Fluorescent signals of dye uptake in controls (median 4.00) and in addition of La^{3+} (median 1.38) are highly significantly different to each other (p=0.002) in a Mann-

Whitney U test. During extracellular stimulation with a defined frequency of 5 Hz for 5 minutes and a FM1-43 concentration of 1 µM, dye uptake is significantly reduced in addition of the pharmacological blocker La^{3+}. To initiate release of previously labeled SVs we used 60 mM K^{+}. This is not comparable with the 5 Hz stimulation protocol, hence we cannot make a statement regarding exocytosis.

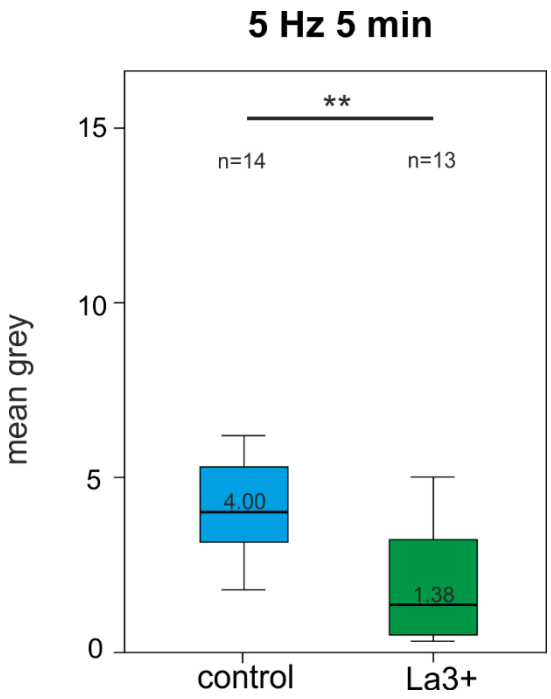

Figure 41: **Addition of La^{3+} shows a highly significant difference in FM1-43 uptake during a 5 Hz stimulation for 5 minutes.** Statistical analysis of FM1-43 uptake during extracellular stimulation with 5 Hz. Controls are shown in blue box plots (n=14), incubation with La^{3+} is shown in green box plots (n=13). Control dye uptake (median=4.0) is highly significantly different (p=0.002) to the uptake under blocking conditions (median=1.38) in a Mann-Whitney U test.

3.5.3 Crawling bursts

With the styryl dye FM1-43 we have shown that fewer SVs are recycled during repetitive stimulation and in 20 mM K^{+} in addition of the pharmacological blocker La^{3+}. Whether this effect would also show up during normal behavior is still not clear. Therefore, we aimed to use a protocol representing a stimulation pattern similar to physiological conditions. To assess motoneuron firing patterns during behavior, we recorded larval motoneurons during crawling-like locomotor patterns in semi-intact preparations intracellularly with patch pipettes in current clamp mode (Figure 42A). Single bursts of action potentials are separated with an interburst interval of 1-2 seconds. Within a burst we analyzed burst duration and intraburst frequency (Figure 42B). Based on these recordings and published data (Kadas et al. 2015) we created a

stimulation protocol based on actual larval crawling (Figure 42C). The protocol consists of 120 Hz bursts lasting for 0.25 seconds which are separated by a 1 second interburst interval.

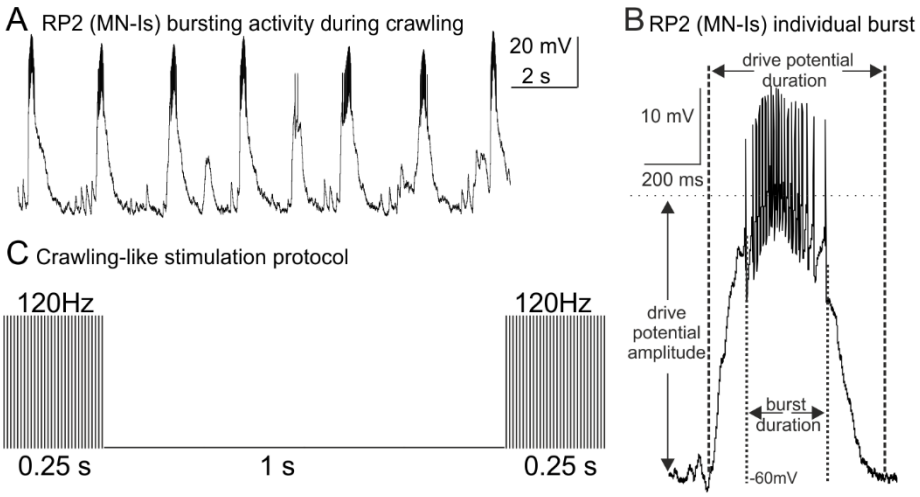

Figure 42: **Larval crawling bursting activity. A** Representative bout of bursting activity recorded from an RP2 (MN-Is) motoneuron during fictive crawling. **B** Enlarged individual burst with parameters used for protocol design. **C** Burst analysis and test experiments yielded a stimulation protocol of 120 Hz bursts which last for 0.25 seconds and are separated by a 1 second interpulse pause (Kadas et al. 2015).

We started with a crawling-like stimulation for 1 minute which corresponds to 50 bursts (Figure 43). Quantification of 5 controls (mean 17.35) and 5 treated with La^{3+} yields no significant difference in fluorescent signal ($p=0.088$) in a T-test. With 50 bursts we reached saturation of dye uptake again like the ones treated with 90 mM K^+. Therefore, we reduced the number of bursts to 20 to load less dye into boutons. Statistical analysis of 12 controls (mean 14.33) and 11 in addition of La^{3+} (mean 6.68) showed a highly significant difference in fluorescent signal ($p=0.004$) in a T-test. If we limited the number of bursts to 5, no synaptic terminals could be recognized in addition of La^{3+}. Consequently, no mean grey measurement could be performed which is reflected by the mean grey value of 0. Analysis yields that the fluorescent signals of 17 controls (mean 6.05) and 17 treated with La^{3+} are highly significantly different to each other in mean grey values ($p<0.001$) in a T-test.

During high activity stimulation protocols like 90 mM K^+, 5 Hz with 4 µM FM1-43, and 50 bursts, synaptic vesicles of the recycling pool are saturated with the dye. Likely every SV will be loaded with FM1-43, some might even have underwent release and recycling a second time. Therefore, to recognize impairments in endocytosis in addition of the pharmacological blocker La^{3+}, dye uptake during stimulation has to be reduced in order to prevent saturation.

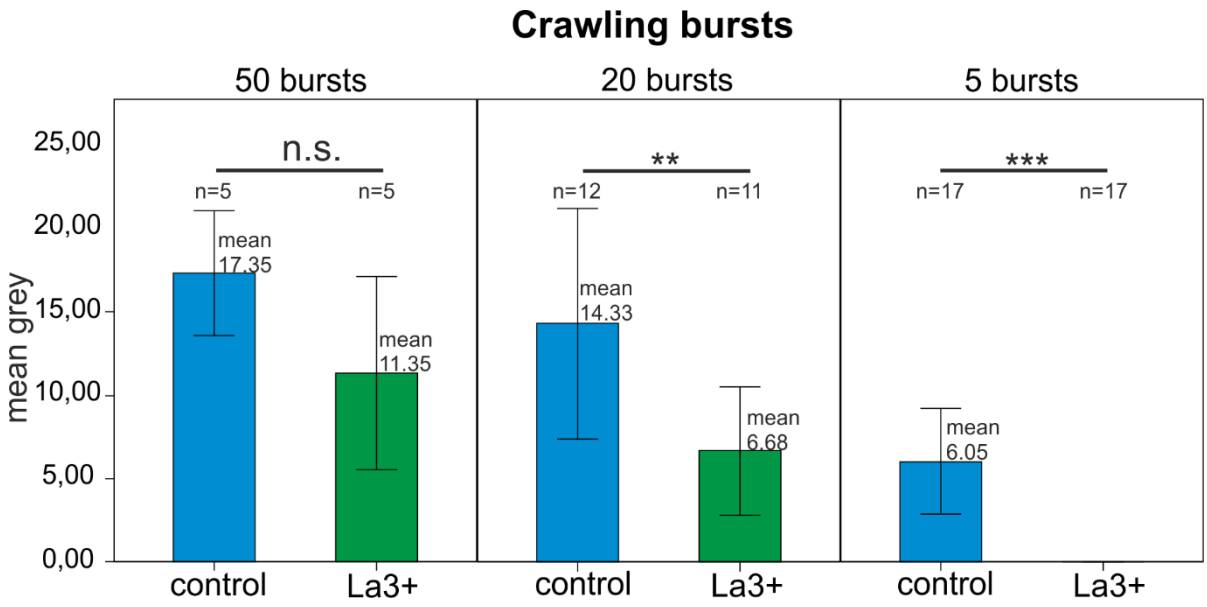

Figure 43: **Addition of La^{3+} shows a highly significant difference in FM1-43 uptake during crawling like stimulation of 5 and 20 bursts. Saturated boutons loaded with FM1-43 during 50 bursts show no significant difference in dye uptake in addition of La^{3+}.** Statistical analysis of FM1-43 uptake during extracellular stimulation with crawling bursts. Controls are shown in blue bars, incubation with La^{3+} is shown in green bars. A stimulation with 50 bursts results in no significant difference (p=0.088) in dye uptake between controls (mean=17.35, n=5) and samples treated with La^{3+} (mean=11.35, n=5). Reduction of the number of bursts to 20 reveals a statistically significant difference (p=0.004) between control dye uptake (mean=14.33, n=12) and uptake in addition of La^{3+} (mean=6.68, n=11). The highest significant difference between control dye uptake (mean=6.05, n=17) and uptake in blocking conditions (mean=0, n=17) is exhibited during stimulation with 5 crawling-like bursts (p<0.001). T-Test was used for analysis in all three comparisons.

3.6 Pre- and postsynaptic Ca^{2+} Imaging with GCaMP3

We could show that addition of the pharmacological blocker La^{3+} reduces synaptic vesicle recycling at larval motoneuron terminals. To demonstrate that presynaptic Ca^{2+} influx through DmCa1D channels mediates enhanced recycling we imaged Ca^{2+} influx directly with the genetically encoded Ca^{2+} indicator GCaMP3. GCaMP3 is coupled to synaptic vesicles via an ectopically expressed rat-synaptophysin (Pech et al. 2015). Upon stimulation we expect presynaptic Ca^{2+} influx through DmCa1A channels, mediating exocytosis, and through DmCa1D channels, enhancing recycling, which will both be detected by GCaMP3. To separate Ca^{2+} influx through DmCa1D channels we added the pharmacological blocker of DmCa1D, lanthanum. We stimulated the nerve projecting onto muscle 6 and 7 of the abdominal segments A2 or A3 with a suction electrode (2.4). All experiments were carried out in 10 µM glutamate to prevent muscle movement. Glutamate will bind to the postsynaptic glutamate receptor (GluR) leading to ongoing postsynaptic Ca^{2+} influx. The postsynaptic membrane will be permanently depolarized leading to sustained maximum contraction of larval crawling muscles. Stimulation of 5 action potentials (APs) was followed by 10 action potentials after a pause of 10 seconds. The number of action potentials was doubled to 20 action potentials again after a

10 second pause. An intraburst frequency of 120 Hz, similar to a larval crawling pattern, was used. The protocol was performed with normal saline and with 1 µM La^{3+} in normal saline. Peak ΔF/F are shown in Figure 44. In control terminals (A-C) fluorescence increases with the increase of action potentials. After incubation with 1 µM La^{3+} this increase in fluorescence is strongly diminished (D-F).

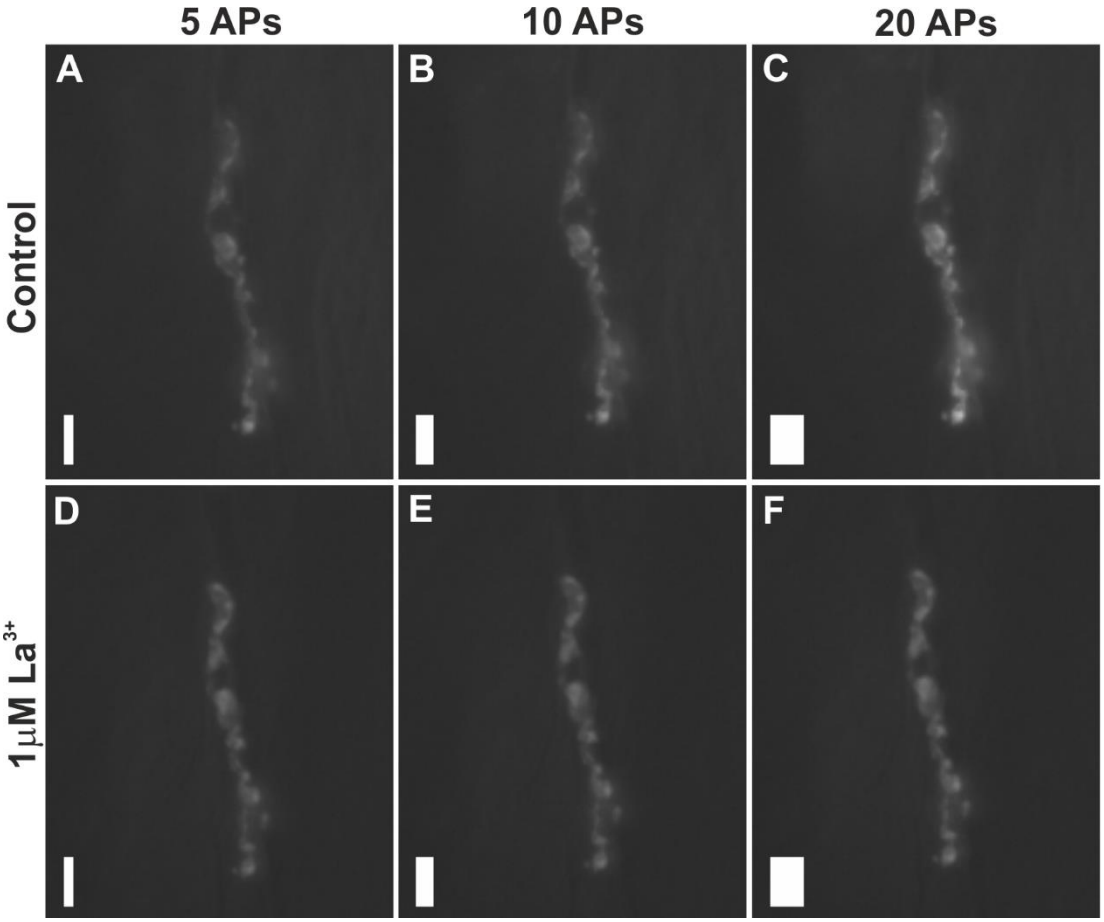

Figure 44: **Presynaptic Ca^{2+}-influx upon stimulation is reduced in addition of La^{3+}.** Ca^{2+} imaging at MN terminals expressing presynaptic GCaMP3. UAS-Syp-GCaMP3 is expressed under control of the motoneuron driver OK3-71-GAL4. **A-C** show control Ca^{2+} signal upon stimulation with 5 action potentials (APs) (**A**), 10 APs (**B**) and 20 APs (**C**). The more action potentials the higher the signal. **D-F** Recordings from the same terminals under blocking conditions of 1 µM La^{3+} show Ca^{2+} signal upon stimulation with 5 action potentials (APs) (**D**), 10 APs (**E**) and 20 APs (**F**). There is only a slight change in fluorescence when the number of APs is increased.

Quantitative analysis of controls (blue bars, n=6) and of La^{3+} application for 3 minutes (green bars, n=6) is shown in Figure 45. During stimulation with 5 APs, incubation in 3 minutes La^{3+} (mean=0.02) reduced ΔF/F by 76 % of the control in glutamate saline (mean=0.12). In addition of La^{3+} (mean=0.06), this reduction is increased to 85 %, relative to controls (mean=0.39) during stimulation with 10 APs. A stimulation with 20 APs decreased ΔF/F by 73 % in addition

of La^{3+} for 3 minutes (mean=0.31) in comparison to the control (mean=1.18). The relative reduction in fluorescence signal in addition of the pharmacological blocker La^{3+} during stimulation with 10 action potentials yields a 10 % higher value. This disparity might be due to very little data points (Figure 45). Furthermore, standard deviation bars show a broad spread of values. Therefore, we tested the relative reduction in fluorescence signal in addition of La^{3+} upon stimulation with 5, 10, and 20 APs for statistically significant differences (Figure 46). An analysis of variance (ANOVA) for a single factor shows no significant difference (p=0.191) in the relative reduction of ΔF/F upon stimulation with 5 APs, 10 APs, and 20 APs after 3 minutes incubation in La^{3+}. If the SV bound construct Syp-GCaMP3 exclusively recognizes Ca^{2+} influx at the presynaptic membrane this would mean DmCa1D channels would mediate around 80 % of this influx. This is not in accordance with former studies, which showed that synaptic transmission is mediated by presynaptic Ca^{2+} influx through DmCa1A channels and DmCa1A null mutant embryos are incapable of facilitating fast synaptic transmission (Kawasaki et al. 2000; McLeod 2006; Hou et al. 2008). A possible explanation is that SVs are located throughout the whole terminal in the different SV pools. Upon stimulation, overall elevations in Ca^{2+} concentration within the terminal will be recognized by the vesicle bound Syp-GCaMP3. Consequently, this construct is not suitable to measure exclusively Ca^{2+} influx at the presynaptic membrane (Pech et al. 2015).

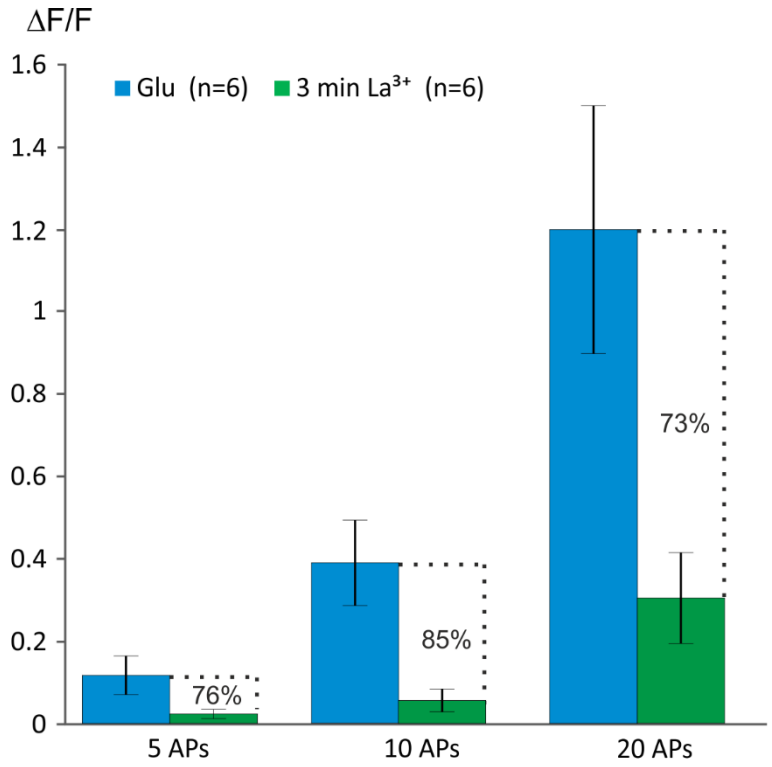

Figure 45: **Presynaptic Ca^{2+}-influx after 3 minutes incubation with La^{3+} is strongly reduced.** Lanthanum dependent changes of ΔF/F in terminals expressing Syp-GCaMP3 after 3 minutes incubation. Expression of UAS-Syp-GCaMP3 is controlled by the motoneuron driver OK3-71-GAL4. 6 terminals of muscle 6 and 7 were stimulated with 5 action potentials (APs), 10 APs and 20 APs. To prevent muscle movement 10 mM Glutamate was added. Blue bars represent control recordings. ΔF/F after 3 min incubation with La^{3+} is shown in green bars.

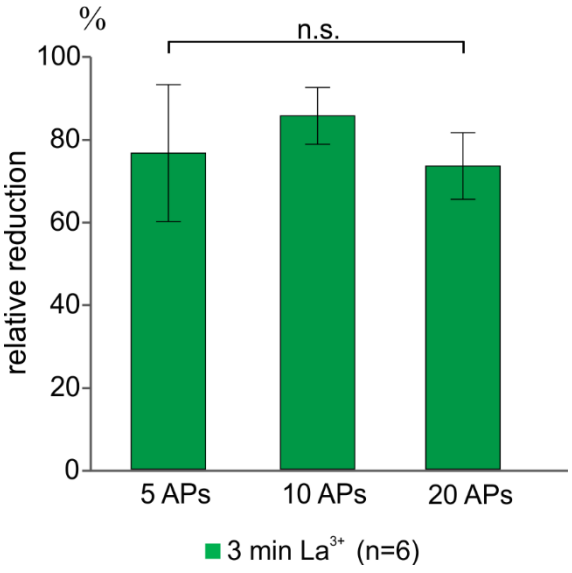

Figure 46: **Relative reductions of the fluorescent signal in addition of La^{3+} during stimulation with 5 APs, 10 APs, and 20 APs are not statistically different.** In addition of La^{3+} the fluorescence signal upon an extracellular stimulation of 5 APs, 10 APs, and 20 APs is strongly reduced to 76%, 85 %, and 73 % (n=6). An analysis of variance (ANOVA) for a single factor yields no significant difference between the three values (p=0.191).

A direct proof to show that DmCa1D channels take part in endocytosis but not in exocytosis is still missing. If DmCa1D plays no part in exocytosis, synaptic transmission has to be unchanged in addition of the pharmacological blocker La^{3+}. Synaptic transmission can be measured by recording evoked postsynaptic potentials (EPSPs). Postsynaptic responses are generated by postsynaptic DmCa1D channels. Therefore, addition of La^{3+} would eliminate EPSPs. A possible way to measure synaptic transmission independently of postsynaptic DmCa1D channels is to directly image postsynaptic Ca^{2+} influx through glutamate receptors (GluRs). A postsynaptic GCaMP3 which localizes to the subsynaptic reticulum seems to exclusively recognize postsynaptic Ca^{2+} influx through GluRs (Guerrero et al. 2005; Peled & Isacoff 2011, 2014). During stimulation with 1 action potential (AP) every 10 seconds synaptic transmission should not be disturbed by adding the DmCa1D blocker La^{3+}, if DmCa1D does not contribute to exocytosis. At a frequency of 0.1 Hz no synaptic depression occurs, hence Ca^{2+} signals of single stimuli within a recording should be similar (Wu et al. 2005). Figure 47 shows images of basic fluorescence (F_0) and fluorescence upon 1 AP (F) on muscles 6 and 7. Control samples (A+B) show increased fluorescence upon stimulation (B). After an incubation time of 3 minutes with 1 µM La^{3+} there is only a slight increase in fluorescence upon stimulation (D). This indicates that DmCa1D channels contribute to exocytosis.

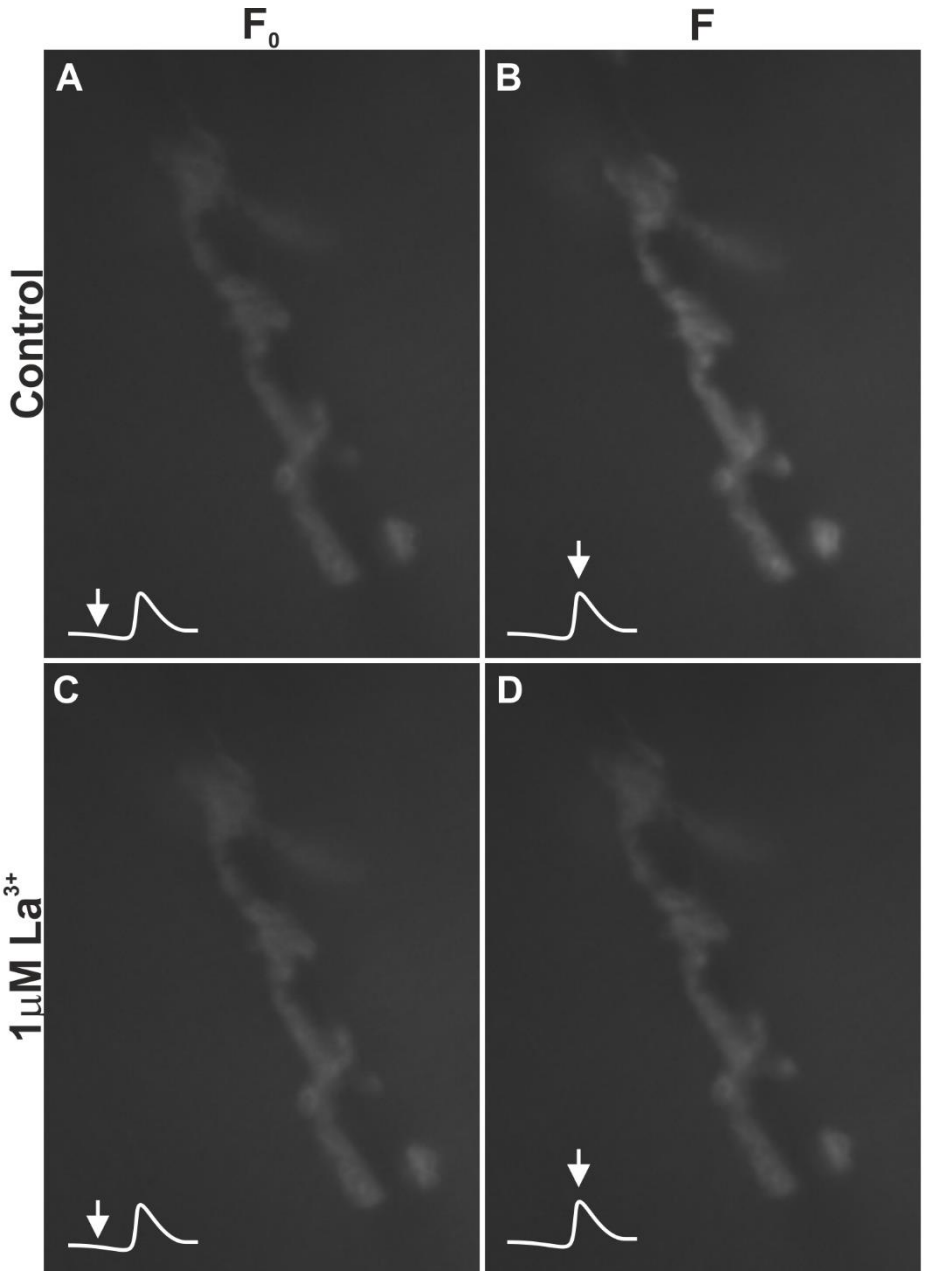

Figure 47: **Addition of La^{3+} reduces postsynaptic Ca^{2+}-influx through GluRs upon stimulation.** Ca^{2+} imaging at the postsynapse of larval NMJs on muscle 6 and 7. MHC-CD8-Synap-GCaMP3-Sh expresses in larval crawling muscles and localizes closely to postsynaptic glutamate receptors. **A+B** show control Ca^{2+} signal before (F_0) and upon stimulation (F) of one action potential. **C+D** Recording from the same terminals under blocking conditions of 3 min incubation with 1 µM La^{3+} show only a slight increase in Ca^{2+} signal before (F_0) and upon stimulation (F) of one action potential.

Quantitative analysis of 5 controls in normal saline (blue bar) and 5 in addition of 3 minutes in 1 µM La^{3+} (green bar) are shown in Figure 48. Controls yield an increase in fluorescence signal of 46 % ($\Delta F/F=0.46$) upon one action potential. After incubation with La^{3+}, this increase adds up to only 15 % ($\Delta F/F=0.15$) which is a reduction of 78 % compared to controls. This indicates that DmCa1D channels mediate to 78 % of Ca^{2+} influx needed for exocytosis.

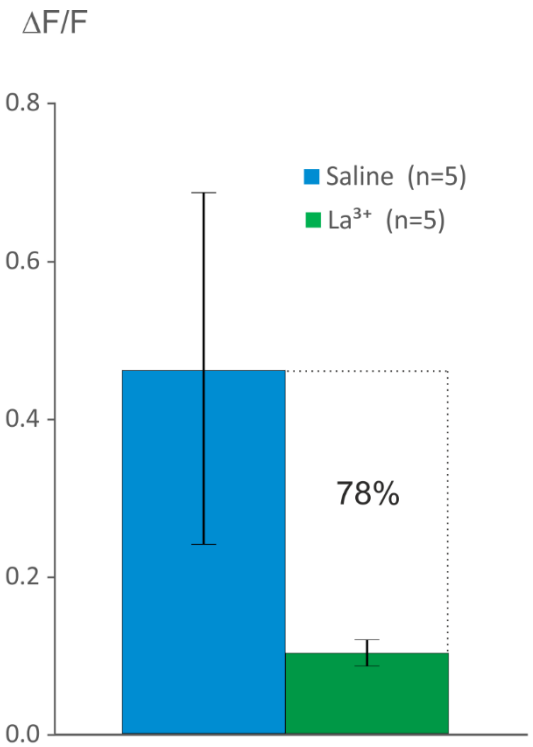

Figure 48: **Postsynaptic Ca^{2+}-influx through GluRs is strongly reduced in addition of La^{3+}.** Lanthanum induced reduction in ΔF/F of the postsynaptically expressed MHC-CD8-Synap-GCaMP3-Sh. Motoneurons projecting onto muscles 6 and 7 were stimulated with one action potential every 10 seconds. Blue bar shows control recordings in normal saline (n=5). ΔF/F after 3 min incubation with La^{3+} is represented by the green bar (n=5). Relative fluorescence shows a reduction of 78 % in comparison to control values.

A reduction of 78 % of postsynaptic calcium influx upon DmCa1D blockade could be caused by two things: If DmCa1D channels contributed to synaptic vesicle release, more postsynaptic glutamate receptors would be activated in the presence of presynaptic Ca^{2+} influx through DmCa1A and DmCa1D channels than compared to presynaptic Ca^{2+} influx through DmCa1A channels only, when DmCa1D channels are blocked by La^{3+}. If this was the case, these data would indicate a clear contribution of DmCa1D channels to synaptic vesicle exocytosis. In fact, the contribution of DmCa1D channels (78 %) would be even higher than that of DmCa1A channels. Several lines of evidence make this possibility highly unlikely. First, my own results show that action potential induced exocytosis, measured with imaging of the styryl dye FM1-43 (3.6), is not affected by a blockade of DmCa1D channels (Figure 40). Second, published data clearly demonstrate that DmCa1A channels are essential and sufficient for fast synaptic transmission (Kawasaki et al. 2000; MacLeod et al. 2006; Hou et al. 2008). And third, a conditional genetic knockdown of DmCa1A channels causes complete paralysis (Kawasaki et al. 2000; Rieckhof et al. 2003; Gu et al. 2009), thus further demonstrating that presynaptic Ca^{2+} influx through DmCa1D channels is not sufficient to induce muscle contraction. If DmCa1D channels contributed to 78 % of the postsynaptic glutamate receptor activation during

neuromuscular transmission, muscle contraction should at least be possible. Therefore, the reduction of postsynaptic muscle Ca^{2+} response to motoneuron firing is highly unlikely a sole consequence of decreased synaptic function. Alternatively, it is possible that the postsynaptically localized GCaMP3 construct, MHC-CD8-SynapGCaMP3-Sh, may also recognize Ca^{2+} influx through DmCa1D channels localized in the larval muscles of *Drosophila* (Ren et a. 1998). To test this we stimulated muscle 6 intracellularly with a sharp glass electrode to prevent Ca^{2+} influx through GluRs. Consequently, we will only initiate Ca^{2+} influx through postsynaptic DmCa1D channels. We analyzed 3 recordings from 3 different animals expressing the postsynaptic GCaMP3 construct (Figure 49). Controls yield an increase in fluorescence of 46 % (ΔF/F=0.46) upon extracellular stimulation of one action potential (blue bar, n=5). During intracellular stimulation of 1 action potential (light blue bar, n=3) we still get an increase in fluorescence of 12 % (ΔF/F=0.12) which is a reduction of 79 % compared to controls. Consequently, the postsynaptically localized construct MHC-CD8-SynapGCaMP3-Sh is not specific for Ca^{2+} influx exclusively through postsynaptic glutamate receptors (GluRs), but also recognizes Ca^{2+} influx through postsynaptic DmCa1D channels.

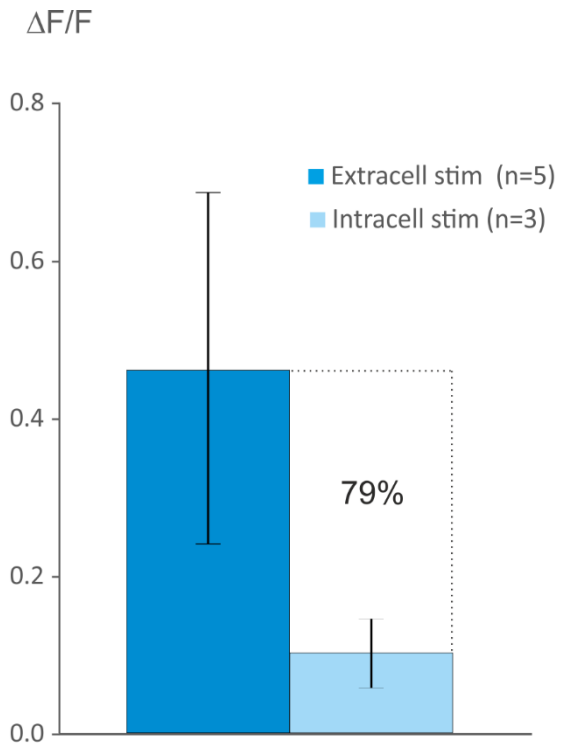

Figure 49: **The postsynaptic GCaMP3 construct recognizes Ca^{2+} influx through GluRs and through DmCa1D channels.** ΔF/F of the postsynaptically expressed MHC-CD8-Synap-GCaMP3-Sh during intracellular stimulation of muscle 6. To test if the SynapGCaMP3 construct also recognizes Ca^{2+} influx through postsynaptic DmCa1D channels we stimulated muscle 6 directly with an intracellular electrode. Stimulation was done with one action potential every 10 seconds. Blue bar shows ΔF/F during extracellular stimulation with a suction electrode (n=5). Intracellular stimulation (light blue bar, n=3) yields a change in fluorescence of 79 % in comparison of extracellular stimulation.

4 Discussion

I hypothesized that DmCa1D channels localize to the periactive zone of synaptic terminals of *Drosophila* larval NMJs to facilitate synaptic vesicle endocytosis. Accordingly, I predicted the subsynaptic location of DmCa1D not at the active zone within motoneuron terminals, but to the surrounding area called the periactive zone. To test this, I used a specific antibody against the DmCa1D channel together with antibodies against proteins localized to different areas within the presynaptic membrane. This prediction of DmCa1D channel localization to the periactive zone is supported by three results: First, DmCa1D channels do not co-localize with Bruchpilot and DmCa1A channels at active zones. Second, it localizes closely to the periactive zone protein Fasciclin II (Marie et al. 2004). And third, DmCa1D channels show partial overlap with the periactive zone protein Endophilin, which is part of the endocytic machinery (Schmidt et al. 1999). Based on these neuroanatomical findings, I predicted that loss of DmCa1D function causes increased synaptic depression. This was tested by recording evoked postsynaptic potentials (EPSPs) in controls and following DmCa1D RNAi knockdown as well as MARCM knockout specifically in a subset of motoneurons. Indeed, the data demonstrate that loss of DmCa1D function increased synaptic depression at motoneuron terminals. However, these results can either be explained by reduced activity dependent SV endocytosis, or alternatively, by a combination of vesicle depletion and reduced synaptic facilitation during repetitive stimulation. It could be possible that residual Ca^{2+}, which entered the cell through DmCa1D channels, mediates synaptic facilitation, which in turn partially compensates for depression caused by vesicle depletion (Zucker & Regehr 2002). Therefore, rigorous testing of my hypothesis required direct measurements of presynaptic vesicle recycling in controls and after blockade of DmCa1D channels. I conducted imaging experiments with the styryl dye FM1-43 which integrates into lipid bilayer membranes. Upon endocytosis, FM1-43 is incorporated into synaptic vesicles. The fluorescence signal corresponds to the rate of SV retrieval. During high potassium induced motoneuron firing and extracellular repetitive stimulation of axon terminals, loss of DmCa1D channels reduced SV endocytosis. These data are in agreement with a direct role of DmCa1D channels augmenting synaptic vesicle recycling, but not with a potential role in SV release. An important question is, whether the contribution of DmCa1D channels to synaptic vesicle endocytosis is relevant for neuromuscular function during behavior. Therefore, we measured motoneuron firing patterns during locomotion in semi-intact preparations and designed stimulation protocols to test the function of DmCa1D in the context of behaviorally relevant motoneuron activity patterns. This indeed demonstrated that loss of DmCa1D channels reduces synaptic vesicle recycling at motoneuron terminals during crawling-like firing

stimulation protocols. To further support the idea that presynaptic DmCa1D channels exclusively support Ca^{2+} dependent synaptic vesicle recycling, I conducted two series of experiments: First, I demonstrated activity dependent Ca^{2+} influx through DmCa1D channels into the presynaptic terminal by combining Ca^{2+} imaging with pharmacological blockade of DmCa1D channels. This demonstrated that the used GCaMP3-construct, which binds to the SV membrane, recognizes Ca^{2+} elevations in the whole terminal and not Ca^{2+} influx exclusively at the presynaptic membrane. Finally, I looked for additional evidence that DmCa1D does not support exocytosis. A direct proof that loss of DmCa1D function does not contribute to synaptic vesicle release at all requires a strict isolation of postsynaptic glutamate receptor (GluR) activation upon presynaptic vesicle release with and without DmCa1D function. This can be achieved by two-electrode voltage clamp recordings. By holding the muscle membrane potential at -80 mV, which is below the activation potential of DmCa1D channels, GluR activation is isolated (Guerrero et al. 2005; Peled & Isacoff 2011, 2014). This experiment was beyond the time frame of this thesis. Below I will outline and discuss my findings point by point.

4.1 Localization and function of DmCa1D channels in different compartments of larval motoneurons

In *Drosophila* larval motoneurons aCC and RP2 the DmCa1D L-type current could be measured in somatodendritic regions using patch clamp (Worrell & Levine 2008). Identification of DmCa1D as the main somatodendritic L-type current was concluded from a significant reduction of L-type current following DmCa1D RNAi knockdown. However, this provides only indirect evidence for the presence of DmCa1D channels in motoneurons, especially because RNAi knockdown throughout development bears the potential danger of indirect developmental defects on the composition of ionic currents of mature neurons. For example, in adult flight motoneurons, genetic loss of DmαG function causes a loss of somatodendritic DmCa1A currents (Ryglewski et al., 2012). Therefore, direct proof for the presence of DmCa1D channels in motoneurons is required. With a specific antibody against the DmCa1D calcium channel (3.1) we were able to directly show its localization in larval motoneurons (MNs) for the first time. The channel localizes to all compartments of these MNs: soma, axon, dendrites and terminals. The role of DmCa1D in axons may be the activation of Ca^{2+} dependent K^+ channels. A collaboration with Dr. Kadas in the Duch lab has shown that this BK current causes a fast hyperpolarization, which in turn augments fast Na^+ channel de-

inactivation, thus increasing maximum motoneuron firing rates during locomotion (Kadas et al. 2015). Based on this, I have demonstrated that action potential conduction along larval motoneuron axons indeed causes axonal Ca^{2+} influx through DmCa1D channels. Additional collaborative data (not shown in this thesis, Kadas, Ryglewski, Worrell & Duch, in preparation) indicate that this axonal Ca^{2+} influx indeed activated BK channels to facilitate motoneuron firing rates, and thus, maximum muscle contraction forces during locomotion. A similar function for Ca^{2+} activated K^{+} channels in maximizing neuronal firing rates has been shown in hippocampal CA1pyramidal cells (Gu et al. 2007) and cerebellar purkinje neurons (Womack & Khodakhah 2002), but so far not in motoneurons. Therefore, this study provides functional data for axonal L-type Ca^{2+} channels in motoneurons for the first time.

I also present immunocytochemical evidence for a dendritic localization of DmCa1D channels in motoneurons. In dendrites, DmCa1D yields a clustered pattern similar to L-type channels in spinal MNs (Heckman et al. 2003). DmCa1D may amplify postsynaptic input by increasing the duration of the synaptic drive potential during crawling burst activity (Kadas et al. in preparation). This also increases motoneuron firing responses to a given synaptic input. Therefore, axonal and dendritic DmCa1D channels increase motoneuron firing rates by different mechanisms, which act cooperatively. The dendritic function was previously well described in spinal motoneurons, which indicates highly conserved roles of dendritic L-type Ca^{2+} channels in excitability control of motoneurons (Heckmann et al. 2003). By contrast, the axonal function has not been described in vertebrates. I speculate that this is a unique specialization of unmyelinated invertebrate motoneurons.

High motoneuron firing rates cause large numbers of SVs to be released. This in turn requires high rates of SV recycling to maintain reliable neuromuscular transmission during ongoing motoneuron firing. In immunocytochemistry experiments with the synaptic vesicle (SV) protein Synaptotagmin we could show localization of DmCa1D to the presynaptic membrane (Figure 21). Therefore, the central aim of my work was to test whether DmCa1D channels augment SV recycling in a Ca^{2+} dependent manner during sustained motoneuron activity. This would mean that DmCa1D channels have three mechanistically different functions in three different compartments of larval motoneurons which all cooperate to ensure maximum muscle force generation.

4.1.1 Immunocytochemical evidence that DmCa1D channels, localized to motoneuron synaptic terminals, are not required for synaptic vesicle release at active zones

I first analyzed the subsynaptic localization of DmCa1D at the neuromuscular junction (NMJ). The presynaptic membrane is divided into active zones (AZ), which are the sites for SV exocytosis, and the active zones surrounding periactive zone (PZ). We used proteins of both zones to reveal DmCa1D localization. At mammalian central synapses and at the frog NMJ VGCCs and the Ca^{2+} sensor at SVs are tightly coupled with a distance of 10-20 nm to enable efficient, fast and precise synaptic transmission (Harlow et al. 2011; Bucurenciu et al. 2008; Eggermann et al. 2011). The active zone consists of highly specialized proteins: RIM (Graf et al. 2012; Müller et al. 2012), RIM-binding protein (Liu et al. 2011), Unc13 (Aravamudan et al. 1999), Liprin-α (Kaufmann et al. 2002; Fouquet et al. 2009), Syd-1 (Owald et al. 2010); Fife (Bruckner et al. 2012) and Bruchpilot (Kittel et al. 2006a; Wagh et al. 2006). The ELKS family member Bruchpilot forms T-bar structures at active zones and it couples VGCCs and SVs to enable fast synaptic transmission (Kittel et al. 2006a, Fouquet et al. 2009; Liu et al. 2011; Matkovich et al. 2013). With super-resolution light microscopy it is shown that AZs consist of single units each containing around 137 Bruchpilot molecules (Ehmann et al. 2014). Within these units voltage-gated DmCa1A channels are clustered (Liu et al. 2011; Maglione & Sgirist 2013). Fast synaptic transmission is possible exclusively at these highly organized structures. Consequently, to directly contribute to synaptic transmission DmCa1D channels have to localize in very close proximity to those units.

We used the T-bar forming CAZ protein Bruchpilot to identify AZs. Bruchpilot is the most commonly used active zone marker in *Drosophila*. A GFP-tagged splice variant of the VGCC DmCa1A, cac1-eGFP, served as second active zone marker (Kawasaki et al. 2002). Stainings with α-Bruchpilot (nc82) and α-DmCa1D (Figure 22) reveal no overlap but an alternating pattern at synaptic boutons. The same can be seen in stainings of α-DmCa1D with the GFP-tagged DmCa1A construct cac1-eGFP (Figure 23). In order to contribute to SV exocytosis DmCa1D channels have to co-localize with Bruchpilot proteins and DmCa1A channels at AZs. Only at AZs the essential tight coupling of VGCCs and SVs is given (Südhof 2012). After the peak in calcium influx is reached upon activity, release of transmitter starts after 200 µs. During these 200 µs, Ca^{2+} will diffuse around 50 nm away from channel pores, whereby AZs, containing multiple release units, are around 300 nm in diameter (Llinas 1977; Fogelson & Zucker 1985; Ehmann et al. 2014). Therefore, the distance between DmCa1D channels and AZs is too large for DmCa1D channels to contribute to exocytosis.

4.1.2 DmCa1D channels localize close to the endocytic machinery at the periactive zone of synaptic terminals

The periactive zone (PZ) at synaptic terminals is defined as the area surrounding active zones (Lahey et al. 1994; Schuster et al. 1996; Thomas et al. 1997; Beumer et al. 1999; Sone et al. 2000). Lacking presence at active zones we assumed DmCa1D localization at the PZ of MN terminals. Because this area occupies a large part of a bouton we had to determine DmCa1D localization within the PZ. For this we used two different proteins which are known to localize at different places at the PZ. Endophilin is part of the endocytic machinery and localizes closely to Dynamin and Dap160 (Micheva et al. 1997; Schmidt et al. 1999; Ringstad et al. 1999; Marie et al. 2004; Dickman et al. 2005). The cell adhesion molecule Fascicilin II (Fas II) is also localized to the PZ. It partially overlaps with proteins needed for endocytosis, but is mainly localized to a distinct area (Roos & Kelly 1998, 1999; Marie et al. 2004). It could be shown that DmCa1D channels localize to the periactive zone marked by Fas II (Figure 25) and Endophilin (Figure 27), thereby, showing partial overlap with both proteins. Endophilin staining was present throughout the whole presynaptic membrane only omitting AZs (Figure 26). This contradicts former studies, which claim that Endophilin localizes to the endocytic machinery at specific sites within the periactive zone (Roos & Kelly 1999; Schmidt et al. 1999; Marie et al. 2004). DmCa1D localization to the periactive zone shows that two different VGCCs exist at larval motoneuron terminals: DmCa1A channels at AZs and DmCa1D channels at the PZ. Localized to two different compartments, both channels likely mediate two different functions.

4.2 Reduction or loss of DmCa1D leads to increased depression at the NMJ

Previous studies at the *Drosophila* larval NMJ showed that at least three different VGCCs mediate Ca^{2+} influx at the presynaptic membrane (Kawasaki et al. 2000; Kuromi et al. 2004; Hou et al. 2008; Kuromi et al. 2010). The DmCa1A channel is known to localize at AZs mediating Ca^{2+} influx needed for fast synaptic transmission (Kawasaki et al. 2000, 2002, 2004; McLeod 2006; Hou et al. 2008; Liu et al. 2008). There is strong evidence for the existence of a La^{3+}-sensitive VGCC facilitating vesicle recycling (Kuromi et al. 2004; Hou et al. 2008; Kuromi et al. 2010). Contribution of Ca^{2+} influx to SV recycling could be shown in synapses of vertebrates and invertebrates (Heuser & Reese 1973; Gad et al. 1998; Guatimosim et al. 1998; Klingauf et al. 1998; Marks & McMahon 1998; Cousin & Robinson 1998, 2000; Neale et al. 1999; Sankaranarayanan and Ryan 2001; Kuromi et al. 2004; Zefirov et al. 2006;

Yamashita et al. 2010). A study at the *Drosophila* NMJ in 2009 attributed this Ca^{2+} influx to a Ca^{2+} hemi-channel named Flower. Localized to the SV membrane, two hemi-channels form a functional channel upon vesicle fusion with the presynaptic membrane (Yao et al. 2009). This protein was not subject of further investigations. I suggest that Ca^{2+} influx, contributing to endocytosis of SVs, is mediated by the VGCC DmCa1D. Endocytosis of SVs mainly takes place at the periactive zone of synaptic terminals involving the endocytic proteins dynamin and clathrin (Miller & Heuser 1984; Murthy & De Camilli 2003; Granseth et al. 2006; Ferguson et al. 2007; Smith et al. 2008; Dittman et al. 2009). Due to DmCa1D localization at the periactive zone of terminals I postulated the hypothesis that this VGCC facilitates Ca^{2+} influx, which regulates synaptic vesicle (SV) endocytosis. Reduction of this retrieval would impair release site clearance (Neher 2010; Haucke et al. 2011). As result, fewer SVs are able to be docked, primed and released. The readily releasable pool of SVs is depleted, which is called synaptic depression (Del Castillo & Katz 1954; Zucker 1989). In order to measure the effect of DmCa1D on synaptic depression we used two genetic tools to achieve a DmCa1D knockdown (RNAi) and knockout (MARCM). During repetitive stimulation with a frequency of 5 Hz, reduction (Figure 32) and loss of DmCa1D (Figure 34) increased synaptic depression at terminals of larval motoneurons aCC and RP2. Increased synaptic depression can be explained on the one hand by impairment of activity dependent retrieval of SVs. On the other hand, reduced residual Ca^{2+} concentrations, leading to reduced synaptic facilitation during repetitive stimulation, can reduce SV exocytosis. In order to distinguish between DmCa1D contributing to synaptic facilitation or SV endocytosis, release and retrieval of SVs has to be regarded separately.

4.3 Loss of DmCa1D reduces the rate of endocytosis but not exocytosis

Separate measuring of exocytosis and endocytosis was conducted with the styryl dye FM1-43. Motoneuron firing was induced with high potassium solution or with repetitive extracellular stimulation. Stimulations, which caused immense synaptic transmission, followed by immense SV retrieval, led to dye saturation of synaptic vesicles. Loss of DmCa1D seemed to have no effect on endocytosis (Figure 38). At several synapses it could be shown that exocytosis and endocytosis are directly coupled by large scaffolding proteins (Shupliakov et al. 1997; Gad et al. 1998; Gundelfinger et al. 2003; Murthy & De Camilli 2003; Dittman et al. 2009; Haucke et al. 2011). To enable fast synaptic transmission SVs have to be released with precise timing, which is given at AZ release sites. Membrane integrity preservation requires release site clearance and membrane retrieval after exocytosis. Furthermore, SV proteins have to be sorted

and retrieved after fusion of SVs with the presynaptic membrane. A large and complex set of structural and functional proteins accomplish these tasks (Gundelfinger et al. 2003). Ca^{2+} seems to be dispensible for endocytosis but rather acts as an activity dependent regulator, thereby enhancing SV retrieval. To highlight the regulative role of Ca^{2+} influx in endocytosis the amount of dye loaded into terminals had to be reduced. Under these conditions, loss of DmCa1D significantly decreased the rate of endocytosis without affecting exocytosis (Figure 40). This is in agreement with the supportive role of DmCa1D in endocytosis but not with DmCa1D contribution to exocytosis.

4.3.1 DmCa1D-enhanced endocytosis is relevant for neuromuscular function during behavior

To test the role of DmCa1D in endocytosis during behavior, we designed stimulation protocols similar to motoneuron firing patterns measured during locomotion. During larval crawling locomotion, motoneurons fire repetitive bursts corresponding to each stride. As mentioned above, exocytosis and endocytosis are automatic coupled by large scaffolding proteins. Because endocytosis takes places even in a Ca^{2+}-free environment (Ramaswami et al. 1994; Ryan et al. 1996; Deak et al. 2004), Ca^{2+}-influx seems to regulate enhancement of endocytosis in an activity dependent manner. Three different endocytic mechanisms are known: Kiss and run, ultrafast endocytosis and clathrin-mediated endocytosis (Kononenko et al. 2013; Zhou et al. 2014). Only the latter seems to be responsive to increased Ca^{2+} levels, below concentrations needed for release initiation (Ferguson et al. 2007). Depending on stimulation intensity, all three retrieval processes can occur (Gundelfinger et al. 2003). SVs retrieved via faster mechanisms like kiss and run or ultrafast endocytosis will be recycled and released again faster than via the slow clathrin-mediated endocytosis (Klingauf et al. 1998; Pyle et al. 2000; Sara et al. 2002). During 5 minutes of high activity, many vesicles will undergo release and retrieval multiple times. It is possible that all SVs of the recycling pool, passing release, retrieval and again release, are loaded with dye. Consequently, a supportive effect of Ca^{2+} in enhancing SV endocytosis will be masked when dye saturation of SVs is reached. Wildtype larvae accomplish 50 to 60 strides per minute at maximum during crawling on agarose plates (Saraswati et al. 2004; Fox et al. 2006). Loss of DmCa1D showed no effect on endocytosis during a maximum crawling speed stimulation protocol (Figure 43). However, in their natural environment, surrounded by food, crawling speed is reduced. And indeed, during lower crawling speed

stimulation protocols, loss of DmCa1D significantly reduces SV endocytosis. DmCa1D seems to play a regulatory role in endocytosis during behaviorally relevant motoneuron firing patterns.

4.4 Activity dependent Ca^{2+} influx through DmCa1D channels into the presynaptic terminal

Evidence for a regulatory role of DmCa1D in endocytosis but no contribution to exocytosis has been already provided above. To show activity dependent presynaptic Ca^{2+} influx through DmCa1D channels, Ca^{2+} imaging combined with pharmacological blockade of DmCa1D channels, was performed. With courtesy of André Fialas lab in Göttingen we received a fly line containing the construct UAS-SypGCaMP3 (Pech et al. 2015). Expressed in motoneurons, GCaMP3 localizes to the membrane of SVs. Upon activation, Ca^{2+} influx through DmCa1A channels reaches a concentration of 10-100 µM to enable SV exocytosis (Augustine 2001; Kawasaki et al. 2000; 2002; 2004; McLeod 2006; Hou et al. 2008). To initiate endocytosis of SVs the increase in Ca^{2+} concentration is much lower, above 1 µM Ca^{2+} retrieval even breaks down (von Gersdorff & Matthews 1994; Marks & McMahon 1998; Cousin & Robinson 2000). Regarding this, imaging of Ca^{2+} influx at the presynaptic membrane would consist of a major part, mediated by DmCa1A channels, and a minor part, mediated by DmCa1D channels. Contradicting to this, our results show that loss of DmCa1D reduces activity dependent presynaptic Ca^{2+} influx about 80 % (Figure 45).

The SypGCaMP3 construct is postulated to recognize presynaptic Ca^{2+} influx (Pech et al. 2015). The ectopically expressed rat-synaptophysin coupled to GCaMP3, localizes to the membrane of SVs. SVs are present in three different pools: the readily releasable pool, the recycling pool and the reserve pool (Rizzoli & Betz 2005). Upon activity, SVs of the readily releasable pool undergo exocytosis and are fused with the presynaptic membrane (Rettig & Neher 2002). Following endocytosis, SVs enter the recycling pool (Harata et al. 2001). SVs of the recycling pool are scattered throughout the whole terminal. During sustained intense release, SVs from the reserve pool are recruited to maintain synaptic transmission (Kuromi & Kidokoro 2000; Ikeda & Bekkers 2009; Kim & Ryan 2010). Consequently, localized to SVs, GCaMP3 is distributed throughout the whole terminal, in the readily releasable pool, the presynaptic membrane, the recycling pool and the reserve pool. During high frequency stimulation Ca^{2+} microdomains occur at active zones mediating exocytosis, which is indicated by increased GCaMP3 signal and might even be strong enough to saturate the Ca^{2+} indicator (Adler et al. 1991; Llinas et al. 1992; Stanley 1993; Neher 1998; Bucurenciu et al. 2008; Pech et al. 2015).

To recruit SVs for the readily releasable pool an increase in Ca^{2+} concentration in the whole terminal might be involved (Dittman & Regehr 1998; Stevens & Wesseling 1998; Wang & Kaczmarek 1998; Neher & Sakaba 2008). Stimulation above 30 Hz promotes recruitment of SVs from the reserve pool at the *Drosophila* NMJ, but initiation is not understood (Kuromi & Kidokoro 2000; Rizzoli & Betz 2005). Regarding the intracellular resting Ca^{2+} concentration at of ~100 nM and the dynamic range of GCaMP3 from ~100-10,000 nM, an increase in $[Ca^{2+}]$ in the whole terminal will also be detected by Syp-GCaMP3 (Tian et al. 2009). DmCa1D channels localize to the presynaptic and axon-terminal membrane. Consequently, loss of DmCa1D will reduce Ca^{2+} influx directly at the presynaptic membrane, but also at the whole membrane of the terminal. The global increase of $[Ca^{2+}]$ will be reduced, which will be detected by every SV in the terminal. With the SV bound Syp-GCaMP3 construct we could show activity dependent Ca^{2+} influx through DmCa1D channels at synaptic terminals. In addition to that it was not possible to isolate Ca^{2+} influx through DmCa1D channels at the presynaptic membrane only.

4.5 Role of DmCa1D in exocytosis

Experiments measuring synaptic depression showed that loss of DmCa1D reduced synaptic transmission (3.5). Whether this is due to impairments in SV endocytosis or exocytosis could not be separated with this experiment. Participation of DmCa1D in exocytosis of synaptic vesicles was investigated using the postsynaptically localized construct MHC-CD8-Synap-GCaMP3-Sh (Guerrero et al. 2005; Peled & Isacoff 2011, 2014). They claim that Ca^{2+} influx mediated by postsynaptic glutamate receptors (GluRs) will be recognized by this GCaMP3-construct, whereas Ca^{2+} influx through postsynaptic DmCa1D channels will not be recognized. Therefore, it should be possible to selectively measure GluR activation, which correlates with the amount of released transmitter. At a frequency of 0.1 Hz no synaptic depression occurs, hence, every Ca^{2+} signal upon a single stimulus should be similar (Wu et al. 2005). Upon stimulation with 1 action potential every 10 seconds, loss of DmCa1D caused a reduction of 78 % in GluR activation (Figure 48). This indicates that DmCa1D channels would contribute to 78 % of synaptic transmission, whereas only 22 % are mediated by DmCa1A channels. This is not in agreement with my own results that loss of DmCa1D has no effect on exocytosis, measured with the styryl dye FM1-43, and furthermore it contradicts the following published data. In DmCa1A null mutant embryos it could be shown that DmCa1A channels are essential and sufficient for fast synaptic transmission (Hou et al. 2008). DmCa1D channels are not

sufficient to induce muscle contraction, which was shown by a conditional genetic knockdown of DmCa1A channels that causes complete paralysis (Kawasaki et al. 2000; Rieckhof et al. 2003; MacLeod et al. 2006; Gu et al. 2009). A reduction of 78 % in GluR activation is highly unlikely caused by reduced synaptic function.

Despite claiming that the construct MHC-CD8-Synap-GCaMP3-Sh would only recognize postsynaptic Ca^{2+} influx through GluRs, but not DmCa1D channels, they used two-electrode voltage clamp (TEVC) to measure Ca^{2+} signals (Guerreo et al. 2005; Peled & Isacoff 2011, 2014). With this method, synaptic transmission is initiated by extracellular stimulation, while the muscle potential is clamped to -80 mV. Transmitter release leads to opening of GluRs following Ca^{2+} influx and membrane depolarization. Holding the muscle potential at -80 mV prevents opening of DmCa1D VGCCs and hence, Ca^{2+} influx through these channels. To test if the postsynaptic GCaMP3 construct does recognize Ca^{2+} influx through postsynaptic DmCa1D channels in current clamp mode, we stimulated the muscle with an intracellular electrode. By directly depolarizing the muscle membrane, synaptic transmission is circumvented and only DmCa1D channels will open to mediate postsynaptic Ca^{2+} influx. During extracellular stimulation, the Ca^{2+} signal upon 1 AP increases to ~50 %, while intracellular stimulation yields an increase in fluorescence of already 12 % (Figure 49). With this experiment we can show that during extracellular stimulation in current clamp mode, the MHC-CD8-Synap-GCaMP3-Sh construct recognizes postsynaptic Ca^{2+} influx through GluRs as well as DmCa1D channels. To eliminate Ca^{2+} influx through DmCa1D channels the method of two-electrode voltage clamp has to be used to hold the membrane potential below VGCC opening. This experiment was beyond the time frame of this thesis. With the conducted experiment we were not able to exclude a role of DmCa1D in exocytosis.

4.6 Conclusion

At several synapses it could be shown that Ca^{2+} plays a role in SV endocytosis (Ceccarelli & Hurlbut 1980; Thomas et al. 1990; Smith & Neher 1997; Gad et al. 1998; Naele et al. 1999; Kuromi & Kidokoro 2002; Kuromi et al. 2004; Wu et al. 2007; Xu et al. 2008; Hosoi et al. 2009). At the *Drosophila* NMJ evidence was given that a Ca^{2+} channel mediates Ca^{2+} influx needed for enhanced SV retrieval at the periactive zone of synaptic terminals (Kuromi et al. 2004; Hou et al. 2008; Kuromi et al. 2010). A proposed complex mechanism by which two SV-bound hemi-channels form a functional channel upon fusion with the presynaptic membrane called Flower, was not subject of further studies (Yao et al. 2009). With this study I show

evidence that Ca^{2+} influx contributing to SV endocytosis is facilitated by the VGCC DmCa1D at motoneuron terminals. With a specific antibody against DmCa1D, channel localization to presynaptic terminals could be shown. DmCa1D channels are not localized at active zones, which are specialized regions within the terminal enabling fast and efficient SV release (Couteaux & Pecot-Dechavassine 1970; Südhof 2012). But, they are localized at the periactive zone, which is the area surrounding active zones (Lahey et al. 1994; Schuster et al. 1996; Thomas et al. 1997; Beumer et al. 1999; Sone et al. 2000). Reduction and loss of DmCa1D channels caused increased synaptic depression. Because this can be explained by impairments in endocytosis and exocytosis, direct imaging of SV retrieval and release with the styryl dye Fm1-43 was conducted (Betz & Bewick 1992; Betz et al. 1996). Loss of DmCa1D showed a reduction in endocytosis during behaviorally relevant motoneuron firing patterns, whereas exocytosis remained unaffected. Ca^{2+} imaging experiments demonstrated, that loss of DmCa1D reduces activity dependent Ca^{2+} influx into synaptic terminals. This could not be shown exclusively at the presynaptic membrane, but at the whole terminal. Whether Ca^{2+} influx through DmCa1D channels contributes to SV release was tested by measuring postsynaptic GluR activation with postsynaptic Ca^{2+} imaging (Guerrero et al. 2005). In current clamp mode it is not possible to exclusively measure postsynaptic Ca^{2+} influx through GluR, because DmCa1D VGCCs open upon membrane depolarization and cause additional Ca^{2+} influx. Isolation of GluR activation can be achieved by using two-electrode voltage clamp. While the muscle membrane potential is clamped to -80 mV, DmCa1D channels will not open. Ca^{2+} influx through postsynaptic GluRs, which corresponds to synaptic transmission, can then be measured via Ca^{2+} imaging or by recording postsynaptic potentials (Guerrero et al. 2005; Peled & Isacoff 2011, 2014). Because of the limited time frame of this thesis I did not conducted these experiments. However, we have evidence that DmCa1D channels do not contribute to SV release. First, we could show that DmCa1D does not localize to active zones of synaptic terminals. To initiate exocytosis of SVs an immense increase in Ca^{2+} concentration is necessary (Augustine et al. 2001). Because such Ca^{2+} concentrations are toxic to the cell these elevations occur only at very small areas (nm) surrounding active zones, called microdomains (Adler et al. 1991; Heidelberger et al. 1994; Schneggenburger & Neher 2000; Gundelfinger et al. 2003). To accomplish this, VGCCs and SVs have to be in close proximity to each other, which is only given at active zones (Meinrenken et al. 2003; Liu et al. 2011; Matkovich et al. 2013; Maglione & Sigrist 2013). The localization of DmCa1D channels to the periactive zone means that they are too far away from active zones to contribute to the Ca^{2+} microdomains (~tens of nanometers) (Harlow et al. 2011; Bucurenciu et al. 2008; Eggermann et al. 2011). Second, in measurements

of the endocytosis rate with the amphiphilic dye FM1-43, exocytosis remained intact after incubation with the pharmacological DmCa1D blocker lanthanum. Together, these data give strong evidence that DmCa1D, localized to the periactive zone of synaptic terminals, is the Ca^{2+} channel, which mediates Ca^{2+} influx needed for enhanced SV endocytosis (Kuromi et al. 2004; Hou et al. 2008; Kuromi et al. 2010). Because exocytosis and endocytosis are coupled through large scaffolding proteins, endocytosis takes place even in a Ca^{2+} free environment (Ramaswami et al. 1994; Ryan et al. 1996; Gundelfinger et al. 2003; Deak et al. 2004; Haucke et al. 2011). Therefore, DmCa1D seems to act as a fine-regulator of enhanced endocytosis in an activity-dependent manner.

5 References

Adler, E. M.; Augustine, G. J.; Duffy, S. N.; Charlton, M. P. (1991): Alien intracellular calcium chelators attenuate neurotransmitter release at the squid giant synapse. In: *The Journal of neuroscience: the official journal of the Society for Neuroscience* 11 (6), S. 1496–1507.

Ahlijanian, M. K.; Westenbroek, R. E.; Catterall, W. A. (1990): Subunit structure and localization of dihydropyridine-sensitive calcium channels in mammalian brain, spinal cord, and retina. In: *Neuron* 4 (6), S. 819–832.

Akerboom, Jasper; Chen, Tsai-Wen; Wardill, Trevor J.; Tian, Lin; Marvin, Jonathan S.; Mutlu, Sevinc et al. (2012): Optimization of a GCaMP calcium indicator for neural activity imaging. In: *The Journal of neuroscience : the official journal of the Society for Neuroscience* 32 (40), S. 13819–13840. DOI: 10.1523/JNEUROSCI.2601-12.2012.

Akerboom, Jasper; Rivera, Jonathan D. Velez; Guilbe, Maria M. Rodriguez; Malave, Elisa C. Alfaro; Hernandez, Hector H.; Tian, Lin et al. (2009): Crystal structures of the GCaMP calcium sensor reveal the mechanism of fluorescence signal change and aid rational design. In: *The Journal of biological chemistry* 284 (10), S. 6455–6464. DOI: 10.1074/jbc.M807657200.

Allbritton, N. L.; Meyer, T.; Stryer, L. (1992): Range of messenger action of calcium ion and inositol 1,4,5-trisphosphate. In: *Science (New York, N.Y.)* 258 (5089), S. 1812–1815.

Andronache, Zoita; Ursu, Daniel; Lehnert, Simone; Freichel, Marc; Flockerzi, Veit; Melzer, Werner (2007): The auxiliary subunit gamma 1 of the skeletal muscle L-type Ca2+ channel is an endogenous Ca2+ antagonist. In: *Proceedings of the National Academy of Sciences of the United States of America* 104 (45), S. 17885–17890. DOI: 10.1073/pnas.0704340104.

Astorga, Guadalupe; Hartel, Steffen; Sanhueza, Magdalena; Bacigalupo, Juan (2012): TRP, TRPL and cacophony channels mediate Ca2+ influx and exocytosis in photoreceptors axons in Drosophila. In: *PloS one* 7 (8), S. e44182. DOI: 10.1371/journal.pone.0044182.

Atwood, H. L.; Govind, C. K.; Wu, C. F. (1993): Differential ultrastructure of synaptic terminals on ventral longitudinal abdominal muscles in Drosophila larvae. In: *Journal of neurobiology* 24 (8), S. 1008–1024. DOI: 10.1002/neu.480240803.

Augustine, G. J. (2001): How does calcium trigger neurotransmitter release? In: *Current opinion in neurobiology* 11 (3), S. 320–326.

Baird, G. S.; Zacharias, D. A.; Tsien, R. Y. (1999): Circular permutation and receptor insertion within green fluorescent proteins. In: *Proceedings of the National Academy of Sciences of the United States of America* 96 (20), S. 11241–11246.

Baker, P. F.; Blaustein, M. P.; Hodgkin, A. L.; Steinhardt, R. A. (1969): The influence of calcium on sodium efflux in squid axons. In: *The Journal of physiology* 200 (2), S. 431–458.

Bate, M. (1990): The embryonic development of larval muscles in Drosophila. In: *Development (Cambridge, England)* 110 (3), S. 791–804.

Bate M (1993). The mesoderm and its derivatives. In: The development of *Drosophila melanogaster* (Bate M, Martinez Arias A, eds), pp 1013–1090. Cold Spring Harbor, NY: Cold Spring Harbor Laboratory.

Bate, M.; Broadie, K. (1995): Wiring by fly: the neuromuscular system of the Drosophila embryo. In: *Neuron* 15 (3), S. 513–525.

Bean, B. P. (1989): Classes of calcium channels in vertebrate cells. In: *Annual review of physiology* 51, S. 367–384. DOI: 10.1146/annurev.ph.51.030189.002055.

Bear M. F., Connors B. W. & Paradiso M. A.: *Neuroscience, Exploring the Brain.* Lippincott Williams & Wilkins, 2007, p. 61; p. 778.

Berridge, M. J. (1991): Cytoplasmic calcium oscillations: a two pool model. In: *Cell calcium* 12 (2-3), S. 63–72.

Berridge, M. J. (1993): Cell signalling. A tale of two messengers. In: *Nature* 365 (6445), S. 388–389. DOI: 10.1038/365388a0.

Berridge, M. J.; Bootman, M. D.; Lipp, P. (1998): Calcium--a life and death signal. In: *Nature* 395 (6703), S. 645–648. DOI: 10.1038/27094.

Berridge, M. J.; Lipp, P.; Bootman, M. D. (2000): The versatility and universality of calcium signalling. In: *Nature reviews. Molecular cell biology* 1 (1), S. 11–21. DOI: 10.1038/35036035.

Betz, W. J.; Bewick, G. S. (1992): Optical analysis of synaptic vesicle recycling at the frog neuromuscular junction. In: *Science (New York, N.Y.)* 255 (5041), S. 200–203.

Betz, W. J.; Mao, F.; Bewick, G. S. (1992): Activity-dependent fluorescent staining and destaining of living vertebrate motor nerve terminals. In: *The Journal of neuroscience : the official journal of the Society for Neuroscience* 12 (2), S. 363–375.

Betz, W. J.; Mao, F.; Smith, C. B. (1996): Imaging exocytosis and endocytosis. In: *Current opinion in neurobiology* 6 (3), S. 365–371.

Beumer, K. J.; Rohrbough, J.; Prokop, A.; Broadie, K. (1999): A role for PS integrins in morphological growth and synaptic function at the postembryonic neuromuscular junction of Drosophila. In: *Development (Cambridge, England)* 126 (24), S. 5833–5846.

Bodi, J.; Nishio, H.; Zhou, Y.; Branton, W. D.; Kimura, T.; Sakakibara, S. (1995): Synthesis of an O-palmitoylated 44-residue peptide amide (PLTX II) blocking presynaptic calcium channels in Drosophila. In: *Peptide research* 8 (4), S. 228–235.

Boehning, Darren; Patterson, Randen L.; Sedaghat, Leela; Glebova, Natalia O.; Kurosaki, Tomohiro; Snyder, Solomon H. (2003): Cytochrome c binds to inositol (1,4,5) trisphosphate receptors, amplifying calcium-dependent apoptosis. In: *Nature cell biology* 5 (12), S. 1051–1061. DOI: 10.1038/ncb1063.

Bossing, T.; Udolph, G.; Doe, C. Q.; Technau, G. M. (1996): The embryonic central nervous system lineages of Drosophila melanogaster. I. Neuroblast lineages derived from the ventral half of the neuroectoderm. In: *Developmental biology* 179 (1), S. 41–64. DOI: 10.1006/dbio.1996.0240.

Brandt, Andreas; Striessnig, Joerg; Moser, Tobias (2003): CaV1.3 channels are essential for development and presynaptic activity of cochlear inner hair cells. In: *The Journal of neuroscience : the official journal of the Society for Neuroscience* 23 (34), S. 10832–10840.

Broadie, K.; Sink, H.; van Vactor, D.; Fambrough, D.; Whitington, P. M.; Bate, M.; Goodman, C. S. (1993): From growth cone to synapse: the life history of the RP3 motor neuron. In: *Development (Cambridge, England). Supplement*, S. 227–238.

Broadie, Kendal S.; Richmond, Janet E. (2002): Establishing and sculpting the synapse in Drosophila and C. elegans. In: *Current opinion in neurobiology* 12 (5), S. 491–498.

Broadus, J.; Skeath, J. B.; Spana, E. P.; Bossing, T.; Technau, G.; Doe, C. Q. (1995): New neuroblast markers and the origin of the aCC/pCC neurons in the Drosophila central nervous system. In: *Mechanisms of development* 53 (3), S. 393–402.

Bucurenciu, Iancu; Kulik, Akos; Schwaller, Beat; Frotscher, Michael; Jonas, Peter (2008): Nanodomain coupling between Ca2+ channels and Ca2+ sensors promotes fast and efficient transmitter release at a cortical GABAergic synapse. In: *Neuron* 57 (4), S. 536–545. DOI: 10.1016/j.neuron.2007.12.026.

Budnik, V. (1996): Synapse maturation and structural plasticity at Drosophila neuromuscular junctions. In: *Current opinion in neurobiology* 6 (6), S. 858–867.

Buraei, Zafir; Yang, Jian (2010): The ss subunit of voltage-gated Ca2+ channels. In: *Physiological reviews* 90 (4), S. 1461–1506. DOI: 10.1152/physrev.00057.2009.

Burk, S. E.; Lytton, J.; MacLennan, D. H.; Shull, G. E. (1989): cDNA cloning, functional expression, and mRNA tissue distribution of a third organellar Ca2+ pump. In: *The Journal of biological chemistry* 264 (31), S. 18561–18568.

Cain, Stuart M.; Snutch, Terrance P. (2010): Contributions of T-type calcium channel isoforms to neuronal firing. In: *Channels (Austin, Tex.)* 4 (6), S. 475–482. DOI: 10.4161/chan.4.6.14106.

Calderon-Rivera, Aida; Andrade, Arturo; Hernandez-Hernandez, Oscar; Gonzalez-Ramirez, Ricardo; Sandoval, Alejandro; Rivera, Manuel et al. (2012): Identification of a disulfide bridge essential for structure and function of the voltage-gated Ca(2+) channel alpha(2)delta-1 auxiliary subunit. In: *Cell calcium* 51 (1), S. 22–30. DOI: 10.1016/j.ceca.2011.10.002.

Campiglio, Marta; Flucher, Bernhard E. (2015): The role of auxiliary subunits for the functional diversity of voltage-gated calcium channels. In: *Journal of cellular physiology* 230 (9), S. 2019–2031. DOI: 10.1002/jcp.24998.

Campos-Ortage J. A. & Hartenstein V.: *The Embryonic Development of Drosophila melanogaster.* Berlin: Springer Verlag. 1985.

Carbone, E.; Lux, H. D. (1984): A low voltage-activated, fully inactivating Ca channel in vertebrate sensory neurones. In: *Nature* 310 (5977), S. 501–502.

Carlin, Kevin P.; Bui, Tuan V.; Dai, Yue; Brownstone, Robert M. (2009): Staircase currents in motoneurons: insight into the spatial arrangement of calcium channels in the dendritic tree. In: *The Journal of neuroscience : the official journal of the Society for Neuroscience* 29 (16), S. 5343–5353. DOI: 10.1523/JNEUROSCI.5458-08.2009.

Catterall, W. A. (2000): Structure and regulation of voltage-gated Ca2+ channels. In: *Annual review of cell and developmental biology* 16, S. 521–555. DOI: 10.1146/annurev.cellbio.16.1.521.

Catterall, William A.; Perez-Reyes, Edward; Snutch, Terrance P.; Striessnig, Joerg (2005): International Union of Pharmacology. XLVIII. Nomenclature and structure-function relationships of voltage-gated calcium channels. In: *Pharmacological reviews* 57 (4), S. 411–425. DOI: 10.1124/pr.57.4.5.

Cauvin, C.; Loutzenhiser, R.; van Breemen, C. (1983): Mechanisms of calcium antagonist-induced vasodilation. In: *Annual review of pharmacology and toxicology* 23, S. 373–396. DOI: 10.1146/annurev.pa.23.040183.002105.

Ceccarelli, B.; Hurlbut, W. P. (1980): Vesicle hypothesis of the release of quanta of acetylcholine. In: *Physiological reviews* 60 (2), S. 396–441.

Ceccarelli, B.; Hurlbut, W. P.; Mauro, A. (1973): Turnover of transmitter and synaptic vesicles at the frog neuromuscular junction. In: *The Journal of cell biology* 57 (2), S. 499–524.

Chang, H.; Ciani, S.; Kidokoro, Y. (1994): Ion permeation properties of the glutamate receptor channel in cultured embryonic Drosophila myotubes. In: *The Journal of physiology* 476 (1), S. 1–16.

Chang, Kenneth; Elledge, Stephen J.; Hannon, Gregory J. (2006): Lessons from Nature: microRNA-based shRNA libraries. In: *Nature methods* 3 (9), S. 707–714. DOI: 10.1038/nmeth923.

Chen, Ren-Shiang; Deng, Tzyy-Chyn; Garcia, Thomas; Sellers, Zachary M.; Best, Philip M. (2007): Calcium channel gamma subunits: a functionally diverse protein family. In: *Cell biochemistry and biophysics* 47 (2), S. 178–186.

Chen, Yingxiao; Song, Xianqiang; Ye, Sheng; Miao, Lin; Zhu, Yun; Zhang, Rong-Guang; Ji, Guangju (2013): Structural insight into enhanced calcium indicator GCaMP3 and GCaMPJ to promote further improvement. In: *Protein & cell* 4 (4), S. 299–309. DOI: 10.1007/s13238-013-2103-4.

Chen, Yu-Hang; Li, Ming-Hui; Zhang, Yun; He, Lin-Ling; Yamada, Yoichi; Fitzmaurice, Aileen et al. (2004): Structural basis of the alpha1-beta subunit interaction of voltage-gated Ca2+ channels. In: *Nature* 429 (6992), S. 675–680. DOI: 10.1038/nature02641.

Chiba, A.; Rose, D. (1998): "Painting" the target: how local molecular cues define synaptic relationships. In: *BioEssays : news and reviews in molecular, cellular and developmental biology* 20 (11), S. 941–948. DOI: 10.1002/(SICI)1521-1878(199811)20:11<941::AID-BIES9>3.0.CO;2-D.

Chiba, A.; Snow, P.; Keshishian, H.; Hotta, Y. (1995): Fasciclin III as a synaptic target recognition molecule in Drosophila. In: *Nature* 374 (6518), S. 166–168. DOI: 10.1038/374166a0.

Choi, James C.; Park, Demian; Griffith, Leslie C. (2004): Electrophysiological and morphological characterization of identified motor neurons in the Drosophila third instar larva central nervous system. In: *Journal of neurophysiology* 91 (5), S. 2353–2365. DOI: 10.1152/jn.01115.2003.

Chu-LaGraff, Q.; Schmid, A.; Leidel, J.; Bronner, G.; Jackle, H.; Doe, C. Q. (1995): huckebein specifies aspects of CNS precursor identity required for motoneuron axon pathfinding. In: *Neuron* 15 (5), S. 1041–1051.

Clapham, D. E. (1995): Calcium signaling. In: *Cell* 80 (2), S. 259–268.

Cochilla, A. J.; Angleson, J. K.; Betz, W. J. (1999): Monitoring secretory membrane with FM1-43 fluorescence. In: *Annual review of neuroscience* 22, S. 1–10. DOI: 10.1146/annurev.neuro.22.1.1.

Contreras, Diego (2006): The role of T-channels in the generation of thalamocortical rhythms. In: *CNS & neurological disorders drug targets* 5 (6), S. 571–585.

Cousin, M. A.; Robinson, P. J. (1998): Ba2+ does not support synaptic vesicle retrieval in rat cerebrocortical synaptosomes. In: *Neuroscience letters* 253 (1), S. 1–4.

Cousin, M. A.; Robinson, P. J. (2000): Ca(2+) influx inhibits dynamin and arrests synaptic vesicle endocytosis at the active zone. In: *The Journal of neuroscience : the official journal of the Society for Neuroscience* 20 (3), S. 949–957.

Couteaux, R.; Pecot-Dechavassine, M. (1970): Synaptic vesicles and pouches at the level of "active zones" of the neuromuscular junction. In: *Comptes rendus hebdomadaires des seances de l'Academie des sciences. Serie D: Sciences naturelles* 271 (25), S. 2346–2349.

Crandall, Shane R.; Govindaiah, G.; Cox, Charles L. (2010): Low-threshold Ca2+ current amplifies distal dendritic signaling in thalamic reticular neurons. In: *The Journal of neuroscience : the official journal of the Society for Neuroscience* 30 (46), S. 15419–15429. DOI: 10.1523/JNEUROSCI.3636-10.2010.

Crivici, A.; Ikura, M. (1995): Molecular and structural basis of target recognition by calmodulin. In: *Annual review of biophysics and biomolecular structure* 24, S. 85–116. DOI: 10.1146/annurev.bb.24.060195.000505.

Davies, Anthony; Kadurin, Ivan; Alvarez-Laviada, Anita; Douglas, Leon; Nieto-Rostro, Manuela; Bauer, Claudia S. et al. (2010): The alpha2delta subunits of voltage-gated calcium channels form GPI-anchored proteins, a posttranslational modification essential for function. In: *Proceedings of the National Academy of Sciences of the United States of America* 107 (4), S. 1654–1659. DOI: 10.1073/pnas.0908735107.

Davis, G. W.; Bezprozvanny, I. (2001): Maintaining the stability of neural function: a homeostatic hypothesis. In: *Annual review of physiology* 63, S. 847–869. DOI: 10.1146/annurev.physiol.63.1.847.

de Lange, R P J; de Roos, A D G; Borst, J. G. G. (2003): Two modes of vesicle recycling in the rat calyx of Held. In: *The Journal of neuroscience : the official journal of the Society for Neuroscience* 23 (31), S. 10164–10173.

Deak, Ferenc; Schoch, Susanne; Liu, Xinran; Sudhof, Thomas C.; Kavalali, Ege T. (2004): Synaptobrevin is essential for fast synaptic-vesicle endocytosis. In: *Nature cell biology* 6 (11), S. 1102–1108. DOI: 10.1038/ncb1185.

DEL CASTILLO, J.; KATZ, B. (1954): Statistical factors involved in neuromuscular facilitation and depression. In: *The Journal of physiology* 124 (3), S. 574–585.

Delgado, R.; Maureira, C.; Oliva, C.; Kidokoro, Y.; Labarca, P. (2000): Size of vesicle pools, rates of mobilization, and recycling at neuromuscular synapses of a Drosophila mutant, shibire. In: *Neuron* 28 (3), S. 941–953.

Dickman, Dion K.; Horne, Jane Anne; Meinertzhagen, Ian A.; Schwarz, Thomas L. (2005): A slowed classical pathway rather than kiss-and-run mediates endocytosis at synapses lacking synaptojanin and endophilin. In: *Cell* 123 (3), S. 521–533. DOI: 10.1016/j.cell.2005.09.026.

Dietrich, Dirk; Kirschstein, Timo; Kukley, Maria; Pereverzev, Alexej; Brelie, Christian von der; Schneider, Toni; Beck, Heinz (2003): Functional specialization of presynaptic Cav2.3 Ca2+ channels. In: *Neuron* 39 (3), S. 483–496.

Dietzl, Georg; Chen, Doris; Schnorrer, Frank; Su, Kuan-Chung; Barinova, Yulia; Fellner, Michaela et al. (2007): A genome-wide transgenic RNAi library for conditional gene inactivation in Drosophila. In: *Nature* 448 (7150), S. 151–156. DOI: 10.1038/nature05954.

DiPolo, Reinaldo; Beauge, Luis (2006): Sodium/calcium exchanger: influence of metabolic regulation on ion carrier interactions. In: *Physiological reviews* 86 (1), S. 155–203. DOI: 10.1152/physrev.00018.2005.

Dittman, J. S.; Regehr, W. G. (1998): Calcium dependence and recovery kinetics of presynaptic depression at the climbing fiber to Purkinje cell synapse. In: *The Journal of neuroscience : the official journal of the Society for Neuroscience* 18 (16), S. 6147–6162.

Dittman, Jeremy; Ryan, Timothy A. (2009): Molecular circuitry of endocytosis at nerve terminals. In: *Annual review of cell and developmental biology* 25, S. 133–160. DOI: 10.1146/annurev.cellbio.042308.113302.

Doe, C. Q.; Hiromi, Y.; Gehring, W. J.; Goodman, C. S. (1988): Expression and function of the segmentation gene fushi tarazu during Drosophila neurogenesis. In: *Science (New York, N.Y.)* 239 (4836), S. 170–175.

Doe, C. Q.; Smouse, D.; Goodman, C. S. (1988): Control of neuronal fate by the Drosophila segmentation gene even-skipped. In: *Nature* 333 (6171), S. 376–378. DOI: 10.1038/333376a0.

Doering, Clinton J.; Zamponi, Gerald W. (2003): Molecular pharmacology of high voltage-activated calcium channels. In: *Journal of bioenergetics and biomembranes* 35 (6), S. 491–505.

Dolmetsch, R. E.; Xu, K.; Lewis, R. S. (1998): Calcium oscillations increase the efficiency and specificity of gene expression. In: *Nature* 392 (6679), S. 933–936. DOI: 10.1038/31960.

Dolphin, Annette C. (2003): Beta subunits of voltage-gated calcium channels. In: *Journal of bioenergetics and biomembranes* 35 (6), S. 599–620.

Dolphin, Annette C. (2009): Calcium channel diversity: multiple roles of calcium channel subunits. In: *Current opinion in neurobiology* 19 (3), S. 237–244. DOI: 10.1016/j.conb.2009.06.006.

Dreosti, Elena; Odermatt, Benjamin; Dorostkar, Mario M.; Lagnado, Leon (2009): A genetically encoded reporter of synaptic activity in vivo. In: *Nature methods* 6 (12), S. 883–889. DOI: 10.1038/nmeth.1399.

Dresbach, T.; Qualmann, B.; Kessels, M. M.; Garner, C. C.; Gundelfinger, E. D. (2001): The presynaptic cytomatrix of brain synapses. In: *Cellular and molecular life sciences : CMLS* 58 (1), S. 94–116. DOI: 10.1007/PL00000781.

Du Lac, S.; Bastiani, M. J.; Goodman, C. S. (1986): Guidance of neuronal growth cones in the grasshopper embryo. II. Recognition of a specific axonal pathway by the aCC neuron. In: *The Journal of neuroscience : the official journal of the Society for Neuroscience* 6 (12), S. 3532–3541.

Dunlap, K.; Luebke, J. I.; Turner, T. J. (1995): Exocytotic Ca2+ channels in mammalian central neurons. In: *Trends in neurosciences* 18 (2), S. 89–98.

Eberl, D. F.; Ren, D.; Feng, G.; Lorenz, L. J.; van Vactor, D.; Hall, L. M. (1998): Genetic and developmental characterization of Dmca1D, a calcium channel alpha1 subunit gene in Drosophila melanogaster. In: *Genetics* 148 (3), S. 1159–1169.

Eckl, Nina. Analyse und Funktion von DmCa1D Calcium-Kanälen in verschiedenen Kompartimenten larvaler *Drosophila* Motoneurone. Masterarbeit, J.-Gutenberg Universität Mainz, 2016.

Eggermann, Emmanuel; Bucurenciu, Iancu; Goswami, Sarit Pati; Jonas, Peter (2011): Nanodomain coupling between Ca(2)(+) channels and sensors of exocytosis at fast mammalian synapses. In: *Nature reviews. Neuroscience* 13 (1), S. 7–21. DOI: 10.1038/nrn3125.

Ehmann, Nadine; van de Linde, Sebastian; Alon, Amit; Ljaschenko, Dmitrij; Keung, Xi Zhen; Holm, Thorge et al. (2014): Quantitative super-resolution imaging of Bruchpilot distinguishes active zone states. In: *Nature communications* 5, S. 4650. DOI: 10.1038/ncomms5650.

Elbashir, S. M.; Martinez, J.; Patkaniowska, A.; Lendeckel, W.; Tuschl, T. (2001): Functional anatomy of siRNAs for mediating efficient RNAi in Drosophila melanogaster embryo lysate. In: *The EMBO journal* 20 (23), S. 6877–6888. DOI: 10.1093/emboj/20.23.6877.

Ellis, S. B.; Williams, M. E.; Ways, N. R.; Brenner, R.; Sharp, A. H.; Leung, A. T. et al. (1988): Sequence and expression of mRNAs encoding the alpha 1 and alpha 2 subunits of a DHP-sensitive calcium channel. In: *Science (New York, N.Y.)* 241 (4873), S. 1661–1664.

Fang, Kun; Colecraft, Henry M. (2011): Mechanism of auxiliary beta-subunit-mediated membrane targeting of L-type (Ca(V)1.2) channels. In: *The Journal of physiology* 589 (Pt 18), S. 4437–4455. DOI: 10.1113/jphysiol.2011.214247.

Ferron, Laurent; Davies, Anthony; Page, Karen M.; Cox, David J.; Leroy, Jerome; Waithe, Dominic et al. (2008): The stargazin-related protein gamma 7 interacts with the mRNA-binding protein heterogeneous nuclear ribonucleoprotein A2 and regulates the stability of specific mRNAs, including CaV2.2. In: *The Journal of neuroscience : the official journal of the Society for Neuroscience* 28 (42), S. 10604–10617. DOI: 10.1523/JNEUROSCI.2709-08.2008.

Fogelson, A. L.; Zucker, R. S. (1985): Presynaptic calcium diffusion from various arrays of single channels. Implications for transmitter release and synaptic facilitation. In: *Biophysical journal* 48 (6), S. 1003–1017. DOI: 10.1016/S0006-3495(85)83863-7.

Fouquet, Wernher; Owald, David; Wichmann, Carolin; Mertel, Sara; Depner, Harald; Dyba, Marcus et al. (2009): Maturation of active zone assembly by Drosophila Bruchpilot. In: *The Journal of cell biology* 186 (1), S. 129–145. DOI: 10.1083/jcb.200812150.

Fox, Lyle E.; Soll, David R.; Wu, Chun-Fang (2006): Coordination and modulation of locomotion pattern generators in Drosophila larvae: effects of altered biogenic amine levels by the tyramine beta hydroxlyase mutation. In: *The Journal of neuroscience : the official journal of the Society for Neuroscience* 26 (5), S. 1486–1498. DOI: 10.1523/JNEUROSCI.4749-05.2006.

Freise, D.; Held, B.; Wissenbach, U.; Pfeifer, A.; Trost, C.; Himmerkus, N. et al. (2000): Absence of the gamma subunit of the skeletal muscle dihydropyridine receptor increases L-type Ca2+ currents and alters channel inactivation properties. In: *The Journal of biological chemistry* 275 (19), S. 14476–14481.

Fujioka, Miki; Lear, Bridget C.; Landgraf, Matthias; Yusibova, Galina L.; Zhou, Jian; Riley, Kristen M. et al. (2003): Even-skipped, acting as a repressor, regulates axonal projections in Drosophila. In: *Development (Cambridge, England)* 130 (22), S. 5385–5400. DOI: 10.1242/dev.00770.

Fuller-Bicer, Geraldine A.; Varadi, Gyula; Koch, Sheryl E.; Ishii, Masakazu; Bodi, Ilona; Kadeer, Nijiat et al. (2009): Targeted disruption of the voltage-dependent calcium channel alpha2/delta-1-subunit. In: *American journal of physiology. Heart and circulatory physiology* 297 (1), S. H117-24. DOI: 10.1152/ajpheart.00122.2009.

Gad, H.; Low, P.; Zotova, E.; Brodin, L.; Shupliakov, O. (1998): Dissociation between Ca2+-triggered synaptic vesicle exocytosis and clathrin-mediated endocytosis at a central synapse. In: *Neuron* 21 (3), S. 607–616.

Gaffield, Michael A.; Betz, William J. (2007): Synaptic vesicle mobility in mouse motor nerve terminals with and without synapsin. In: *The Journal of neuroscience : the official journal of the Society for Neuroscience* 27 (50), S. 13691–13700. DOI: 10.1523/JNEUROSCI.3910-07.2007.

Galli, T.; Haucke, V. (2001): Cycling of synaptic vesicles: how far? How fast! In: *Science's STKE : signal transduction knowledge environment* 2001 (88), S. re1. DOI: 10.1126/stke.2001.88.re1.

Galli, Thierry; Haucke, Volker (2004): Cycling of synaptic vesicles: how far? How fast! In: *Science's STKE : signal transduction knowledge environment* 2004 (264), S. re19. DOI: 10.1126/stke.2642004re19.

Gersdorff, H. von; Matthews, G. (1994): Inhibition of endocytosis by elevated internal calcium in a synaptic terminal. In: *Nature* 370 (6491), S. 652–655. DOI: 10.1038/370652a0.

Gorczyca, M.; Augart, C.; Budnik, V. (1993): Insulin-like receptor and insulin-like peptide are localized at neuromuscular junctions in Drosophila. In: *The Journal of neuroscience : the official journal of the Society for Neuroscience* 13 (9), S. 3692–3704.

Grenningloh, G.; Rehm, E. J.; Goodman, C. S. (1991): Genetic analysis of growth cone guidance in Drosophila: fasciclin II functions as a neuronal recognition molecule. In: *Cell* 67 (1), S. 45–57.

Grillner, Sten; Markram, Henry; Schutter, Erik de; Silberberg, Gilad; LeBeau, Fiona E. N. (2005): Microcircuits in action--from CPGs to neocortex. In: *Trends in neurosciences* 28 (10), S. 525–533. DOI: 10.1016/j.tins.2005.08.003.

Gu, Huaiyu; Jiang, Shaojuan Amy; Campusano, Jorge M.; Iniguez, Jorge; Su, Hailing; Hoang, Andy An et al. (2009): Cav2-type calcium channels encoded by cac regulate AP-independent neurotransmitter release at cholinergic synapses in adult Drosophila brain. In: *Journal of neurophysiology* 101 (1), S. 42–53. DOI: 10.1152/jn.91103.2008.

Gu, Ning; Vervaeke, Koen; Storm, Johan F. (2007): BK potassium channels facilitate high-frequency firing and cause early spike frequency adaptation in rat CA1 hippocampal pyramidal cells. In: *The Journal of physiology* 580 (Pt.3), S. 859–882. DOI: 10.1113/jphysiol.2006.126367.

Guatimosim, C.; Romano-Silva, M. A.; Gomez, M. V.; Prado, M. A. (1998): Recycling of synaptic vesicles at the frog neuromuscular junction in the presence of strontium. In: *Journal of neurochemistry* 70 (6), S. 2477–2483.

Guerrero, Giovanna; Reiff, Dierk F.; Agarwal, Gautam; Ball, Robin W.; Borst, Alexander; Goodman, Corey S.; Isacoff, Ehud Y. (2005): Heterogeneity in synaptic transmission along a Drosophila larval motor axon. In: *Nature neuroscience* 8 (9), S. 1188–1196. DOI: 10.1038/nn1526.

Gunteski-Hamblin, A. M.; Greeb, J.; Shull, G. E. (1988): A novel Ca2+ pump expressed in brain, kidney, and stomach is encoded by an alternative transcript of the slow-twitch muscle sarcoplasmic reticulum Ca-ATPase gene. Identification of cDNAs encoding Ca2+ and other cation-transporting ATPases using an oligonucleotide probe derived from the ATP-binding site. In: *The Journal of biological chemistry* 263 (29), S. 15032–15040.

Gurnett, C. A.; Waard, M. de; Campbell, K. P. (1996): Dual function of the voltage-dependent Ca2+ channel alpha 2 delta subunit in current stimulation and subunit interaction. In: *Neuron* 16 (2), S. 431–440.

Haley, Benjamin; Hendrix, David; Trang, Vinh; Levine, Michael (2008): A simplified miRNA-based gene silencing method for Drosophila melanogaster. In: *Developmental biology* 321 (2), S. 482–490. DOI: 10.1016/j.ydbio.2008.06.015.

Hallermann, Stefan; Heckmann, Manfred; Kittel, Robert J. (2010): Mechanisms of short-term plasticity at neuromuscular active zones of Drosophila. In: *HFSP journal* 4 (2), S. 72–84. DOI: 10.2976/1.3338710.

Halpern, M. E.; Chiba, A.; Johansen, J.; Keshishian, H. (1991): Growth cone behavior underlying the development of stereotypic synaptic connections in Drosophila embryos. In: *The Journal of neuroscience : the official journal of the Society for Neuroscience* 11 (10), S. 3227–3238.

Hara, Yusuke; Koganezawa, Masayuki; Yamamoto, Daisuke (2015): The Dmca1D channel mediates Ca(2+) inward currents in Drosophila embryonic muscles. In: *Journal of neurogenetics* 29 (2-3), S. 117–123. DOI: 10.3109/01677063.2015.1054991.

Harata, N.; Ryan, T. A.; Smith, S. J.; Buchanan, J.; Tsien, R. W. (2001): Visualizing recycling synaptic vesicles in hippocampal neurons by FM 1-43 photoconversion. In: *Proceedings of the National Academy of Sciences of the United States of America* 98 (22), S. 12748–12753. DOI: 10.1073/pnas.171442798.

Hardingham, G. E.; Chawla, S.; Johnson, C. M.; Bading, H. (1997): Distinct functions of nuclear and cytoplasmic calcium in the control of gene expression. In: *Nature* 385 (6613), S. 260–265. DOI: 10.1038/385260a0.

Harlow, M. L.; Ress, D.; Stoschek, A.; Marshall, R. M.; McMahan, U. J. (2001): The architecture of active zone material at the frog's neuromuscular junction. In: *Nature* 409 (6819), S. 479–484. DOI: 10.1038/35054000.

Harrelson, A. L.; Goodman, C. S. (1988): Growth cone guidance in insects: fasciclin II is a member of the immunoglobulin superfamily. In: *Science (New York, N.Y.)* 242 (4879), S. 700–708.

Hartwig, Cortnie L.; Worrell, Jason; Levine, Richard B.; Ramaswami, Mani; Sanyal, Subhabrata (2008): Normal dendrite growth in Drosophila motor neurons requires the AP-1 transcription factor. In: *Developmental neurobiology* 68 (10), S. 1225–1242. DOI: 10.1002/dneu.20655.

Haucke, Volker; Neher, Erwin; Sigrist, Stephan J. (2011): Protein scaffolds in the coupling of synaptic exocytosis and endocytosis. In: *Nature reviews. Neuroscience* 12 (3), S. 127–138. DOI: 10.1038/nrn2948.

Heckman, C. J.; Lee, Robert H.; Brownstone, Robert M. (2003): Hyperexcitable dendrites in motoneurons and their neuromodulatory control during motor behavior. In: *Trends in neurosciences* 26 (12), S. 688–695. DOI: 10.1016/j.tins.2003.10.002.

Heidelberger, R.; Heinemann, C.; Neher, E.; Matthews, G. (1994): Calcium dependence of the rate of exocytosis in a synaptic terminal. In: *Nature* 371 (6497), S. 513–515. DOI: 10.1038/371513a0.

Held H (1893) Die zentrale Gehörleitung. Archiv für Anatomie und Physiologie. Anat Abt 201–248.

Heuser, J. E.; Reese, T. S. (1973): Evidence for recycling of synaptic vesicle membrane during transmitter release at the frog neuromuscular junction. In: *The Journal of cell biology* 57 (2), S. 315–344.

Hida, Yamato; Ohtsuka, Toshihisa (2010): CAST and ELKS proteins: structural and functional determinants of the presynaptic active zone. In: *Journal of biochemistry* 148 (2), S. 131–137. DOI: 10.1093/jb/mvq065.

Ho, R., Chang, S. & Goodman, C. S. (1981) Neurosci. Abstr. 7, 348.

Hoang, B.; Chiba, A. (2001): Single-cell analysis of Drosophila larval neuromuscular synapses. In: *Developmental biology* 229 (1), S. 55–70. DOI: 10.1006/dbio.2000.9983.

Hosoi, Nobutake; Holt, Matthew; Sakaba, Takeshi (2009): Calcium dependence of exo- and endocytotic coupling at a glutamatergic synapse. In: *Neuron* 63 (2), S. 216–229. DOI: 10.1016/j.neuron.2009.06.010.

Hou, Jiamei; Tamura, Takuya; Kidokoro, Yoshiaki (2008): Delayed synaptic transmission in Drosophila cacophonynull embryos. In: *Journal of neurophysiology* 100 (5), S. 2833–2842. DOI: 10.1152/jn.90342.2008.

Hounsgaard, J.; Mintz, I. (1988): Calcium conductance and firing properties of spinal motoneurones in the turtle. In: *The Journal of physiology* 398, S. 591–603.

Hua, Yunfeng; Sinha, Raunak; Thiel, Cora S.; Schmidt, Roman; Huve, Jana; Martens, Henrik et al. (2011): A readily retrievable pool of synaptic vesicles. In: *Nature neuroscience* 14 (7), S. 833–839. DOI: 10.1038/nn.2838.

Hui, Enfu; Johnson, Colin P.; Yao, Jun; Dunning, F. Mark; Chapman, Edwin R. (2009): Synaptotagmin-mediated bending of the target membrane is a critical step in Ca(2+)-regulated fusion. In: *Cell* 138 (4), S. 709–721. DOI: 10.1016/j.cell.2009.05.049.

Ikeda, Kaori; Bekkers, John M. (2009): Counting the number of releasable synaptic vesicles in a presynaptic terminal. In: *Proceedings of the National Academy of Sciences of the United States of America* 106 (8), S. 2945–2950. DOI: 10.1073/pnas.0811017106.

Iniguez, Jorge; Schutte, Soleil S.; O'Dowd, Diane K. (2013): Cav3-type alpha1T calcium channels mediate transient calcium currents that regulate repetitive firing in Drosophila antennal lobe PNs. In: *Journal of neurophysiology* 110 (7), S. 1490–1496. DOI: 10.1152/jn.00368.2013.

Isope, Philippe; Hildebrand, Michael E.; Snutch, Terrance P. (2012): Contributions of T-type voltage-gated calcium channels to postsynaptic calcium signaling within Purkinje neurons. In: *Cerebellum (London, England)* 11 (3), S. 651–665. DOI: 10.1007/s12311-010-0195-4.

Jahn, Reinhard; Scheller, Richard H. (2006): SNAREs--engines for membrane fusion. In: *Nature reviews. Molecular cell biology* 7 (9), S. 631–643. DOI: 10.1038/nrm2002.

Jan, L. Y.; Jan, Y. N. (1982): Antibodies to horseradish peroxidase as specific neuronal markers in Drosophila and in grasshopper embryos. In: *Proceedings of the National Academy of Sciences of the United States of America* 79 (8), S. 2700–2704.

Jay, S. D.; Sharp, A. H.; Kahl, S. D.; Vedvick, T. S.; Harpold, M. M.; Campbell, K. P. (1991): Structural characterization of the dihydropyridine-sensitive calcium channel alpha 2-subunit and the associated delta peptides. In: *The Journal of biological chemistry* 266 (5), S. 3287–3293.

Jia, X. X.; Gorczyca, M.; Budnik, V. (1993): Ultrastructure of neuromuscular junctions in Drosophila: comparison of wild type and mutants with increased excitability. In: *Journal of neurobiology* 24 (8), S. 1025–1044. DOI: 10.1002/neu.480240804.

Johansen, J.; Halpern, M. E.; Johansen, K. M.; Keshishian, H. (1989): Stereotypic morphology of glutamatergic synapses on identified muscle cells of Drosophila larvae. In: *The Journal of neuroscience : the official journal of the Society for Neuroscience* 9 (2), S. 710–725.

Johansen C., Krishnamurthy L., Saxena N.P., Sethi S.C. Genotypic variation in moisture response of chickpea grown under line-source sprinklers in a semi-arid tropical environment. Field Crop Res.1994;37:103–112.

Jongh, K. S. de; Warner, C.; Catterall, W. A. (1990): Subunits of purified calcium channels. Alpha 2 and delta are encoded by the same gene. In: *The Journal of biological chemistry* 265 (25), S. 14738–14741.

Kang, Myoung-Goo; Campbell, Kevin P. (2003): Gamma subunit of voltage-activated calcium channels. In: *The Journal of biological chemistry* 278 (24), S. 21315–21318. DOI: 10.1074/jbc.R300004200.

KATZ, B. (1971): Quantal mechanism of neural transmitter release. In: *Science (New York, N.Y.)* 173 (3992), S. 123–126.

KATZ, B.; MILEDI, R. (1965): PROPAGATION OF ELECTRIC ACTIVITY IN MOTOR NERVE TERMINALS. In: *Proceedings of the Royal Society of London. Series B, Biological sciences* 161, S. 453–482.

KATZ, B.; MILEDI, R. (1969): Spontaneous and evoked activity of motor nerve endings in calcium Ringer. In: *The Journal of physiology* 203 (3), S. 689–706.

Katz B.: *The release of neural transmitter substances.* C. C. Thomas, Springfield, 1969.

Kavalali, Ege T.; Jorgensen, Erik M. (2014): Visualizing presynaptic function. In: *Nature neuroscience* 17 (1), S. 10–16. DOI: 10.1038/nn.3578.

Kawasaki, F.; Felling, R.; Ordway, R. W. (2000): A temperature-sensitive paralytic mutant defines a primary synaptic calcium channel in Drosophila. In: *The Journal of neuroscience : the official journal of the Society for Neuroscience* 20 (13), S. 4885–4889.

Kawasaki, Fumiko; Collins, Stephen C.; Ordway, Richard W. (2002): Synaptic calcium-channel function in Drosophila: analysis and transformation rescue of temperature-sensitive paralytic and lethal mutations of cacophony. In: *The Journal of neuroscience : the official journal of the Society for Neuroscience* 22 (14), S. 5856–5864.

Kawasaki, Fumiko; Zou, Beiyan; Xu, Xia; Ordway, Richard W. (2004): Active zone localization of presynaptic calcium channels encoded by the cacophony locus of Drosophila. In: *The Journal of neuroscience : the official journal of the Society for Neuroscience* 24 (1), S. 282–285. DOI: 10.1523/JNEUROSCI.3553-03.2004.

Kidokoro, Yoshiaki; Kuromi, Hiroshi; Delgado, Ricardo; Maureira, Carlos; Oliva, Carolina; Labarca, Pedro (2004): Synaptic vesicle pools and plasticity of synaptic transmission at the Drosophila synapse. In: *Brain research. Brain research reviews* 47 (1-3), S. 18–32. DOI: 10.1016/j.brainresrev.2004.05.004.

Kiehn, O. (1991): Plateau potentials and active integration in the 'final common pathway' for motor behaviour. In: *Trends in neurosciences* 14 (2), S. 68–73.

Kiehn, O.; Kjaerulff, O.; Tresch, M. C.; Harris-Warrick, R. M. (2000): Contributions of intrinsic motor neuron properties to the production of rhythmic motor output in the mammalian spinal cord. In: *Brain research bulletin* 53 (5), S. 649–659.

Kiehn, Ole; Kullander, Klas (2004): Central pattern generators deciphered by molecular genetics. In: *Neuron* 41 (3), S. 317–321.

Kim, Sung Hyun; Ryan, Timothy A. (2010): CDK5 serves as a major control point in neurotransmitter release. In: *Neuron* 67 (5), S. 797–809. DOI: 10.1016/j.neuron.2010.08.003.

King, Glenn F. (2007): Modulation of insect Ca(v) channels by peptidic spider toxins. In: *Toxicon : official journal of the International Society on Toxinology* 49 (4), S. 513–530. DOI: 10.1016/j.toxicon.2006.11.012.

Kitagawa, S.; Nakagaki, M. (1981): Influence of phenomenological coefficients on reverse permeation and overshooting phenomenon of ions. In: *Yakugaku zasshi : Journal of the Pharmaceutical Society of Japan* 101 (9), S. 780–790.

Kittel, Julie A.; DeBeer, Bryann B.; Kimbrel, Nathan A.; Matthieu, Monica M.; Meyer, Eric C.; Gulliver, Suzy Bird; Morissette, Sandra B. (2016): Does body mass index moderate the association between posttraumatic stress disorder symptoms and suicidal ideation in Iraq/Afghanistan veterans? In: *Psychiatry research* 244, S. 123–129. DOI: 10.1016/j.psychres.2016.07.039.

Kittel, R. J.; Hallermann, S.; Thomsen, S.; Wichmann, C.; Sigrist, S. J.; Heckmann, M. (2006): Active zone assembly and synaptic release. In: *Biochemical Society transactions* 34 (Pt 5), S. 939–941. DOI: 10.1042/BST0340939.

Kittel, Robert J.; Wichmann, Carolin; Rasse, Tobias M.; Fouquet, Wernher; Schmidt, Manuela; Schmid, Andreas et al. (2006): Bruchpilot promotes active zone assembly, Ca2+ channel clustering, and vesicle release. In: *Science (New York, N.Y.)* 312 (5776), S. 1051–1054. DOI: 10.1126/science.1126308.

Klingauf, J.; Kavalali, E. T.; Tsien, R. W. (1998): Kinetics and regulation of fast endocytosis at hippocampal synapses. In: *Nature* 394 (6693), S. 581–585. DOI: 10.1038/29079.

Kononenko, Natalia L.; Pechstein, Arndt; Haucke, Volker (2013): The tortoise and the hare revisited. In: *eLife* 2, S. e01233. DOI: 10.7554/eLife.01233.

Kuromi, H.; Kidokoro, Y. (2000): Tetanic stimulation recruits vesicles from reserve pool via a cAMP-mediated process in Drosophila synapses. In: *Neuron* 27 (1), S. 133–143.

Kuromi, H.; Ueno, K.; Kidokoro, Y. (2010): Two types of Ca2+ channel linked to two endocytic pathways coordinately maintain synaptic transmission at the Drosophila synapse. In: *The European journal of neuroscience* 32 (3), S. 335–346. DOI: 10.1111/j.1460-9568.2010.07300.x.

Kuromi, Hiroshi; Honda, Atsuko; Kidokoro, Yoshiaki (2004): Ca2+ influx through distinct routes controls exocytosis and endocytosis at drosophila presynaptic terminals. In: *Neuron* 41 (1), S. 101–111.

Kuromi, Hiroshi; Kidokoro, Yoshiaki (2002): Selective replenishment of two vesicle pools depends on the source of Ca2+ at the Drosophila synapse. In: *Neuron* 35 (2), S. 333–343.

Kuromi, Hiroshi; Kidokoro, Yoshiaki (2005): Exocytosis and endocytosis of synaptic vesicles and functional roles of vesicle pools: lessons from the Drosophila neuromuscular junction. In: *The Neuroscientist : a review journal bringing neurobiology, neurology and psychiatry* 11 (2), S. 138–147. DOI: 10.1177/1073858404271679.

Lacerda, A. E.; Kim, H. S.; Ruth, P.; Perez-Reyes, E.; Flockerzi, V.; Hofmann, F. et al. (1991): Normalization of current kinetics by interaction between the alpha 1 and beta subunits of the skeletal muscle dihydropyridine-sensitive Ca2+ channel. In: *Nature* 352 (6335), S. 527–530. DOI: 10.1038/352527a0.

Lahey, T.; Gorczyca, M.; Jia, X. X.; Budnik, V. (1994): The Drosophila tumor suppressor gene dlg is required for normal synaptic bouton structure. In: *Neuron* 13 (4), S. 823–835.

Landgraf, M.; Bossing, T.; Technau, G. M.; Bate, M. (1997): The origin, location, and projections of the embryonic abdominal motorneurons of Drosophila. In: *The Journal of neuroscience : the official journal of the Society for Neuroscience* 17 (24), S. 9642–9655.

Landis, D. M.; Hall, A. K.; Weinstein, L. A.; Reese, T. S. (1988): The organization of cytoplasm at the presynaptic active zone of a central nervous system synapse. In: *Neuron* 1 (3), S. 201–209.

Lee, Jihye; Ueda, Atsushi; Wu, Chun-Fang (2014): Distinct roles of Drosophila cacophony and Dmca1D Ca(2+) channels in synaptic homeostasis: genetic interactions with slowpoke Ca(2+) -activated BK channels in presynaptic excitability and postsynaptic response. In: *Developmental neurobiology* 74 (1), S. 1–15. DOI: 10.1002/dneu.22120.

Leube, R. E. (1995): The topogenic fate of the polytopic transmembrane proteins, synaptophysin and connexin, is determined by their membrane-spanning domains. In: *Journal of cell science* 108 (Pt 3), S. 883–894.

Li, Haiyan; Foss, Sarah M.; Dobryy, Yuriy L.; Park, C. Kevin; Hires, Samuel Andrew; Shaner, Nathan C. et al. (2011): Concurrent imaging of synaptic vesicle recycling and calcium dynamics. In: *Frontiers in molecular neuroscience* 4, S. 34. DOI: 10.3389/fnmol.2011.00034.

Lipscombe, Diane; Pan, Jennifer Qian; Gray, Annette C. (2002): Functional diversity in neuronal voltage-gated calcium channels by alternative splicing of Ca(v)alpha1. In: *Molecular neurobiology* 26 (1), S. 21–44. DOI: 10.1385/MN:26:1:021.

Littleton, J. T.; Ganetzky, B. (2000): Ion channels and synaptic organization: analysis of the Drosophila genome. In: *Neuron* 26 (1), S. 35–43.

Liu, Karen S. Y.; Siebert, Matthias; Mertel, Sara; Knoche, Elena; Wegener, Stephanie; Wichmann, Carolin et al. (2011): RIM-binding protein, a central part of the active zone, is essential for neurotransmitter release. In: *Science (New York, N.Y.)* 334 (6062), S. 1565–1569. DOI: 10.1126/science.1212991.

Llinas, R.; Sugimori, M.; Silver, R. B. (1992): Presynaptic calcium concentration microdomains and transmitter release. In: *Journal of physiology, Paris* 86 (1-3), S. 135–138.

Llinas, R. R. (1977): Depolarization-release coupling systems in neurons. In: *Neurosciences Research Program bulletin* 15 (4), S. 555–687.

Lytton, J.; MacLennan, D. H. (1988): Molecular cloning of cDNAs from human kidney coding for two alternatively spliced products of the cardiac Ca2+-ATPase gene. In: *The Journal of biological chemistry* 263 (29), S. 15024–15031.

Lytton, J.; Zarain-Herzberg, A.; Periasamy, M.; MacLennan, D. H. (1989): Molecular cloning of the mammalian smooth muscle sarco(endo)plasmic reticulum Ca2+-ATPase. In: *The Journal of biological chemistry* 264 (12), S. 7059–7065.

Macleod, G. T.; Chen, L.; Karunanithi, S.; Peloquin, J. B.; Atwood, H. L.; McRory, J. E. et al. (2006): The Drosophila cacts2 mutation reduces presynaptic Ca2+ entry and defines an important element in Cav2.1 channel inactivation. In: *The European journal of neuroscience* 23 (12), S. 3230–3244. DOI: 10.1111/j.1460-9568.2006.04873.x.

Maglione, Marta; Sigrist, Stephan J. (2013): Seeing the forest tree by tree: super-resolution light microscopy meets the neurosciences. In: *Nature neuroscience* 16 (7), S. 790–797. DOI: 10.1038/nn.3403.

Marder, Eve; Bucher, Dirk; Schulz, David J.; Taylor, Adam L. (2005): Invertebrate central pattern generation moves along. In: *Current biology : CB* 15 (17), S. R685-99. DOI: 10.1016/j.cub.2005.08.022.

Marder, Eve; Prinz, Astrid A. (2002): Modeling stability in neuron and network function: the role of activity in homeostasis. In: *BioEssays : news and reviews in molecular, cellular and developmental biology* 24 (12), S. 1145–1154. DOI: 10.1002/bies.10185.

Marie, Bruno; Sweeney, Sean T.; Poskanzer, Kira E.; Roos, Jack; Kelly, Regis B.; Davis, Graeme W. (2004): Dap160/intersectin scaffolds the periactive zone to achieve high-fidelity endocytosis and normal synaptic growth. In: *Neuron* 43 (2), S. 207–219. DOI: 10.1016/j.neuron.2004.07.001.

Marks, B.; McMahon, H. T. (1998): Calcium triggers calcineurin-dependent synaptic vesicle recycling in mammalian nerve terminals. In: *Current biology : CB* 8 (13), S. 740–749.

Martens, Sascha; McMahon, Harvey T. (2008): Mechanisms of membrane fusion: disparate players and common principles. In: *Nature reviews. Molecular cell biology* 9 (7), S. 543–556. DOI: 10.1038/nrm2417.

Matkovic, Tanja; Siebert, Matthias; Knoche, Elena; Depner, Harald; Mertel, Sara; Owald, David et al. (2013): The Bruchpilot cytomatrix determines the size of the readily releasable pool of synaptic vesicles. In: *The Journal of cell biology* 202 (4), S. 667–683. DOI: 10.1083/jcb.201301072.

Meinrenken, Christoph J.; Borst, J. Gerard G.; Sakmann, Bert (2003): Local routes revisited: the space and time dependence of the Ca2+ signal for phasic transmitter release at the rat calyx of Held. In: *The Journal of physiology* 547 (Pt 3), S. 665–689. DOI: 10.1113/jphysiol.2002.032714.

Micheva, K. D.; Ramjaun, A. R.; Kay, B. K.; McPherson, P. S. (1997): SH3 domain-dependent interactions of endophilin with amphiphysin. In: *FEBS letters* 414 (2), S. 308–312.

Milani, D.; Malgaroli, A.; Guidolin, D.; Fasolato, C.; Skaper, S. D.; Meldolesi, J.; Pozzan, T. (1990): Ca2+ channels and intracellular Ca2+ stores in neuronal and neuroendocrine cells. In: *Cell calcium* 11 (2-3), S. 191–199.

Mittelstaedt, Tobias; Alvarez-Baron, Elena; Schoch, Susanne (2010): RIM proteins and their role in synapse function. In: *Biological chemistry* 391 (6), S. 599–606. DOI: 10.1515/BC.2010.064.

Mohrmann, Ralf; Wit, Heidi de; Verhage, Matthijs; Neher, Erwin; Sorensen, Jakob B. (2010): Fast vesicle fusion in living cells requires at least three SNARE complexes. In: *Science (New York, N.Y.)* 330 (6003), S. 502–505. DOI: 10.1126/science.1193134.

Morrissette, J.; Heisermann, G.; Cleary, J.; Ruoho, A.; Coronado, R. (1993): Cyclic ADP-ribose induced Ca2+ release in rabbit skeletal muscle sarcoplasmic reticulum. In: *FEBS letters* 330 (3), S. 270–274.

Moss, Fraser J.; Viard, Patricia; Davies, Anthony; Bertaso, Federica; Page, Karen M.; Graham, Alex et al. (2002): The novel product of a five-exon stargazin-related gene abolishes Ca(V)2.2 calcium channel expression. In: *The EMBO journal* 21 (7), S. 1514–1523. DOI: 10.1093/emboj/21.7.1514.

Murthy, Venkatesh N.; Camilli, Pietro de (2003): Cell biology of the presynaptic terminal. In: *Annual review of neuroscience* 26, S. 701–728. DOI: 10.1146/annurev.neuro.26.041002.131445.

Nakai, J.; Ohkura, M.; Imoto, K. (2001): A high signal-to-noise Ca(2+) probe composed of a single green fluorescent protein. In: *Nature biotechnology* 19 (2), S. 137–141. DOI: 10.1038/84397.

Neale, E. A.; Bowers, L. M.; Jia, M.; Bateman, K. E.; Williamson, L. C. (1999): Botulinum neurotoxin A blocks synaptic vesicle exocytosis but not endocytosis at the nerve terminal. In: *The Journal of cell biology* 147 (6), S. 1249–1260.

Neher, E. (1998): Vesicle pools and Ca2+ microdomains: new tools for understanding their roles in neurotransmitter release. In: *Neuron* 20 (3), S. 389–399.

Neher, Erwin (2010): What is Rate-Limiting during Sustained Synaptic Activity: Vesicle Supply or the Availability of Release Sites. In: *Frontiers in synaptic neuroscience* 2, S. 144. DOI: 10.3389/fnsyn.2010.00144.

Neher, Erwin; Sakaba, Takeshi (2008): Multiple roles of calcium ions in the regulation of neurotransmitter release. In: *Neuron* 59 (6), S. 861–872. DOI: 10.1016/j.neuron.2008.08.019.

Newton, C. L.; Mignery, G. A.; Sudhof, T. C. (1994): Co-expression in vertebrate tissues and cell lines of multiple inositol 1,4,5-trisphosphate (InsP3) receptors with distinct affinities for InsP3. In: *The Journal of biological chemistry* 269 (46), S. 28613–28619.

Ni, Jian-Quan; Liu, Lu-Ping; Binari, Richard; Hardy, Robert; Shim, Hye-Seok; Cavallaro, Amanda et al. (2009): A Drosophila resource of transgenic RNAi lines for neurogenetics. In: *Genetics* 182 (4), S. 1089–1100. DOI: 10.1534/genetics.109.103630.

Ni, Jian-Quan; Markstein, Michele; Binari, Richard; Pfeiffer, Barret; Liu, Lu-Ping; Villalta, Christians et al. (2008): Vector and parameters for targeted transgenic RNA interference in Drosophila melanogaster. In: *Nature methods* 5 (1), S. 49–51. DOI: 10.1038/nmeth1146.

Ni, Jian-Quan; Zhou, Rui; Czech, Benjamin; Liu, Lu-Ping; Holderbaum, Laura; Yang-Zhou, Donghui et al. (2011): A genome-scale shRNA resource for transgenic RNAi in Drosophila. In: *Nature methods* 8 (5), S. 405–407. DOI: 10.1038/nmeth.1592.

Nowycky, M. C.; Fox, A. P.; Tsien, R. W. (1985): Three types of neuronal calcium channel with different calcium agonist sensitivity. In: *Nature* 316 (6027), S. 440–443.

Obermair, Gerald J.; Kugler, Gerlinde; Baumgartner, Sabine; Tuluc, Petronel; Grabner, Manfred; Flucher, Bernhard E. (2005): The Ca2+ channel alpha2delta-1 subunit determines Ca2+ current kinetics in skeletal muscle but not targeting of alpha1S or excitation-contraction coupling. In: *The Journal of biological chemistry* 280 (3), S. 2229–2237. DOI: 10.1074/jbc.M411501200.

Obermair, Gerald J.; Tuluc, Petronel; Flucher, Bernhard E. (2008): Auxiliary Ca(2+) channel subunits: lessons learned from muscle. In: *Current opinion in pharmacology* 8 (3), S. 311–318. DOI: 10.1016/j.coph.2008.01.008.

Ohtsuka, Toshihisa; Takao-Rikitsu, Etsuko; Inoue, Eiji; Inoue, Marie; Takeuchi, Masakazu; Matsubara, Kaho et al. (2002): Cast: a novel protein of the cytomatrix at the active zone of synapses that forms a ternary complex with RIM1 and munc13-1. In: *The Journal of cell biology* 158 (3), S. 577–590. DOI: 10.1083/jcb.200202083.

Orrenius, Sten; Zhivotovsky, Boris; Nicotera, Pierluigi (2003): Regulation of cell death: the calcium-apoptosis link. In: *Nature reviews. Molecular cell biology* 4 (7), S. 552–565. DOI: 10.1038/nrm1150.

Patel, N. H.; Schafer, B.; Goodman, C. S.; Holmgren, R. (1989): The role of segment polarity genes during Drosophila neurogenesis. In: *Genes & development* 3 (6), S. 890–904.

Pech, Ulrike; Revelo, Natalia H.; Seitz, Katharina J.; Rizzoli, Silvio O.; Fiala, Andre (2015): Optical dissection of experience-dependent pre- and postsynaptic plasticity in the Drosophila brain. In: *Cell reports* 10 (12), S. 2083–2095. DOI: 10.1016/j.celrep.2015.02.065.

Pederson PL, Carafoli E (1987) Ion motive ATPases. I. Ubiquity, properties and significance to cell function. Trends Biochem Sci 12:146-150.

Peled, Einat S.; Isacoff, Ehud Y. (2011): Optical quantal analysis of synaptic transmission in wild-type and rab3-mutant Drosophila motor axons. In: *Nature neuroscience* 14 (4), S. 519–526. DOI: 10.1038/nn.2767.

Peled, Einat S.; Newman, Zachary L.; Isacoff, Ehud Y. (2014): Evoked and spontaneous transmission favored by distinct sets of synapses. In: *Current biology : CB* 24 (5), S. 484–493. DOI: 10.1016/j.cub.2014.01.022.

Peng, I-Feng; Wu, Chun-Fang (2007): Drosophila cacophony channels: a major mediator of neuronal Ca2+ currents and a trigger for K+ channel homeostatic regulation. In: *The Journal of neuroscience : the official journal of the Society for Neuroscience* 27 (5), S. 1072–1081. DOI: 10.1523/JNEUROSCI.4746-06.2007.

Perez-Reyes, E.; Kim, H. S.; Lacerda, A. E.; Horne, W.; Wei, X. Y.; Rampe, D. et al. (1989): Induction of calcium currents by the expression of the alpha 1-subunit of the dihydropyridine receptor from skeletal muscle. In: *Nature* 340 (6230), S. 233–236. DOI: 10.1038/340233a0.

Perkins, Lizabeth A.; Holderbaum, Laura; Tao, Rong; Hu, Yanhui; Sopko, Richelle; McCall, Kim et al. (2015): The Transgenic RNAi Project at Harvard Medical School: Resources and Validation. In: *Genetics* 201 (3), S. 843–852. DOI: 10.1534/genetics.115.180208.

Pielage, Jan; Fetter, Richard D.; Davis, Graeme W. (2006): A postsynaptic spectrin scaffold defines active zone size, spacing, and efficacy at the Drosophila neuromuscular junction. In: *The Journal of cell biology* 175 (3), S. 491–503. DOI: 10.1083/jcb.200607036.

Platzer, J.; Engel, J.; Schrott-Fischer, A.; Stephan, K.; Bova, S.; Chen, H. et al. (2000): Congenital deafness and sinoatrial node dysfunction in mice lacking class D L-type Ca2+ channels. In: *Cell* 102 (1), S. 89–97.

Pragnell, M.; Waard, M. de; Mori, Y.; Tanabe, T.; Snutch, T. P.; Campbell, K. P. (1994): Calcium channel beta-subunit binds to a conserved motif in the I-II cytoplasmic linker of the alpha 1-subunit. In: *Nature* 368 (6466), S. 67–70. DOI: 10.1038/368067a0.

Pyle, J. L.; Kavalali, E. T.; Piedras-Renteria, E. S.; Tsien, R. W. (2000): Rapid reuse of readily releasable pool vesicles at hippocampal synapses. In: *Neuron* 28 (1), S. 221–231.

Ramaswami, M.; Krishnan, K. S.; Kelly, R. B. (1994): Intermediates in synaptic vesicle recycling revealed by optical imaging of Drosophila neuromuscular junctions. In: *Neuron* 13 (2), S. 363–375.

Reid, Christopher A.; Bekkers, John M.; Clements, John D. (2003): Presynaptic Ca2+ channels: a functional patchwork. In: *Trends in neurosciences* 26 (12), S. 683–687. DOI: 10.1016/j.tins.2003.10.003.

Ren, D.; Xu, H.; Eberl, D. F.; Chopra, M.; Hall, L. M. (1998): A mutation affecting dihydropyridine-sensitive current levels and activation kinetics in Drosophila muscle and mammalian heart calcium channels. In: *The Journal of neuroscience : the official journal of the Society for Neuroscience* 18 (7), S. 2335–2341.

Rettig, Jens; Neher, Erwin (2002): Emerging roles of presynaptic proteins in Ca++-triggered exocytosis. In: *Science (New York, N.Y.)* 298 (5594), S. 781–785. DOI: 10.1126/science.1075375.

Reuter, H. (1983): Calcium channel modulation by neurotransmitters, enzymes and drugs. In: *Nature* 301 (5901), S. 569–574.

Reuter, H.; Seitz, N. (1968): The dependence of calcium efflux from cardiac muscle on temperature and external ion composition. In: *The Journal of physiology* 195 (2), S. 451–470. DOI: 10.1113/jphysiol.1968.sp008467.

Richards, Mark W.; Butcher, Adrian J.; Dolphin, Annette C. (2004): Ca2+ channel beta-subunits: structural insights AID our understanding. In: *Trends in pharmacological sciences* 25 (12), S. 626–632. DOI: 10.1016/j.tips.2004.10.008.

Rieckhof, Gabrielle E.; Yoshihara, Motojiro; Guan, Zhuo; Littleton, J. Troy (2003): Presynaptic N-type calcium channels regulate synaptic growth. In: *The Journal of biological chemistry* 278 (42), S. 41099–41108. DOI: 10.1074/jbc.M306417200.

Ringstad, N.; Gad, H.; Low, P.; Di Paolo, G.; Brodin, L.; Shupliakov, O.; Camilli, P. de (1999): Endophilin/SH3p4 is required for the transition from early to late stages in clathrin-mediated synaptic vesicle endocytosis. In: *Neuron* 24 (1), S. 143–154.

Rizzoli, Silvio O.; Betz, William J. (2005): Synaptic vesicle pools. In: *Nature reviews. Neuroscience* 6 (1), S. 57–69. DOI: 10.1038/nrn1583.

Roos, J.; Kelly, R. B. (1998): Dap160, a neural-specific Eps15 homology and multiple SH3 domain-containing protein that interacts with Drosophila dynamin. In: *The Journal of biological chemistry* 273 (30), S. 19108–19119.

Roos, J.; Kelly, R. B. (1999): The endocytic machinery in nerve terminals surrounds sites of exocytosis. In: *Current biology : CB* 9 (23), S. 1411–1414.

Ryan, T. A.; Smith, S. J.; Reuter, H. (1996): The timing of synaptic vesicle endocytosis. In: *Proceedings of the National Academy of Sciences of the United States of America* 93 (11), S. 5567–5571.

Ryglewski, Stefanie; Lance, Kimberly; Levine, Richard B.; Duch, Carsten (2012): Ca(v)2 channels mediate low and high voltage-activated calcium currents in Drosophila motoneurons. In: *The Journal of physiology* 590 (4), S. 809–825. DOI: 10.1113/jphysiol.2011.222836.

Sakaba, T.; Neher, E. (2001): Calmodulin mediates rapid recruitment of fast-releasing synaptic vesicles at a calyx-type synapse. In: *Neuron* 32 (6), S. 1119–1131.

Sankaranarayanan, S.; Ryan, T. A. (2001): Calcium accelerates endocytosis of vSNAREs at hippocampal synapses. In: *Nature neuroscience* 4 (2), S. 129–136. DOI: 10.1038/83949.

Sara, Yildirim; Mozhayeva, Marina G.; Liu, Xinran; Kavalali, Ege T. (2002): Fast vesicle recycling supports neurotransmission during sustained stimulation at hippocampal synapses. In: *The Journal of neuroscience : the official journal of the Society for Neuroscience* 22 (5), S. 1608–1617.

Saraswati, Sudipta; Fox, Lyle E.; Soll, David R.; Wu, Chun-Fang (2004): Tyramine and octopamine have opposite effects on the locomotion of Drosophila larvae. In: *Journal of neurobiology* 58 (4), S. 425–441. DOI: 10.1002/neu.10298.

Satzler, Kurt; Sohl, Leander F.; Bollmann, Johann H.; Borst, J. Gerard G.; Frotscher, Michael; Sakmann, Bert; Lubke, Joachim H. R. (2002): Three-dimensional reconstruction of a calyx of Held and its postsynaptic principal neuron in the medial nucleus of the trapezoid body. In: *The Journal of neuroscience : the official journal of the Society for Neuroscience* 22 (24), S. 10567–10579.

Schaefer, Jennifer E.; Worrell, Jason W.; Levine, Richard B. (2010): Role of intrinsic properties in Drosophila motoneuron recruitment during fictive crawling. In: *Journal of neurophysiology* 104 (3), S. 1257–1266. DOI: 10.1152/jn.00298.2010.

Schmid, A.; Chiba, A.; Doe, C. Q. (1999): Clonal analysis of Drosophila embryonic neuroblasts: neural cell types, axon projections and muscle targets. In: *Development (Cambridge, England)* 126 (21), S. 4653–4689.

Schmid, Andreas; Hallermann, Stefan; Kittel, Robert J.; Khorramshahi, Omid; Frolich, Andreas M. J.; Quentin, Christine et al. (2008): Activity-dependent site-specific changes of glutamate receptor composition in vivo. In: *Nature neuroscience* 11 (6), S. 659–666. DOI: 10.1038/nn.2122.

Schmidt, A.; Wolde, M.; Thiele, C.; Fest, W.; Kratzin, H.; Podtelejnikov, A. V. et al. (1999): Endophilin I mediates synaptic vesicle formation by transfer of arachidonate to lysophosphatidic acid. In: *Nature* 401 (6749), S. 133–141. DOI: 10.1038/43613.

Schneggenburger, R.; Neher, E. (2000): Intracellular calcium dependence of transmitter release rates at a fast central synapse. In: *Nature* 406 (6798), S. 889–893. DOI: 10.1038/35022702.

Schoch, Susanne; Gundelfinger, Eckart D. (2006): Molecular organization of the presynaptic active zone. In: *Cell and tissue research* 326 (2), S. 379–391. DOI: 10.1007/s00441-006-0244-y.

Schuster, Christoph M.; Davis, Graeme W.; Fetter, Richard D.; Goodman, Corey S. (1996): Genetic Dissection of Structural and Functional Components of Synaptic Plasticity. I. Fasciclin II Controls Synaptic Stabilization and Growth. In: *Neuron* 17 (4), S. 641–654. DOI: 10.1016/S0896-6273(00)80197-X.

Shupliakov, O.; Low, P.; Grabs, D.; Gad, H.; Chen, H.; David, C. et al. (1997): Synaptic vesicle endocytosis impaired by disruption of dynamin-SH3 domain interactions. In: *Science (New York, N.Y.)* 276 (5310), S. 259–263.

Singer, D.; Biel, M.; Lotan, I.; Flockerzi, V.; Hofmann, F.; Dascal, N. (1991): The roles of the subunits in the function of the calcium channel. In: *Science (New York, N.Y.)* 253 (5027), S. 1553–1557.

Sink, H.; Whitington, P. M. (1991): Location and connectivity of abdominal motoneurons in the embryo and larva of Drosophila melanogaster. In: *Journal of neurobiology* 22 (3), S. 298–311. DOI: 10.1002/neu.480220309.

Sipos, I.; Pika-Hartlaub, U.; Hofmann, F.; Flucher, B. E.; Melzer, W. (2000): Effects of the dihydropyridine receptor subunits gamma and alpha2delta on the kinetics of heterologously expressed L-type Ca2+ channels. In: *Pflugers Archiv : European journal of physiology* 439 (6), S. 691–699.

Sitsapesan, R.; McGarry, S. J.; Williams, A. J. (1994): Cyclic ADP-ribose competes with ATP for the adenine nucleotide binding site on the cardiac ryanodine receptor Ca(2+)-release channel. In: *Circulation research* 75 (3), S. 596–600.

Smith, C.; Neher, E. (1997): Multiple forms of endocytosis in bovine adrenal chromaffin cells. In: *The Journal of cell biology* 139 (4), S. 885–894.

Sone, M.; Suzuki, E.; Hoshino, M.; Hou, D.; Kuromi, H.; Fukata, M. et al. (2000): Synaptic development is controlled in the periactive zones of Drosophila synapses. In: *Development (Cambridge, England)* 127 (19), S. 4157–4168.

Spangler, S. A.; Hoogenraad, C. C. (2007): Liprin-alpha proteins: scaffold molecules for synapse maturation. In: *Biochemical Society transactions* 35 (Pt 5), S. 1278–1282. DOI: 10.1042/BST0351278.

Srinivasan, Subhashini; Lance, Kimberley; Levine, Richard B. (2012): Contribution of EAG to excitability and potassium currents in Drosophila larval motoneurons. In: *Journal of neurophysiology* 107 (10), S. 2660–2671. DOI: 10.1152/jn.00201.2011.

Srinivasan, Subhashini; Lance, Kimberley; Levine, Richard B. (2012): Segmental differences in firing properties and potassium currents in Drosophila larval motoneurons. In: *Journal of neurophysiology* 107 (5), S. 1356–1365. DOI: 10.1152/jn.00200.2011.

Stanley, E. F. (1993): Presynaptic calcium channels and the transmitter release mechanism. In: *Annals of the New York Academy of Sciences* 681, S. 368–372.

Steriade, M. (2006): Grouping of brain rhythms in corticothalamic systems. In: *Neuroscience* 137 (4), S. 1087–1106. DOI: 10.1016/j.neuroscience.2005.10.029.

Stevens, C. F.; Wesseling, J. F. (1998): Activity-dependent modulation of the rate at which synaptic vesicles become available to undergo exocytosis. In: *Neuron* 21 (2), S. 415–424.

Sudhof, T. C. (1995): The synaptic vesicle cycle: a cascade of protein-protein interactions. In: *Nature* 375 (6533), S. 645–653. DOI: 10.1038/375645a0.

Sudhof, Thomas C. (2004): The synaptic vesicle cycle. In: *Annual review of neuroscience* 27, S. 509–547. DOI: 10.1146/annurev.neuro.26.041002.131412.

Sudhof, Thomas C. (2012): The presynaptic active zone. In: *Neuron* 75 (1), S. 11–25. DOI: 10.1016/j.neuron.2012.06.012.

Sudhof, Thomas C.; Rothman, James E. (2009): Membrane fusion: grappling with SNARE and SM proteins. In: *Science (New York, N.Y.)* 323 (5913), S. 474–477. DOI: 10.1126/science.1161748.

Sulkowski, Mikolaj J.; Iyer, Srividya Chandramouli; Kurosawa, Mathieu S.; Iyer, Eswar Prasad R.; Cox, Daniel N. (2011): Turtle functions downstream of Cut in differentially regulating class specific dendrite morphogenesis in Drosophila. In: *PloS one* 6 (7), S. e22611. DOI: 10.1371/journal.pone.0022611.

Susin, Santos A.; Zamzami, Naoufal; Kroemer, Guido (1998): Mitochondria as regulators of apoptosis. Doubt no more. In: *Biochimica et Biophysica Acta (BBA) - Bioenergetics* 1366 (1-2), S. 151–165. DOI: 10.1016/S0005-2728(98)00110-8.

Takamori, Shigeo; Holt, Matthew; Stenius, Katinka; Lemke, Edward A.; Gronborg, Mads; Riedel, Dietmar et al. (2006): Molecular anatomy of a trafficking organelle. In: *Cell* 127 (4), S. 831–846. DOI: 10.1016/j.cell.2006.10.030.

Tanabe, T.; Takeshima, H.; Mikami, A.; Flockerzi, V.; Takahashi, H.; Kangawa, K. et al. (1987): Primary structure of the receptor for calcium channel blockers from skeletal muscle. In: *Nature* 328 (6128), S. 313–318. DOI: 10.1038/328313a0.

Tejedor, F. J.; Bokhari, A.; Rogero, O.; Gorczyca, M.; Zhang, J.; Kim, E. et al. (1997): Essential role for dlg in synaptic clustering of Shaker K+ channels in vivo. In: *The Journal of neuroscience : the official journal of the Society for Neuroscience* 17 (1), S. 152–159.

Thomas, J. B.; Bastiani, M. J.; Bate, M.; Goodman, C. S. (1984): From grasshopper to Drosophila: a common plan for neuronal development. In: *Nature* 310 (5974), S. 203–207.

Thomas, P.; Surprenant, A.; Almers, W. (1990): Cytosolic Ca2+, exocytosis, and endocytosis in single melanotrophs of the rat pituitary. In: *Neuron* 5 (5), S. 723–733.

Thomas, U.; Kim, E.; Kuhlendahl, S.; Koh, Y. H.; Gundelfinger, E. D.; Sheng, M. et al. (1997): Synaptic clustering of the cell adhesion molecule fasciclin II by discs-large and its role in the regulation of presynaptic structure. In: *Neuron* 19 (4), S. 787–799.

Tian, Lin; Hires, S. Andrew; Mao, Tianyi; Huber, Daniel; Chiappe, M. Eugenia; Chalasani, Sreekanth H. et al. (2009): Imaging neural activity in worms, flies and mice with improved GCaMP calcium indicators. In: *Nature methods* 6 (12), S. 875–881. DOI: 10.1038/nmeth.1398.

Tsien, R. W.; Lipscombe, D.; Madison, D. V.; Bley, K. R.; Fox, A. P. (1988): Multiple types of neuronal calcium channels and their selective modulation. In: *Trends in neurosciences* 11 (10), S. 431–438.

Tsien, R. W.; Tsien, R. Y. (1990): Calcium channels, stores, and oscillations. In: *Annual review of cell biology* 6, S. 715–760. DOI: 10.1146/annurev.cb.06.110190.003435.

Tukey J. W.: *Exploratory data analysis.* Addison-Wesley, 1977.

Tuluc, Petronel; Molenda, Natalia; Schlick, Bettina; Obermair, Gerald J.; Flucher, Bernhard E.; Jurkat-Rott, Karin (2009): A CaV1.1 Ca2+ channel splice variant with high conductance and voltage-sensitivity alters EC coupling in developing skeletal muscle. In: *Biophysical journal* 96 (1), S. 35–44. DOI: 10.1016/j.bpj.2008.09.027.

Turrigiano, Gina G. (1999): Homeostatic plasticity in neuronal networks. The more things change, the more they stay the same. In: *Trends in neurosciences* 22 (5), S. 221–227. DOI: 10.1016/S0166-2236(98)01341-1.

Udolph, G.; Luer, K.; Bossing, T.; Technau, G. M. (1995): Commitment of CNS progenitors along the dorsoventral axis of Drosophila neuroectoderm. In: *Science (New York, N.Y.)* 269 (5228), S. 1278–1281.

van den Bogaart, Geert; Holt, Matthew G.; Bunt, Gertrude; Riedel, Dietmar; Wouters, Fred S.; Jahn, Reinhard (2010): One SNARE complex is sufficient for membrane fusion. In: *Nature structural & molecular biology* 17 (3), S. 358–364. DOI: 10.1038/nsmb.1748.

van Petegem, Filip; Clark, Kimberly A.; Chatelain, Franck C.; Minor, Daniel L., JR (2004): Structure of a complex between a voltage-gated calcium channel beta-subunit and an alpha-subunit domain. In: *Nature* 429 (6992), S. 671–675. DOI: 10.1038/nature02588.

Verstreken, Patrik; Kjaerulff, Ole; Lloyd, Thomas E.; Atkinson, Richard; Zhou, Yi; Meinertzhagen, Ian A.; Bellen, Hugo J. (2002): Endophilin mutations block clathrin-mediated endocytosis but not neurotransmitter release. In: *Cell* 109 (1), S. 101–112.

Verstreken, Patrik; Ohyama, Tomoko; Bellen, Hugo J. (2008): FM 1-43 labeling of synaptic vesicle pools at the Drosophila neuromuscular junction. In: *Methods in molecular biology (Clifton, N.J.)* 440, S. 349–369. DOI: 10.1007/978-1-59745-178-9_26.

Wagh, Dhananjay A.; Rasse, Tobias M.; Asan, Esther; Hofbauer, Alois; Schwenkert, Isabell; Durrbeck, Heike et al. (2006): Bruchpilot, a protein with homology to ELKS/CAST, is required for structural integrity and function of synaptic active zones in Drosophila. In: *Neuron* 49 (6), S. 833–844. DOI: 10.1016/j.neuron.2006.02.008.

Wang, L. Y.; Kaczmarek, L. K. (1998): High-frequency firing helps replenish the readily releasable pool of synaptic vesicles. In: *Nature* 394 (6691), S. 384–388. DOI: 10.1038/28645.

Wang, Xiaolu; Hu, Bin; Zieba, Agata; Neumann, Nicole G.; Kasper-Sonnenberg, Monika; Honsbein, Annegret et al. (2009): A protein interaction node at the neurotransmitter release site: domains of Aczonin/Piccolo, Bassoon, CAST, and rim converge on the N-terminal domain of Munc13-1. In: *The Journal of neuroscience : the official journal of the Society for Neuroscience* 29 (40), S. 12584–12596. DOI: 10.1523/JNEUROSCI.1255-09.2009.

Watanabe, Shigeki; Liu, Qiang; Davis, M. Wayne; Hollopeter, Gunther; Thomas, Nikita; Jorgensen, Nels B.; Jorgensen, Erik M. (2013): Ultrafast endocytosis at Caenorhabditis elegans neuromuscular junctions. In: *eLife* 2, S. e00723. DOI: 10.7554/eLife.00723.

Watanabe, Shigeki; Rost, Benjamin R.; Camacho-Perez, Marcial; Davis, M. Wayne; Sohl-Kielczynski, Berit; Rosenmund, Christian; Jorgensen, Erik M. (2013): Ultrafast endocytosis at mouse hippocampal synapses. In: *Nature* 504 (7479), S. 242–247. DOI: 10.1038/nature12809.

Wojcik, Sonja M.; Brose, Nils (2007): Regulation of membrane fusion in synaptic excitation-secretion coupling: speed and accuracy matter. In: *Neuron* 55 (1), S. 11–24. DOI: 10.1016/j.neuron.2007.06.013.

Womack, Mary D.; Khodakhah, Kamran (2002): Characterization of large conductance Ca2+-activated K+ channels in cerebellar Purkinje neurons. In: *The European journal of neuroscience* 16 (7), S. 1214–1222.

Worrell, Jason W.; Levine, Richard B. (2008): Characterization of voltage-dependent Ca2+ currents in identified Drosophila motoneurons in situ. In: *Journal of neurophysiology* 100 (2), S. 868–878. DOI: 10.1152/jn.90464.2008.

Wu, Joy S.; Luo, Liqun (2006): A protocol for mosaic analysis with a repressible cell marker (MARCM) in Drosophila. In: *Nature protocols* 1 (6), S. 2583–2589. DOI: 10.1038/nprot.2006.320.

Wu, Ling-Gang; Hamid, Edaeni; Shin, Wonchul; Chiang, Hsueh-Cheng (2014): Exocytosis and endocytosis: modes, functions, and coupling mechanisms. In: *Annual review of physiology* 76, S. 301–331. DOI: 10.1146/annurev-physiol-021113-170305.

Wu, Ling-Gang; Ryan, Timothy A.; Lagnado, Leon (2007): Modes of vesicle retrieval at ribbon synapses, calyx-type synapses, and small central synapses. In: *The Journal of neuroscience : the official journal of the Society for Neuroscience* 27 (44), S. 11793–11802. DOI: 10.1523/JNEUROSCI.3471-07.2007.

Wu, Ying; Kawasaki, Fumiko; Ordway, Richard W. (2005): Properties of short-term synaptic depression at larval neuromuscular synapses in wild-type and temperature-sensitive paralytic mutants of Drosophila. In: *Journal of neurophysiology* 93 (5), S. 2396–2405. DOI: 10.1152/jn.01108.2004.

Xing, Bin; Ashleigh Long, A.; Harrison, Douglas A.; Cooper, Robin L. (2005): Developmental consequences of neuromuscular junctions with reduced presynaptic calcium channel function. In: *Synapse (New York, N.Y.)* 57 (3), S. 132–147. DOI: 10.1002/syn.20165.

Xu, Chang; Liu, Wenying; Wang, Yuanxiang; Chen, Zhongxian; Ji, Yi (2009): Depressed exocytosis and endocytosis of type II alveolar epithelial cells are responsible for the surfactant deficiency in the lung of newborn

with congenital diaphragmatic hernia. In: *Medical hypotheses* 72 (2), S. 160–162. DOI: 10.1016/j.mehy.2008.09.012.

Yamashita, Takayuki; Eguchi, Kohgaku; Saitoh, Naoto; Gersdorff, Henrique von; Takahashi, Tomoyuki (2010): Developmental shift to a mechanism of synaptic vesicle endocytosis requiring nanodomain Ca2+. In: *Nature neuroscience* 13 (7), S. 838–844. DOI: 10.1038/nn.2576.

Yamashita, Takayuki; Hige, Toshihide; Takahashi, Tomoyuki (2005): Vesicle endocytosis requires dynamin-dependent GTP hydrolysis at a fast CNS synapse. In: *Science (New York, N.Y.)* 307 (5706), S. 124–127. DOI: 10.1126/science.1103631.

Yao, Chi-Kuang; Lin, Yong Qi; Ly, Cindy V.; Ohyama, Tomoko; Haueter, Claire M.; Moiseenkova-Bell, Vera Y. et al. (2009): A synaptic vesicle-associated Ca2+ channel promotes endocytosis and couples exocytosis to endocytosis. In: *Cell* 138 (5), S. 947–960. DOI: 10.1016/j.cell.2009.06.033.

Zefirov, A. L.; Abdrakhmanov, M. M.; Mukhamedyarov, M. A.; Grigoryev, P. N. (2006): The role of extracellular calcium in exo- and endocytosis of synaptic vesicles at the frog motor nerve terminals. In: *Neuroscience* 143 (4), S. 905–910. DOI: 10.1016/j.neuroscience.2006.08.025.

Zhai, R. Grace; Bellen, Hugo J. (2004): The architecture of the active zone in the presynaptic nerve terminal. In: *Physiology (Bethesda, Md.)* 19, S. 262–270. DOI: 10.1152/physiol.00014.2004.

Zheng, W.; Feng, G.; Ren, D.; Eberl, D. F.; Hannan, F.; Dubald, M.; Hall, L. M. (1995): Cloning and characterization of a calcium channel alpha 1 subunit from Drosophila melanogaster with similarity to the rat brain type D isoform. In: *The Journal of neuroscience : the official journal of the Society for Neuroscience* 15 (2), S. 1132–1143.

Zhou, Lujia; McInnes, Joseph; Verstreken, Patrik (2014): Ultrafast synaptic endocytosis cycles to the center stage. In: *Developmental cell* 28 (1), S. 5–6. DOI: 10.1016/j.devcel.2013.12.017.

Zito, K.; Fetter, R. D.; Goodman, C. S.; Isacoff, E. Y. (1997): Synaptic clustering of Fascilin II and Shaker: essential targeting sequences and role of Dlg. In: *Neuron* 19 (5), S. 1007–1016.

Zito, K.; Parnas, D.; Fetter, R. D.; Isacoff, E. Y.; Goodman, C. S. (1999): Watching a synapse grow: noninvasive confocal imaging of synaptic growth in Drosophila. In: *Neuron* 22 (4), S. 719–729.

Zucker, R. S. (1989): Short-term synaptic plasticity. In: *Annual review of neuroscience* 12, S. 13–31. DOI: 10.1146/annurev.ne.12.030189.000305.

6 Appendix

6.1 MARCM cross

1. **<u>Pretest for the complementary test:</u>**

$+\,;\,\frac{1D\ X10}{CyO-GFP}\,;\,+\quad \mathbf{X} \quad +\,;\,\frac{1D\ X7}{CyO}\,;\,+$

➔ Proof of the lethality of X7/X10, only Cy flies should come up

2. **<u>Pretest for heatshock timing in hsFLP flies:</u>**

$\frac{hsFLP\ GFP}{hsFLP\ GFP}\,;\,\frac{\{FRT40A\ ry+\}\ tub-Gal80}{\{FRT40A\ ry+\}\ tub-Gal80}\,;\frac{tub-Gal4}{tub-Gal4}\ \mathbf{X}\ w\,;\,\frac{sna[ScO]\ \{FRT40A\ ry+\}}{CyO}\,;\,+$

F1 $\frac{hsFLP\ GFP}{w}\,;\,\frac{\{FRT40A\ ry+\}\ tub-Gal80}{sna[ScO]\ \{FRT40A\ ry+\}}\,;\,\frac{tub-Gal4}{+}$

➔ In F1 embryos 30 min heatshock when aCC/RP2 is born

3. **<u>1D X10 in ry$^-$ background:</u>**

In(2LR)bw^{v1} = Plum-Balancer = Plum

"1*D X*10" and "1*D X*7" are null-mutant alleles of the *Drosophila* gene *Ca-α1D*

1a) $+\,;\,\frac{\text{Plum}}{CyO}\,;\,\frac{CxD}{TM6b}\quad \mathbf{X}\quad +\,;\,\frac{1D\ X10}{CyO-GFP}\,;\,+$

F1 $+\,;\,\frac{\text{Plum}}{1D\ X10}\,;\,\frac{+}{TM6b}$

1b) $+\,;\,\frac{\text{Plum}}{CyO}\,;\,\frac{CxD}{TM6b}\quad \mathbf{X}\quad +\,;\,+\,;\,\frac{ry-}{ry-}$

F1 $+\,;\,\frac{\text{CyO}}{+}\,;\,\frac{CxD}{ry-}$

2) $\frac{+}{+}$; $\frac{\text{Plum}}{1D\ X10}$; $\frac{+}{TM6b}$ **X** + ; $\frac{\text{CyO}}{+}$; $\frac{CxD}{ry-}$ (1a **X** 1b)

F1 + ; $\frac{CyO}{1D\ X10}$; $\frac{ry-}{TM6b}$

3) + ; $\frac{CyO}{1D\ X10}$; $\frac{ry-}{TM6b}$ **X** + ; $\frac{CyO}{1D\ X10}$; $\frac{ry-}{TM6b}$ (2 **X** 2)

F1 + ; $\frac{CyO}{1D\ X10}$; $\frac{ry-}{ry-}$

4. **Frt-site in ry⁻ background:**

1a) $\frac{+}{+}$; $\frac{Plum}{CyO}$; $\frac{CxD}{TM6b}$ **X** *w* ; $\frac{sna[ScO]\{FRT40A\ ry+\}}{CyO}$; +

F1 + ; $\frac{\text{Plum}}{sna[ScO]\{FRT40A\ ry+\}}$; $\frac{+}{TM6b}$

1b) + ; $\frac{\text{Plum}}{CyO}$; $\frac{CxD}{TM6b}$ **X** + ; + ; $\frac{ry-}{ry-}$

F1 $\frac{+}{+}$; $\frac{\text{CyO}}{+}$; $\frac{CxD}{ry-}$

2) + ; $\frac{\text{Plum}}{sna[ScO]\ \{FRT40A\ ry+\}}$; $\frac{+}{TM6b}$ **X** $\frac{+}{+}$; $\frac{\text{CyO}}{+}$; $\frac{CxD}{ry-}$ (1a **X** 1b)

F1 $\frac{+}{+}$; $\frac{\text{CyO}}{sna[ScO]\ \{FRT40A\ ry+\}}$; $\frac{ry-}{TM6b}$

3) $\frac{+}{+}$; $\frac{\text{CyO}}{sna[ScO]\ \{FRT40A\ ry+\}}$; $\frac{ry-}{TM6b}$ **X** + ; $\frac{\text{CyO}}{sna[ScO]\ \{FRT40A\ ry+\}}$; $\frac{ry-}{TM6b}$ (2 **X** 2)

F1 $\frac{+}{+}$; $\frac{sna[ScO]\ \{FRT40A\ ry+\}}{CyO}$; $\frac{ry-}{ry-}$

5. Combination of 1DX10 and FRT-site

CyO = CyO Cy^1 dp^{lv1} cn^1 pr^1

1D X10 = b^1 $1D^{X10}$ pr^1 cn^1 wx^{wxt} bw^1

1) + ; $\frac{\text{CyO Cy1 dpIv1 cn1 pr1}}{\text{b1 1DX10 pr1 cn1 wxwxt bw1}}$; $\frac{ry-}{ry-}$ **X** $\frac{+}{+}$; $\frac{\text{sna[ScO] \{FRT40A ry+\}}}{\text{CyO}}$; $\frac{ry-}{ry-}$

➔ Crossing over in the gametes of the F1 females:

F1 $\frac{+}{+}$; $\frac{\text{b1 1DX10 pr1 cn1 wxwxt bw1}}{\text{sna[ScO] \{FRT40A ry+\}}}$; $\frac{ry-}{ry-}$ X $\frac{+}{+}$; $\frac{\text{SM6aCy1al1cn2Pdplvlsp2}}{\text{vasKG01651}}$; $\frac{ry-}{ry-}$

Possible Crossing over result:

F1 $\frac{+}{+}$; $\frac{\text{b1 1DX10 pr1 \{FRT40A ry+\}}}{\text{sna[ScO] cn1 wxwxt bw1}}$; $\frac{ry-}{ry-}$ X $\frac{+}{+}$; $\frac{\text{SM6aCy1al1cn2Pdplvlsp2}}{\text{vasKG01651}}$; $\frac{ry-}{ry-}$

- Cy
- Wildtype eye color (FRT ry+)
- No sna[Sco]

➔ F2 $\frac{+}{Y}$; $\frac{\text{b1 1DX10 pr1 \{FRT40A ry+\}}}{\text{SM6aCy1al1cn2Pdplvlsp2}}$; $\frac{ry-}{ry-}$

6. <u>Complementary test and increase of potential recombination events:</u>

➔ many 1DX7-females with one male (single potential recombination event) in one vial

$$+\ ;\ \frac{b1\ 1DX7\ pr1\ cn1\ wxwxt\ bw1}{CyO\ Cy1\ cn1\ dplvl\ pr1{-}GFP}\ ;\ +\quad \mathbf{X} \quad \frac{+}{Y}\ ;\ \frac{b1\ 1DX10\ pr1\ \{FRT40A\ ry+\}}{\mathrm{SM6aCy1al1cn2Pdplvlsp2}}\ ;\ \frac{ry-}{ry-}$$

- Pick CyO-GFP larvae and keep till lethality proof

$$\mathrm{F1}\ \frac{+}{+}\ ;\ \frac{b1\ 1DX10\ pr1\ \{FRT40A\ ry+\}}{b1\ 1DX7\ pr1\ cn1\ wxwxt\ bw1}\ ;\ \frac{ry-}{+}$$ ➔lethal? (only Cy offspring)

Select for: $\frac{+}{+}\ ;\ \frac{b1\ 1DX10\ pr1\ \{FRT40A\ ry+\}}{Cy1\ cn1\ dplvl\ pr1{-}GFP}\ ;\ \frac{ry-}{+}$

<u>Gene locations:</u>

sna (ScO)	35D2
Ca-α1D	35E5-6
"FRT40A"	40A1

6.2 Effect of La^{3+} on EPSPs

6.2 Effect of lanthanum on EPSPs

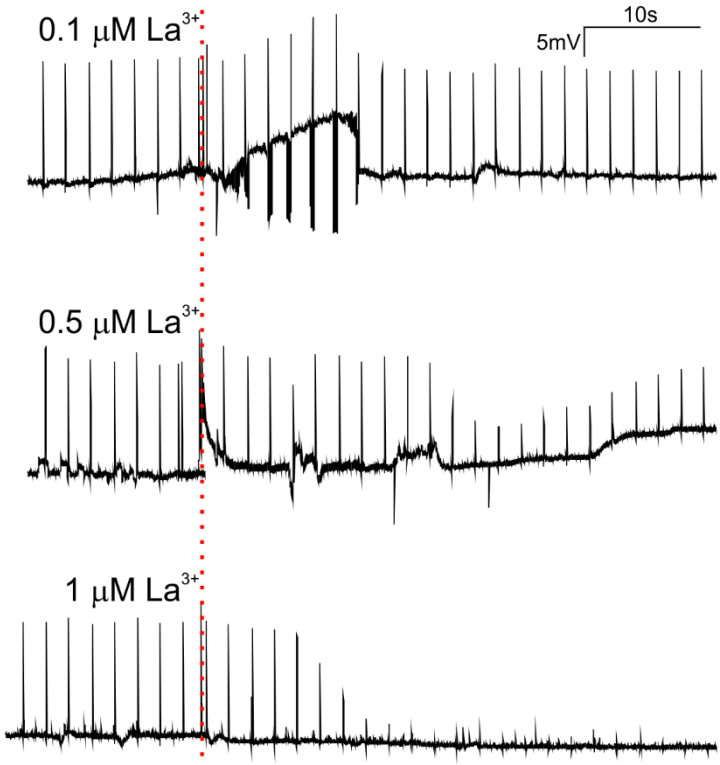

Fig..: Change in EPSP amplitude due to application (red line) of different La^{3+} concentrations. PSPs of larval crawling muscles were evoked through 0.5 Hz stimulation of the axon with a suction electrode. Application of 0.1 µM La^{3+} leads to a small reduction in EPSP amplitude of 5-10 %. One third of EPSP amplitude is left when incubation was done with 0.5 µM La^{3+}. EPSPs are eliminated when 1 µM La^{3+} was added.